Bivariate Splines for Image Enhancements based on Variational Models

by

Qianying Hong

(Under the direction of Ming-jun Lai)

Abstract

In this work, we use bivariate splines to find the approximations of the solutions to two variational models, the ROF model and the TV-L^p model. The reason to use bivariate splines is because of the simplicity of their construction, their accuracy of evaluation and their capability to approximate functions defined on domains of complex shape. We start by showing that both the ROF model and the TV-L^p model have solutions in the spline space, and the solutions are unique and stable. Then we go on to prove that the solutions in the spline space approximate the solutions in the Sobolev space or the BV space. Two iterative numerical algorithms are given to compute the bivariate spline solutions and their convergence are proved. Numerical examples of the applications of the bivariate spline approximations in image inpainting, image resizing, wrinkle removing and image denoising are given. The convergence of the iterative numerical algorithms is examined. Finally, we propose an edge-adaptive triangulation algorithm which triangulates an image according to its edges. To find the edges, we use the Chan-Vese Active Contour Model, which is also a variational model.

Index words: Bivariate Splines, Variational Model, ROF Model, TV-L^p Model, Level Set, Active Contour, Image Enhancement, Triangulation.

Bivariate Splines for Image Enhancements based on Variational Models

by

Qianying Hong

B.S., Sun Yat-sen University, 2003

M.S., Sun Yat-sen University, 2005

M.S., University of Georgia, 2011

A Thesis Submitted to the Graduate Faculty

of The University of Georgia in Partial Fulfillment

of the

Requirements for the Degree

Doctor of Philosophy

Athens, Georgia

2011

Bivariate Splines for Image Enhancements based on Variational Models

by

Qianying Hong

Approved:

Major Professor: Ming-jun Lai

Committee: Ming-jun Lai
Malcolm R. Adams
Alexander Petukhov
Robert Varley

Electronic Version Approved:

Maureen Grasso
Dean of the Graduate School
The University of Georgia
August 2011

Dedication

Dedicated to my father Hong Youwen and my mother Jin Rifen.

Acknowledgments

I would like to acknowledge the following persons who have made this dissertations possible. First, I owe my profound gratitude to the advice and guidance from my advisor, Dr. Mingjun Lai throughout my Ph.D study. He has always made available his support to me in a number of ways through the years. This thesis would not have been possible without his generous advice, constant support and encouragement.

I would also like to thank the rest of my committee: Professor Malcolm R. Adams, Alexander Petukhov, and Robert Varley, for their time to review this thesis.

Finally, I would take this opportunity to express my deepest gratitude to my parents for their unconditioned love and support.

Special thanks go to my husband, Dr. Jingyue Wang, for helping me proofread my thesis. He has also made a lot of valuable suggestions to this thesis through numerous discussions. Also his love and encouragement have given me tremendous support to my study.

Table of Contents

Page

Acknowledgments v

List of Figures viii

List of Tables xi

Chapter

1 Introduction 1

2 Preliminary 4

2.1 Bivariate Splines 4

2.2 Energy Models for Image Restoration 9

2.3 Bounded Variational Penalty Methods 12

2.4 Mollifier and Mollification 17

2.5 Convex Functions and Subdifferential 20

2.6 Inequalities 22

3 Bivariate Spline Approximation for the ROF Model 24

3.1 Existence and Uniqueness of Solutions S_f in $S_d^r(\triangle)$ 26

3.2 Properties of Minimizer of Continuous Functional 29

3.3 Approximation of S_f and s_f to u_f 29

3.4 A Fixed Point Algorithm and its Convergence 39

3.5 Numerical Results 44

4 Bivariate Spline Approximation to a TV-L^p Model 53

4.1 A Statistical Explanation of the TV-L^p Model 55

4.2 Basic Properties of the (ϵ, η)-version TV-L^p Model 59
4.3 Bivariate Spline Approximation of the TV-L^p Model . . . 63
4.4 A Numerical Algorithm 67
4.5 Numerical Examples 74
5 Image Segmentation and Triangulation 81
5.1 Level Set Method 81
5.2 Active Contour Model 83
5.3 Edge-adaptive Triangulation 87
5.4 Numerical Results 89
Bibliography 102

List of Figures

3.1 Example of inpainting by our fitting spline. We use the domain decomposition technique in our computation. 46

3.2 Example of inpainting by our fitting spline. A specified region of a 50% data-corrupted image is recovered. 47

3.3 Example of inpainting by our fitting spline. A specified region of a 60% data-corrupted image is recovered. 48

3.4 Images are scaled by 10 times by using our spline method, bilinear and bicubic interpolation respectively. 49

3.5 Images are enlarged by 10 times by using our spline method, Bicubic and Bilinear interpolation respectively. 49

3.6 Images are enlarged by 10 times by using our spline method, bilinear and bicubic interpolation respectively. 50

3.7 Images are scaled by 10 times by using our spline method, bilinear and bicubic interpolation respectively. 50

3.8 Wrinkles around the eyes and the logo "corbis" are removed. 51

3.9 A face with wrinkles on the left and the face with reduced wrinkles on the right. We use $d = 3$ and $r = 1$ in our computation. 52

3.10 Enlarged details of 4 positions where wrinkles are removed. 52

4.1 Distribution of Laplacian noises of $p = 1$, $p = 1.5$ and $p = 2$. 74

4.2 Triangulations used to test convergence of the algorithm. 75

4.3 Convergency of numerical algorithm on seven different regions. X-axis: number of iterations; Y-axis: $\|u^{(k+1)} - u^{(k)}\|_{L^2(\Omega)}$. 78

4.4 Convergency of numerical algorithm in different p values. X-axis: number of iterations; Y-axis: $\|u^{(k+1)} - u^{(k)}\|_{L^2(\Omega)}$. 79
4.5 Clean image 79
4.6 Noised image of $p = 1$ and the denoised image with the TV-L^p model of $p = 1$ 79
4.7 Noised image of $p = 1.5$ and the denoised image with the TV-L^p model of $p = 1.5$ 80
4.8 Noised image of $p = 2$ and the denoised image with the TV-L^p model of $p = 2$ 80
5.1 Interface involves under forces. 81
5.2 Demonstration of the topology's changing of an interface with level set method. Figure is created by Oleg Alexandrov. 82
5.3 Application of iterative active contours in image segmentation. 87
5.4 Demonstration of the six steps in the edge-adaptive triangulation algorithm. Blue lines are boundaries. Black curves are edges. In each step, points will be deleted are marked in black, and points will be added are marked in blue. . . 94
5.5 (a) An image of a zebra. (b) The structure tensor of the zebra. (c)ACM-segmentation of the structure tensor in (b). (d)The edge of the ACM-segmentation. 95
5.6 (a) An image of a leopard. (b) The structure tensor of the leopard. (c) The ACM-segmentation of the structure tensor in (b). (d) The edge of the ACM-segmentation. 96
5.7 Original image of some special textures. (b) The structure tensor of the texture image. (c) ACM-segmentation of the structure tensor in (b). (d) Boundary of the ACM-segmentation. 97
5.8 ACM-Segmentations based on grey level and gradient level respectively . . . 98

5.9 In (a), some data are clustered together. In (b) the locations of clustered data are identified by ACM-segmentation. In (c) the identified locations are compared to the clustered data. In (d) the true locations of the clustered data are compared to the ACM-identified locations. 99

5.10 (a) The original image of clouds. (b) ACM-segment. (c) is the triangulation based on ACM-segmentation with original image as the background. (d) is the triangulation and edges from the ACM-segmentation. 100

5.11 (a) is the original image of peppers. (b) is the ACM-segmentation. (c) is the triangulation based on the ACM-segmentation with original image as the background. (d) is the triangulation and the edges. 101

List of Tables

4.1 Denoising of p-exponential noises of $p = 1$ by TVL^1, $TVL^{1.5}$ and TVL^2 models 76

4.2 Denoising of p-exponential noises of $p = 1.5$ by TVL^1, $TVL^{1.5}$ and TVL^2 models 76

4.3 Denoising of p-exponential noises of $p = 2$ by TVL^1, $TVL^{1.5}$ and TVL^2 models 77

Chapter 1

Introduction

Many problems in computer vision, e.g., image processing can be formulated as minimization problems. Among them an influential one is the ROF model proposed by Rudin, Osher and Fatemi in [48], which solves the following minimization problem

$$\min_{u\in \mathrm{BV}(\Omega)} \int_\Omega |\nabla u| dx + \frac{1}{\lambda}\int_\Omega |u-f|^2 dx.$$

The ROF model has been studied extensively. See [48], [1], [13], [5], [11], [24], and many references in [51]. Many numerical methods have been proposed to find the numerical approximation. Wang and Lucier have shown in [57] that if $\Omega = [0,1]^2$ the unit square, and f is a $k \times k$ matrix, the minimizer u of the following functional

$$E_k(u) = \sum_{i,j=0}^{k-1} h^2 |(\nabla u)_{ij}| + \frac{1}{2\lambda}\sum_{i,j=0}^{k-1} h^2 (u_{ij} - g_{ij})^2, \quad h = \frac{1}{k},$$

converges to the solution of ROF model in BV space as $h \to 0$. However, their proof can not be easily extended to the case when Ω is a non-rectangular polygon. To solve this problem, we propose to use spline functions to solve the ROF model. A bivariate spline function is a piece-wise polynomial function defined on a triangulation of a polygonal domain with enough smoothness. The main reason we use splines is due to their capability to approximate functions on complicated regions and their accuracy of evaluation, which is critical in image resizing and inpainting. Our main contribution in this dissertation is that we show that the minimizer in a finite dimensional space, such as bivariate spline space, converges to the minimizer in (1) the space of bounded variation $\mathrm{BV}(\Omega)$, when the domain Ω is a rectangle, (2) the Sobolev space $W^{1,1}(\Omega)$, when Ω is a polygon. Moreover, we give an iterative algorithm to compute the bivariate spline approximation and prove the convergence.

For the image denoising problem, we assume the original image $u_0 : \Omega \subset \mathbb{R}^2 \to \mathbb{R}$ is corrupted by a white noise $\epsilon \sim N(0, \sigma^2)$, so that the corrupted image is $f = u_0 + \epsilon$. In statistic settings, by the maximum likelihood method, the best estimation of σ^2 is $\int_\Omega |u_0 - f|^2$. This gives one reason we use the L^2 term as the fidelity term in the ROF model. However, if we generalize the distribution of the error term ϵ from normal distribution to the whole Laplacian distribution family, then by the maximum likelihood method, the fidelity term also needs to be adapted. That is the reason why we introduce a more general model–the TV-L^p model, in which the fidelity term is an L^p term. Similar to the method we use to study the ROF model, we also use the minimizer in a finite dimensional space, e.g. the spline space, to approximate the minimizer in the BV space. A similar approximation property is deduced. Finally, we give an iterative algorithm to compute the bivariate spline approximation and establish the convergence.

It is known that when the size of the triangulation is small enough, the spline function can approximate a discontinuous function well, but the computation time increases simultaneously. Therefore, in some applications, e.g. image denoising, we might want to decompose the image into several regions in each the image is sufficiently smooth, instead of finding the spline approximation on the whole image domain. The active contour method proposed in [16] by Tony F. Chan and Luminita A. Vese is another energy-based method which has its application in image segmentation. In this dissertation, we propose an edge-adaptive triangulation algorithm which triangulates a region based on the region's segmentation by the Chan-Vese active contour model. We also give a finite difference scheme to find the numerical solution of the active contour model. Several numerical examples of image segmentation and edge-adaptive triangulation algorithm are given at the end of the chapter.

This dissertation is divided into five chapters. In Chapter 2, we review some preliminary knowledge. First we review the properties of the bivariate splines we use in our numerical analysis. Next we give an analysis of the underlying reason to use the ROF model for image processing, e.g. image denoising. Then we review some properties of the BV space used

in the ROF model, especially some important results concerning the well-posedness of the minimization problem. Finally in this chapter, we review some basic mathematical tools used in this dissertation, such as mollification, subdifferential convex function, and some basic inequalities. In Chapter 3 and Chapter 4, we show our main results of this dissertation: the analysis of the ROF and TV-L^p model in the finite dimensional space. Finally, in Chapter 5 we explain the Chan-Vese active contour method and the edge-adaptive triangulation algorithm.

Chapter 2

Preliminary

2.1 Bivariate Splines

In this section we outline some basic properties and theories of bivariate splines which will be used in our application to the ROF model and TV-L^p model. We refer to [38] for most spline results presented in this section. Let Ω be a polynomial domain in $\mathbb{R}^2$. Let $\triangle := \{t_1, ..., t_N\}$ be a collection of triangles such that $\Omega = \bigcup_{i=1}^{N} t_i$ and if a pair of triangles in $\triangle$ intersect, then their intersection is either a common vertex or a common edge. For each t, we write $|t|$ for the length of its longest edge, and ρ_t for the radius of the largest disk that can be inscribed in t. We call the ratio $\kappa_t := \dfrac{|t|}{\rho_t}$ the shape parameter of t, $|\triangle| := \max\{|t|,\, t \in \triangle\}$ the size of the triangulation and denote $\rho_\triangle := \max\{\rho_t,\, t \in \triangle\}$.

Definition 2.1.1 (β-Quasi-Uniform Triangulation) . *Let $0 < \beta < \infty$. A triangulation $\triangle$ is a β-quasi-uniform triangulation provided that*

$$\frac{|\triangle|}{\rho_\triangle} \leq \beta.$$

Definition 2.1.2 (Spline Space) *Fix $r \geq 0$ and $d > r$. Let $C^r(\Omega)$ be the class of all r^{th} continuously differentiable functions over Ω. We call*

$$S_d^r(\triangle) = \{s \in C^r(\Omega),\ s|_t \in \mathcal{P}_d, \forall t \in \triangle\}$$

the spline space of degree d and smoothness r over triangulation $\triangle$, where $\mathcal{P}_d$ is the space of all polynomials of degree $\leq d$ and t is a triangle in $\triangle$.

When working with polynomials on triangulations, the barycentric coordinates are more handy than the Cartesian coordinates. Let $t = \langle (x_1, y_1), (x_2, y_2), (x_3, y_3) \rangle = \langle v_1, v_2, v_3 \rangle$ be a non-degenerate triangle. Then any point $v := (x, y)$ has a unique representation of the form $v = b_1 v_1 + b_2 v_2 + b_3 v_3$ with $b_1 + b_2 + b_3 = 1$. The number b_1, b_2, b_3 are called barycentric coordinates of the point v with respect to the triangle t. We use the Bernstein-Bézier polynomials to form a basis for polynomials over a given triangle. Therefore we can write any polynomial of degree d over a single triangle uniquely in terms of Bernstein-Bézier polynomials. We call this the B-form of a polynomial.

Definition 2.1.3 (Bernstein-Bézier Polynomials) *A Bernstein-Bézier polynomial of degree d is defined by*

$$B_{ijk}^d(x, y) = \frac{d!}{i!j!k!} b_1^i b_2^j b_3^k,$$

where i, j, k are non-negative integers with $i + j + k = d$.

Theorem 2.1.1 *The set*

$$\mathcal{B}^d := \{B_{ijk}^d\}_{i+j+k=d}$$

of Bernstein-Bézier polynomials is a basis for the space of polynomials $\mathcal{P}_d$.

Definition 2.1.4 *(B-Form). Let $s \in \mathcal{P}_d$ satisfy*

$$s|_t = \sum_{i+j+k=d} c_{ijk} B_{ijk}^d(x, y).$$

We use the coefficient vector $\mathbf{c} = [c_{ijk},\ i + j + k = d,\ t \in \triangle]$ to denote a spline function in the non-continuous spline space $S_d^{-1}(\triangle)$ [38].

Next we explain the conditions on which polynomials over each single triangle can be connected smoothly to form our splines on Ω.

Theorem 2.1.2 *(Smoothness). Let $t = \langle v_1, v_2, v_3 \rangle$ and $\tilde{t} = \langle v_4, v_3, v_2 \rangle$ be triangles sharing the edge $e := \langle v_2, v_3 \rangle$. Let*

$$p(v) = \sum_{i+j+k=d} c_{ijk} B_{ijk}^d(v)$$

and

$$\tilde{p}(v) = \sum_{i+j+k=d} \tilde{c}_{ijk} \tilde{B}^d_{ijk}(v)$$

where $\{B^d_{ijk}\}$ *and* $\{\tilde{B}^d_{ijk}\}$ *are Bernstein-Bézier polynomials associated to* t *and* $\tilde{t}$ *respectively. Suppose* u *is any direction not parallel to* e*. Denote* D^n_u *the* n^{th} *directional derivative in* u*. Then*

$$D^n_u p(v) = D^n_u \tilde{p}(v),$$

$v \in e$, $n = 0, ..., r$ *if and only if*

$$\tilde{c}_{ijk} = \sum_{\nu+\mu+\kappa=n} c_{\nu,k+\mu,j+\kappa} B^n_{\nu\mu\kappa}(v_4)$$

for $j + k = d - n$ *and* $n = 0, ..., r$*.*

Let $\mathbf{c}$ be the coefficient vector of the B-form of our spline. In practice we can write the smoothness condition in a linear system $H\mathbf{c} = 0$, where H is a rectangular matrix determined by the conditions imposed in Theorem 2.1.2.

Next we review some calculus facts of spline functions.

Theorem 2.1.3 (Integration) *Let* p *be a polynomial written in B-form over a triangle* t *with coefficients* $c_{ijk}, i + j + k = d$*. Then*

$$\int_t p(x, y)dxdy = \frac{A_t}{\binom{d+2}{2}} \sum_{i+j+k=d} c_{ijk},$$

where A_t *is the area of* t*.*

Theorem 2.1.4 (Inner Product)

$$\int_t B_{ijk}(x, y) B_{\nu\mu\kappa}(x, y)dxdy = A_t \frac{\binom{i+\nu}{i}\binom{j+\mu}{j}\binom{k+\kappa}{k}}{\binom{2d}{d}\binom{2d+2}{2}}.$$

Scattered data fitting using splines by discrete least squares and the Lagrange multiplier method are a typical application of splines. Given scattered data $\{(x_i, y_i, f(x_i, y_i)), i =$

$1, ..., N\}$ where N is a relatively large number. Let Ω be the convex hull of the given data location and $\triangle$ a triangulation of Ω. We look for $l_f \in S_d^r(\triangle)$ such that

$$\sum_{i=1}^{N} |l_f(x_i, y_i) - f(x_i, y_i)|^2 = \min_{l \in S_d^{-1}(\triangle)} |l(x_i, y_i) - f(x_i, y_i)|^2 \tag{2.1}$$

$$\text{subject to } Hc = 0.$$

Here $\mathbf{c}$ is the coefficient vector of the B-form of spline function, and $H\mathbf{c} = 0$ is the smoothness conditions imposed in the Theorem 2.1.2.

If the data locations are evenly distributed over $\triangle$ with respect to d, then for each triangle t, the matrix $B_t := [B_{ijk}^d(x_l, y_l)|_t, i+j+k = d, (x_l, y_l) \in t]$ is of full rank. Since there are $\binom{d+2}{2}$ such combinations of triples (i, j, k) subject to $0 \leq i, j, k < \infty$ and $i + j + k = d$, the size of B_t is M_t-by-$\binom{d+2}{2}$, where M_t is the number of points (x_l, y_l)'s in t. Let $B := \text{diag}(B_t, t \in \triangle)$, then any spline function $s \in S_d^r(\Omega)$ can be written as $s = B\mathbf{c}$ for some coefficient vector $\mathbf{c}$. Suppose there are R triangles in $\triangle$, then $B^\top B$ is a full rank square matrix of size $R\binom{d+2}{2}$-by-$R\binom{d+2}{2}$. To solve the constrained discrete least square problem we use the Lagrange multiplier method. Let

$$L(\mathbf{c}) := \sum_{i=1}^{N} |l(x_i - y_i) - f(x_i, y_i)|^2 = \|B\mathbf{c} - \mathbf{f}\|^2$$

where $\mathbf{f}$ is the vector of $f(x_i, y_i)$'s, and

$$G(\mathbf{c}, \alpha) = L(\mathbf{c}) + \alpha^\top H\mathbf{c}.$$

By the Lagrange multiplier method, we solve

$$\frac{\partial}{\partial \mathbf{c}} G(\mathbf{c}, \alpha) = 2B^\top B\mathbf{c} - 2B^\top \mathbf{f} + H^\top \alpha = 0$$

$$\frac{\partial}{\partial \alpha} G(\mathbf{c}, \alpha) = H\mathbf{c} = 0.$$

This is equivalent to solve the linear system

$$\begin{pmatrix} H^\top & 2B^\top B \\ 0 & H \end{pmatrix} \begin{pmatrix} \alpha \\ \mathbf{c} \end{pmatrix} = \begin{pmatrix} 2B^\top \mathbf{f} \\ 0 \end{pmatrix}.$$

One of the main reasons we want to use splines is because they have a nice property: the optimal approximation order. We denote by $W^{k,p}(\Omega)$ the Sobolev space of locally integrable functions $u : \Omega \to \mathbb{R}$ such that for each multi-index α with $|\alpha| \leq k$, $D^\alpha u$ exists in the weak sense and belongs to $L^p(\Omega)$. Define $|f|_{W^{m,p}(\Omega)}$ the L^p norm of the m^{th} derivatives of f over Ω, i.e.,

$$|u|_{W^{k,p}(\Omega)} := \left(\sum_{\nu+\mu=k} \|D_1^\nu D_2^\mu u\|^p_{L^p(\Omega)} \right)^{1/p}, \quad for\ 1 \leq p \leq \infty, \tag{2.2}$$

and define $\|f\|_{L^p(\Omega)} = \left(\frac{1}{A_\Omega} \int_\Omega |f(x)|^p dx \right)^{1/p}$.

We first use the so-called Markov's inequality to compare the size of the derivative of a polynomial with the size of the polynomial itself on a given triangle t. (See [38] for a proof.)

Theorem 2.1.5 (Markov's inequality) *Let $t := \langle v_1, v_2, v_3 \rangle$ be a triangle, and fix $1 \leq q \leq \infty$. Then there exists a constant K depending only on d such that for every polynomial $p \in \mathcal{P}_d$, and any nonnegative integers α and β with $0 \leq \alpha + \beta \leq d$,*

$$\|D_1^\alpha D_2^\beta p\|_{L^q(t)} \leq \frac{K}{\rho_t^{\alpha+\beta}} \|p\|_{L^q(t)}, \quad 0 \leq \alpha + \beta \leq d, \tag{2.3}$$

where ρ_t denotes the radius of the largest circle inscribed in t.

Next we have the following approximation property (cf. [37] and [38]):

Theorem 2.1.6 *Assume $d \geq 3r + 2$ and let $\triangle$ be a triangulation of Ω. Then there exists a quasi-interpolatory operator $Qf \in S_d^r(\triangle)$ mapping $f \in L_1(\Omega)$ into $S_d^r(\triangle)$ such that Qf achieves the optimal approximation order: if $f \in W^{m+1,p}(\Omega)$,*

$$\|D_1^\alpha D_2^\beta (Qf - f)\|_{L^p(\Omega)} \leq C|\triangle|^{m+1-\alpha-\beta} |f|_{W^{m+1,p}(\Omega)} \tag{2.4}$$

for all $\alpha + \beta \leq m + 1$ with $0 \leq m \leq d$. Here the constant C depends only on the degree d and the smallest angle $\theta_\triangle$ and may be dependent on the Lipschitz condition on the boundary of Ω.

We suppose that the data locations $\mathcal{Q} = \{x_i, i = 1, \cdots, n\}$ satisfy the conditions (cf. [33]), that for every $s \in S_d^r(\Omega)$ and every triangle $t \in \triangle$, there exist a positive constant F_1, independent of s and t, such that

$$F_1 \|s\|_{L^\infty(t)} \leq (\sum_{v \in t} s(v)^2)^{1/2}. \tag{2.5}$$

And let F_2 be the largest number of data sites in a triangle $t \in \triangle$ so we have

$$\left\{ \sum_{v \in t} s(v)^2 \right\}^{1/2} \leq F_2 \|s\|_{L^\infty(t)}. \tag{2.6}$$

Then we have the following approximation property of the least square minimizer l_f of (2.1).

Theorem 2.1.7 *Suppose that $d \geq 3r + 2$ and $\triangle$ is a β quasi-uniform triangulation, and there exist two positive constants F_1 and F_2 such that (2.5) and (2.6) are satisfied. Then there exists a constant C depending on d and β such that for every function f in the Sobolev space $W^{m+1,\infty}(\Omega)$ with $0 \leq m \leq d$ such that*

$$\|f - l_f\|_{\Omega,\infty} \leq C \frac{F_2}{F_1} |\triangle|^{m+1} |f|_{W^{m+1,\infty}(\Omega)}.$$

2.2 Energy Models for Image Restoration

Variational and PDE-based approaches have been well studied in image restoration problems. One early model is introduced in 1977 by Tikhonov and Arsenin to find the minimizer of the following functional

$$F(u) = \int_\Omega |u - u_0|^2 dx + \lambda \int_\Omega |\nabla u|^2 dx, \tag{2.7}$$

where ∇ is the standard gradient. The first term in $F(u)$ measures the fidelity to the data. The second is a regularization term. We search for a u that best fits the data so that its gradient is small simultaneously. The parameter λ is a positive weighting constant. The minimization problem admits a unique solution in the functional space

$$W^{1,2}(\Omega) = \{u \in L^2(\Omega); \nabla u \in L^2(\Omega)\},$$

characterized by the Euler-Lagrange equation

$$u - u_0 - \lambda \triangle u = 0 \tag{2.8}$$

with the Neumann boundary condition

$$\frac{\partial u}{\partial n} = 0 \quad \text{on } \partial\Omega \ (n \text{ is the outward normal to } \partial\Omega).$$

However, this is not a good solution to the image restoration problems, because the Laplacian operator has very strong isotropic smoothing properties which annihilate noises but also edges as it evolves. In (2.7), the regularization term penalizes too much the gradients corresponding to edges. The reason is because in the Euler-Lagrange equation of (2.7), the regularization term is transformed to the laplacian diffusion operator δ, which diffuses along the edges but also across the edges. One may decrease p in order to preserve the edges as much as possible. That gives one reason why we should discuss the following model, with $1 \leq p < 2$.

$$E(u) = \int_\Omega |u - u_0|^2 dx + \lambda \int_\Omega |\nabla u|^p dx. \tag{2.9}$$

Furthermore, Rudin, Osher, and Fatemi [47, 48] proposed to use the BV norm to measure the magnitude of u, that is to find the minimizer in the $\mathrm{BV}(\Omega)$ space. Let us analyze the following energy (cf. [6, 7]) for the influence of the smoothing term,

$$E(u) = \frac{1}{2} \int_\Omega |u_0 - u|^2 dx + \lambda \int_\Omega \phi(|\nabla u|) dx, \tag{2.10}$$

which is characterized by the Euler-Lagrange equation:

$$u - u_0 - \lambda \mathrm{div} \left(\frac{\phi'(|\nabla u|)}{|\nabla u|} \nabla u \right) = 0. \tag{2.11}$$

It can be shown that its diffusion term $\mathrm{div} \left(\frac{\phi'(|\nabla u|)}{|\nabla u|} \nabla u \right)$ can be decomposed into a weighted sum of the second derivative in normal and tangent directions to the contour lines (lines along which the intensity is constant). More precisely, for each point x where $|\nabla u(x)| \neq 0$, its normal direction is characterized by the vector $N(x) = \frac{\nabla u(x)}{|\nabla u(x)|} = \frac{1}{|\nabla u(x)|}(u_x, u_y)$

and tangent direction by $T(x) = \dfrac{1}{|\nabla u(x)|}(-u_y, u_x)$, $|T(x)| = 1$, $T(x)$ orthogonal to $N(x)$. We denote by u_{TT} and u_{NN} the second derivatives of u in T-direction and N-direction respectively, i.e.,

$$u_{TT} = T^\top \nabla^2 u T, \quad u_{NN} = N^\top \nabla^2 u N.$$

Here

$$\nabla^2 u = \begin{pmatrix} u_{xx} & u_{xy} \\ u_{yx} & u_{yy} \end{pmatrix}.$$

Define the projection operator $P_N = NN^\top$, and $P_T = TT^\top$. Since $N \cdot T = 0$, we have $P_N + P_T = I$, where I is the identity matrix. It follows that

$$\begin{aligned} u_{NN} + u_{TT} &= T^\top \nabla^2 u T + N^\top \nabla^2 u N = \mathrm{tr}(T^\top \nabla^2 u T + N^\top \nabla^2 u N) \\ &= \mathrm{tr}(\nabla^2 u (TT^\top + NN^\top)) = \mathrm{tr}(\nabla^2 u) = \Delta u = \mathrm{div}(\nabla u). \end{aligned}$$

We can go on to show that

$$\begin{aligned} \mathrm{div}\left(\frac{\nabla u}{|\nabla u|}\right) &= \nabla\left(\frac{1}{|\nabla u|}\right) \cdot \nabla u + \frac{1}{|\nabla u|}\mathrm{div}(\nabla u) \\ &= -\frac{1}{|\nabla u|^2}\left(\nabla |\nabla u| \cdot \nabla u\right) + \frac{1}{|\nabla u|}(u_{TT} + u_{NN}) \\ &= \frac{1}{|\nabla u|}\left(-\nabla^2 u \frac{\nabla u}{|\nabla u|} \cdot \frac{\nabla u}{|\nabla u|} + u_{TT} + u_{NN}\right) \\ &= \frac{1}{|\nabla u|}(-u_{NN} + u_{TT} + u_{NN}) = \frac{u_{TT}}{|\nabla u|}. \end{aligned}$$

Now we can rewrite the diffusion term of (2.11) as a weighted sum of u_{NN} and u_{TT}:

$$\begin{aligned} & \mathrm{div}\left(\frac{\phi'(|\nabla u|)}{|\nabla u|}\nabla u\right) \\ = \; & \nabla(\phi'(|\nabla u|)) \cdot \frac{\nabla u}{|\nabla u|} + \phi'(|\nabla u|)\mathrm{div}\left(\frac{\nabla u}{|\nabla u|}\right) \\ = \; & \phi''(|\nabla u|)\left(\nabla^2 u \frac{\nabla u}{|\nabla u|} \cdot \frac{\nabla u}{|\nabla u|}\right) + \phi'(|\nabla u|)\frac{u_{TT}}{|\nabla u|} \\ = \; & \phi''(|\nabla u|)u_{NN} + \frac{\phi'(|\nabla u|)}{|\nabla u|}u_{TT}. \end{aligned}$$

In a neighborhood of an edge C, an image presents a strong gradient. If we want to preserve the edge, it is preferable to diffuse along C (in the T-direction) and not across it.

In another words, we would like to annihilate the diffusion in the N-direction. That is:

$$\lim_{s\to+\infty} \frac{\phi'(s)}{s} = \beta > 0,$$

and

$$\lim_{s\to+\infty} \phi''(s) = 0.$$

However, it is possible that both $\frac{\phi'(s)}{s}$ and $\phi''(s)$ will approaches to 0 as $s \to \infty$, so we can assume $\frac{\phi'(s)}{s}$ and $\phi''(s)$ both converge to zero but at different rates:

$$\lim_{s\to+\infty} \frac{\phi''(s)}{\phi'(s)/s} = 0.$$

Suppose $\phi(s) = s^z$ then we have

$$\lim_{s\to+\infty} \frac{z(z-1)s^{z-2}s}{zs^{z-1}} = z - 1 = 0$$

$$\phi(s) \simeq s$$

To summarize, the assumption imposed on $\phi(s)$ are

$$\begin{cases} \phi : [0,\infty) \mapsto [0,\infty); \\ \phi''(0) > 0; \\ \phi(s) \simeq s, \text{when } s \to +\infty \end{cases}$$

For example, $\phi(s) = |s|$, and $\phi(s) = \sqrt{\epsilon + s^2}$ are two such suitable candidates. Especially, when $\phi(s) = \sqrt{1+s^2}$, the smoothing term in the energy model is the surface area of s, and the corresponding diffusion term $\operatorname{div}\left(\frac{\nabla s}{\sqrt{1+|\nabla s|^2}}\right)$ is the curvature of the surface function s.

2.3 Bounded Variational Penalty Methods

One reason we solve the minimization problem (2.10) in the BV space instead of the classical Sobolev space, e.g. $W^{1,1}$, is because in a lot of applications the quantity we study can be discontinuous across hypersurfaces, or edges in image processing. The classical Sobolev space

is sometimes too smooth for these applications. Therefore we relax the problem to the BV space, i.e., to solve the following unconstrained minimization problem in BV space

$$\min_{u\in BV} J(u) + \frac{1}{\lambda}\int_\Omega \|u-f\|^2 dx. \tag{2.12}$$

where $J(u) = \int_\Omega |\nabla u| dx$ is the total variation of u. In [50], a slightly more general penalty functional than the BV seminorm is considered, denoted J_ϵ. For sufficiently smooth u, J_ϵ can be written as

$$J_\epsilon(u) = \int_\Omega \sqrt{\epsilon + |\nabla u|^2} dx, \tag{2.13}$$

where $\epsilon \geq 0$. A variation definition of J_ϵ that extends (2.13) to nonsmooth function u is given in [1]. Also in [1], the existence and uniqueness of (2.12) are discussed as well as the effect of taking small $\epsilon > 0$ rather than $\epsilon = 0$.

Let us review some properties of BV functions. Let Ω be a region in $\mathbb{R}^d$, $d = 1, 2, 3$, whose boundary $\partial\Omega$ is Lipschitz continuous.

Definition 2.3.1 (BV **Seminorm)** *For $u : \mathbb{R} \to \mathbb{R}^d$, let*

$$J_0(u) = \sup_{\mathbf{v}\in\mathcal{V}} \int_\Omega (-u\, div(\mathbf{v})) dx,$$

where the set of test functions

$$\mathcal{V} := \{\mathbf{v} \in C_0^1(\Omega; \mathbb{R}^d) \,:\, |\mathbf{v}| \leq 1 \, for\ all\ x \in \Omega)\}.$$

We call $J_0(u)$ the BV seminorm, or total variation of u.

If $u \in C^1(\Omega)$, one can show using integration by parts that

$$J_0(u) = \int_\Omega |\nabla u| dx,$$

because

$$-\int_\Omega u \mathrm{div}(\mathbf{v}) dx + \int_{\partial\Omega} u \underbrace{(\mathbf{v}\cdot\mathbf{n})}_{=0} dx = \int_\Omega \nabla u \cdot \mathbf{v} dx. \tag{2.14}$$

Taking the supremum over $\mathcal{V}$, we have

$$\sup_{\mathbf{v}\in\mathcal{V}} \int_\Omega \nabla u \cdot \mathbf{v} dx = \int_\Omega |\nabla u| dx.$$

Definition 2.3.2 (BV **Space)** *The space of functions of bounded variation on* Ω *is defined by*

$$\mathrm{BV}(\Omega) = \{u \in L^1(\Omega) : J_0(u) < \infty\}.$$

The BV norm is given by

$$\|u\|_{BV} := \|u\|_1 + J_0(u).$$

It can be seen that $\mathrm{BV}(\Omega)$ is complete, therefore a Banach space. And it is easy to see that $W^{1,1}(\Omega) \subset \mathrm{BV}(\Omega) \subset L^1(\Omega)$. Since $W^{1,1}$ is dense in L^1, for any $u \in \mathrm{BV}(\Omega)$, there exists a sequence in $W^{1,1}(\Omega)$ converging to u in L^1. The following theorem shows that every function u in $\mathrm{BV}(\Omega)$ can be approximated, in a certain sense, by C^∞ functions, and consequently by $W^{1,1}$ functions.

Theorem 2.3.1 *(cf. [30]) Let* $u \in \mathrm{BV}(\Omega)$*. Then there exists a sequence* $\{u_j\}$ *in* $C^\infty(\Omega)$ *such that*

$$\lim_{j\to\infty} \int_\Omega |u_j - u| dx = 0,$$

and

$$\lim_{j\to\infty} \int_\Omega |\nabla u_j| dx = \int_\Omega |\nabla u| dx.$$

Since $C^\infty(\Omega)$ is dense in $W^{1,1}(\Omega)$ with respect to L^1 topology, the above theorem holds for $\{u_j\}$ in $W^{1,1}(\Omega)$ also.

Remark. On another hand, the above theorem also shows that why we should use the the BV space instead of $W^{1,1}$ space. It is because the convergent sequence in $W^{1,1}(\Omega)$ might converge to a minimizer in the BV space.

Now, we give a definition of J_ϵ for nonsmooth functions according to [1]. Let us identify the convex functional $f(\mathbf{x}) = \sqrt{|\mathbf{x}|^2 + \epsilon}$ with its second conjugate, or Fenchel transform

$$\sqrt{\epsilon + |\mathbf{x}|^2} = \sup\{\mathbf{x}\cdot\mathbf{y} + \sqrt{\epsilon(1 - |\mathbf{y}|^2)} \,:\, |\mathbf{y}| \le 1\}, \tag{2.15}$$

the supremum being attained for $y = \dfrac{\mathbf{x}}{\sqrt{\epsilon + |\mathbf{x}|^2}}$. For non-smooth u, define

$$J_\epsilon(u) := \sup_{\mathbf{v}\in\mathcal{V}} \int_\Omega \left(-u\mathrm{div}(\mathbf{v}) + \sqrt{\epsilon(1 - |\mathbf{v}|^2)}\right) dx. \tag{2.16}$$

Theorem 2.3.2 *(cf.[1]) If $u \in W^{1,1}(\Omega)$, then*

$$J_\epsilon(u) = \int_\Omega \sqrt{\epsilon + |\nabla u|^2} dx.$$

Proof. Integration by parts gives

$$\int_\Omega \left(-u\mathrm{div}(\mathbf{v}) + \sqrt{\epsilon(1-|\mathbf{v}|^2)} \right) dx = \int_\Omega \left(\nabla u \cdot \mathbf{v} + \sqrt{\epsilon(1-|\mathbf{v}|^2)} \right) dx$$

It follows from (2.15) that

$$\int_\Omega \left(-u\ \mathrm{div}(\mathbf{v}) + \sqrt{\epsilon(1-|\mathbf{v}|^2)} \right) dx \leq \int_\Omega \sqrt{\epsilon + |\nabla u|^2} dx.$$

Consequently, $J_\epsilon(u) \leq \int_\Omega \sqrt{\epsilon + |\nabla u|^2} dx$. On the other hand, take $\bar{\mathbf{v}} = \dfrac{\nabla u}{\sqrt{\epsilon + |\nabla u|^2}}$, and observe that

$$\int_\Omega \left(-u\mathrm{div}(\bar{\mathbf{v}}) + \sqrt{\epsilon(1-|\bar{\mathbf{v}}|^2)} \right) dx = \int_\Omega \sqrt{\epsilon + |\nabla u|^2} dx,$$

and $\bar{\mathbf{v}} \in C(\Omega; \mathbb{R}^d)$ with $|\bar{\mathbf{v}}(x)| \leq 1$ for all $x \in \Omega$. By multiplying $\bar{\mathbf{v}}$ by a suitable characteristic function compactly supported in Ω and then mollifying, one can obtain $\mathbf{v} \in \mathcal{V} \cap C_0^\infty(\Omega)$ for which $\int_\Omega \left(-u\mathrm{div}(\mathbf{v}) + \sqrt{\epsilon(1-|\mathbf{v}|^2)} \right) dx$ is arbitrarily close to $\int_\Omega \sqrt{\epsilon + |\nabla u|^2}$. ■

Theorem 2.3.3 (Convexity) *For $\epsilon \geq 0$, J_ϵ is convex.*

Proof. Let $0 \leq \gamma \leq 1$ and $u_1, u_2 \in L^p(\omega)$. For any $\mathbf{v} \in \mathcal{V}$,

$$\begin{aligned} & \int_\Omega \left(\gamma u_1 + (1-\gamma)u_2)\mathrm{div}(v) + \sqrt{\epsilon(1-|\mathbf{v}|^2)} \right) dx \\ = \ & \gamma \int_\Omega \left(u_1 \mathrm{div}(v) + \sqrt{\epsilon(1-|\mathbf{v}|^2)} \right) dx + (1-\gamma) \int_\Omega \left(u_2 \mathrm{div}(v) + \sqrt{\epsilon(1-|\mathbf{v}|^2)} \right) dx \\ \leq \ & \gamma J_\epsilon(u_1) + (1-\gamma) J_\epsilon(u_2). \end{aligned}$$

Taking the supremum in the top line over $\mathbf{v} \in \mathcal{V}$ gives the convexity of J_ϵ. ■

The next theorem shows that both J_0 and J_ϵ are effective in $\mathrm{BV}(\Omega)$, and J_0 is the pointwise limit of J_ϵ.

Theorem 2.3.4 *(cf. [1]) (i) For any $\epsilon > 0$ and $u \in L^1(\Omega)$, $J_0(u) < \infty$ if and only if $J_\epsilon < \infty$; (ii) For any $u \in \mathrm{BV}(\Omega)$,*

$$\lim_{\epsilon \to 0} J_\epsilon(u) = J_0(u).$$

Define the BV-bounded set

$$\mathcal{D} := \{u \in \mathrm{BV}(\Omega),\ \|u\|_{BV} \leq B\},$$

for some constant $B > 0$. Let d be the dimension of the Euclidean space. Now, we discuss the relative compactness of the BV-bounded set $\mathcal{D}$ in $L^p(\Omega)$, the lower semicontinuity and the coerciveness of J_ϵ, which are critical for the existence and uniqueness of the minimizer for (2.12).

Theorem 2.3.5 *(cf. [1]) If $\mathcal{D}$ is a* BV*-bounded set, then $\mathcal{D}$ is relatively compact in $L^p(\Omega)$ for $1 \leq p \leq \dfrac{d}{d-1}$. $\mathcal{D}$ is bounded, and hence weakly compact for dimensions $d \geq 2$, in $L^p(\Omega)$ for $p = \dfrac{d}{d-1}$.*

Theorem 2.3.6 *(cf. [1]) For any $\epsilon \geq 0$, J_ϵ is weakly lower semicontinuous with respect to the L^p topology for $1 \leq p < \infty$.*

Proof. Let u_n weakly converges to $\bar{u}$ in $L^p(\Omega)$. For any $\mathbf{v} \in \mathcal{V}$, $\mathrm{div}(\mathbf{v}) \in C(\Omega)$ and hence,

$$\begin{aligned}
\int_\Omega \left(-\bar{u}\mathrm{div}(\mathbf{v}) + \sqrt{\epsilon(1-|\mathbf{v}|^2)}\right) dx &= \lim_{n\to\infty} \int_\Omega \left(-u_n \mathrm{div}(\mathbf{v}) + \sqrt{\epsilon(1-|\mathbf{v}|^2)}\right) dx \\
&= \liminf_{n\to\infty} \int_\Omega \left(-u_n \mathrm{div}(\mathbf{v}) + \sqrt{\epsilon(1-|\mathbf{v}|^2)}\right) dx \\
&\leq J_\epsilon(u_n).
\end{aligned}$$

Take the supremum over $\mathbf{v} \in \mathcal{V}$ gives $J_\epsilon(\bar{u}) \leq \liminf_{n\to\infty} J_\epsilon(u_n)$ ■

We call a functional F BV**-coercive** if

$$F(u) \to \infty \text{ whenever } \|u\|_{BV} \to \infty.$$

One can prove:

Lemma 2.3.1 *(cf. [1]) Let*

$$F(u) = J_\epsilon(u) + \frac{1}{\lambda}\|u - f\|_2^2.$$

with $\epsilon \geq 0$, then $F(u)$ is weakly lower semicontinuous and BV*-coercive.*

Finally, we give the following theorem on the existence and uniqueness of the solution to (2.12).

Theorem 2.3.7 *(cf. [1]) Suppose that F is* BV*-coercive. If $1 \leq p < \dfrac{d}{d-1}$ and F is semi-continuous, then problem*

$$\min_{u \in L^p(\Omega)} F(u)$$

has a solution. If in addition $p = \dfrac{d}{d-1}$, dimension $d \geq 2$, and F is weakly lower semi-continuous, then a solution also exists. In either case, the solution is unique if F is strictly convex.

2.4 Mollifier and Mollification

Definition 2.4.1 *Define $\eta \in C^\infty(\Omega)$, by*

$$\eta(x) := \begin{cases} C \exp\left(\frac{1}{|x|^2-1}\right), & \text{if } |x| < 1 \\ 0, & \text{if } |x| \geq 1, \end{cases} \tag{2.17}$$

where the constant $C > 0$ is selected so that

$$\int_\Omega \eta dx = 1.$$

For each $\epsilon > 0$, when $x \in \mathbb{R}^d$, set

$$\eta_\epsilon(x) := \frac{C}{\epsilon^d} \eta\left(\frac{x}{\epsilon}\right).$$

we call η the standard mollifier. The function $\eta_\epsilon \in C^\infty$ and satisfies

$$\int_\Omega \eta_\epsilon = 1, \quad spt(\eta_\epsilon) \subset B(0, \epsilon).$$

Definition 2.4.2 *Suppose $f : \Omega \to \mathbb{R}$ is locally integrable, we define its mollification*

$$f^\epsilon := \eta_\epsilon * f \quad \text{in } \Omega,$$

i.e., for $x \in \Omega$

$$f^\epsilon(x) = \int_{\Omega_\epsilon} \eta_\epsilon(x-y) f(y) dy = \int_{B(0,\epsilon)} \eta_\epsilon(y) f(x-y) dy,$$

where $\Omega_\epsilon := \{x : \ dist(x, \Omega) < \epsilon\}$

Theorem 2.4.1 (Properties of mollifiers) *(i)* $f^\epsilon \in C^\infty(\Omega_\epsilon)$.

(ii) $f^\epsilon \to f$ *a.e. as* $\epsilon \to 0$.

(iii) If $f \in C(\Omega)$, *then* $f^\epsilon \to f$ *uniformly on compact subsets of* Ω.

(iv) If $1 \le p \le \infty$ *and* $f \in L^p_{loc}(\Omega)$, *then* $f^\epsilon \to f$ *in* $L^p_{loc}(\Omega)$.

See [26] for the proofs of these properties and more properties of mollifiers.

Lemma 2.4.1 *(cf. [56]) If* $u \in \mathrm{BV}(\Omega)$, *then*

$$\int_\Omega |\nabla u^\epsilon| \le \int_\Omega |\nabla u|.$$

Lemma 2.4.2 *If* $x \in \mathbb{R}^d$,

$$|D_i^k \eta_\epsilon(x)| \le \frac{C}{\epsilon^{d+k}},\ i = 1, ..., d.$$

Proof. Let $t = \frac{|x|^d}{\epsilon^d} - 1$, then $\eta_\epsilon(x) = \frac{1}{\epsilon^d}\eta(t(x))$. We claim that when $-1 \le t < 0$,

$$\eta^{(k)}(t) = P\left(\frac{1}{t}\right)\exp\left(\frac{1}{t}\right),$$

for some polynomial P. This is true for $t = 0$. Now inductively, if $\eta^{(n)}(t) = P(\frac{1}{t})\exp(\frac{1}{t})$, then

$$\eta^{(n+1)}(t) = P'\left(\frac{1}{t}\right)\left(-\frac{1}{t^2}\right)\exp\left(\frac{1}{t}\right) + P\left(\frac{1}{t}\right)\exp\left(\frac{1}{t}\right)\left(-\frac{1}{t^2}\right).$$

Noting that $P'(1/t)\left(-\frac{1}{t^2}\right) + P(1/t)\left(-\frac{1}{t^2}\right)$ is also a polynomial in $\frac{1}{t}$, we proved the claim. Let $z = -\frac{1}{t}$, when $|x| \le \epsilon$, or equivalently $-1 < t < 0$, we have $1 < z < \infty$. Therefore

$$\lim_{t\to 0} P(\frac{1}{t})\exp(\frac{1}{t}) = \lim_{z\to\infty}\frac{P(-z)}{\exp(z)} < \infty,$$

and consequently

$$\lim_{t\to 0}|\eta^{(k)}(t)| < \infty, \quad \text{for } k \ge 1.$$

By the Faádi Bruno's formula of the chain rule (cf. [27]), we have

$$D_i^k \eta(t(x)) = \sum C\eta^{(m_1+m_2+...+m_k)}(t)\cdot\prod_{j=1}^{k}(D_i^j t(x))^{m_j},$$

where the sum is over all $k-$tuple of nonnegative integers $(m_1, .., m_k)$ satisfying the constraint

$$1 \cdot m_1 + 2 \cdot m_2 + ... + n \cdot m_k = k.$$

As $D_i^j t(x) = 0$, for $j > 2$, the constraint becomes

$$1 \cdot m_1 + 2 \cdot m_2 = k.$$

Since $|x| \leq \epsilon$,

$$\begin{aligned} |\prod_{j=1}^{k}(D_i^j t(x))^{m_j}| &= |(D_i t(x))^{m_1}(D_i^2 t(x))^{m_2}| = \left(\frac{2|x|}{\epsilon^2}\right)^{m_1}\left(\frac{2}{\epsilon^2}\right)^{m_2} \\ &\leq \left(\frac{2\epsilon}{\epsilon^2}\right)^{m_1}\left(\frac{2}{\epsilon^2}\right)^{m_2} = \frac{2^{m_1+m_2}}{\epsilon^{m_1+2m_2}} = \frac{2^{m_1+m_2}}{\epsilon^k}. \end{aligned}$$

Using the above inequality and the fact that $|\eta^{(k)}|$ is bounded for all k, we attain the desired inequality

$$|D_i^k \eta_\epsilon(x)| = \frac{1}{\epsilon^d}|D_i^k \eta(t(x))| \leq \frac{C}{\epsilon^{d+k}}.$$

■

Lemma 2.4.3 *If $u \in W^{1,p}(\Omega)$ for $p \geq 1$, then*

$$\|u^\epsilon - u\|_{L^p(\Omega)} \leq C|u|_{W^{1,p}(\Omega)} \cdot \epsilon \tag{2.18}$$

for a positive constant C independent of ϵ and f.

Proof.

$$\begin{aligned} |u^\epsilon - u| &= \left|\int_{B(x,\epsilon)} \eta_\epsilon(x-y)u(y)\,dy - \int_{B(x,\epsilon)} \eta_\epsilon(x-y)\,dy u(x)\right| \\ &\leq \left|\int_{B(x,\epsilon)} \eta_\epsilon(x-y)(u(y)-u(x))\,dy\right|. \end{aligned} \tag{2.19}$$

Let $z(t) = u(x + t(y-x))$, then $\dot{z}(t) = \nabla u(x + t(y-x)) \cdot (y-x)$. We can rewrite $u(y) - u(x)$ as

$$u(y) - u(x) = \int_0^1 \dot{z}(t)dt = \int_0^1 \nabla u(x + t(y-x)) \cdot (y-x)\,dt.$$

Note that $|y-x| \le \epsilon$, then

$$|u(y)-u(x)| \le \int_0^1 |\nabla u(x+t(y-x))|\,dt \cdot \epsilon.$$

Apply the above inequality to (2.19),

$$\begin{aligned}|u^\epsilon - u| &\le \int_{B(x,\epsilon)} \eta_\epsilon(x-y)|u(y)-u(x)|\,dy \\ &\le \int_{B(x,\epsilon)} \eta_\epsilon(x-y) \int_0^1 |\nabla u(x+t(y-x))|\,dt \cdot \epsilon\,dy.\end{aligned}$$

Now take the p power on both sides, and use the convexity of power function of $p \ge 1$(twice),

$$\begin{aligned}|u^\epsilon - u|^p &\le \left(\int_{B(x,\epsilon)} \eta_\epsilon(x-y) \int_0^1 |\nabla u(x+t(y-x))|\,dt \cdot \epsilon\,dy\right)^p \\ &\le \int_{B(x,\epsilon)} \eta_\epsilon(x-y) \left(\int_0^1 |\nabla u(x+t(y-x))|\,dt\right)^p \epsilon^p\,dy \quad \text{(by Jensen's inequality)} \\ &\le \int_{B(x,\epsilon)} \epsilon^p \eta_\epsilon(x-y) \int_0^1 |\nabla u(x+t(y-x))|^p\,dt\,dy\end{aligned}$$

Integrate both sides over Ω and use the fact that η_ϵ is bounded by

$$\eta_\epsilon(x) \le \frac{C}{\epsilon^2}, \quad \text{when } x \in \mathbb{R}^2,$$

then

$$\begin{aligned}\int_\Omega |u^\epsilon - u|^p\,dx &\le \int_\Omega \int_{B(x,\epsilon)} \epsilon^p \eta_\epsilon(x-y) \int_0^1 |\nabla u(x+t(y-x))|^p\,dt\,dy\,dx \\ &\le C \int_\Omega \int_{B(0,\epsilon)} \epsilon^{p-2} \int_0^1 |\nabla u(x+tz))|^p\,dt\,dz\,dx \qquad (\text{let } z = y-x) \\ &\le C \int_0^1 \int_{B(0,\epsilon)} \epsilon^{p-2} \int_\Omega |\nabla u(x+tz)|^p\,dx\,dz\,dt \\ &\le C|u|^p_{W^{1,p}(\Omega_\epsilon)} \epsilon^p \le C'|u|^p_{W^{1,p}(\Omega)} \epsilon^p.\end{aligned}$$

The last inequality comes from an extension theorem from E. M. Stein(cf. [49]). Taking pth root on both sides gives the result. ■

2.5 Convex Functions and Subdifferential

Since the functionals we study are convex, we discuss some basic properties of convex functions. First we give the definition of subdifferential(or subgradient).

Definition 2.5.1 *If $F : U \to R$ is a convex function defined on a convex open set $U \in \mathbb{R}^n$, a vector $v \in \mathbb{R}^d$ is called a subgradient at a point u_0 in U if for any u in U one has*

$$F(u) - F(u_0) \geq \langle v, u - u_0 \rangle. \tag{2.20}$$

The set of subgradients at u_0 is called the subdifferential at u_0 and is denoted by $\partial F(u)$.

We have the well-known non-expansive property for the minimizer of a convex functional.

Theorem 2.5.1 (Non-expansive) *Let*

$$I(u, f) := G(u) + \frac{1}{\lambda} \int_\Omega |u - f|^2 dx, \tag{2.21}$$

where G is a convex functional. If u_f and u_g are the minimizers of $I(u, f)$ and $I(u, g)$ respectively, for some given functions f and g in $L^2(\Omega)$, then

$$\|u_f - u_g\|_2 \leq \|f - g\|_2.$$

Proof. Since G is convex, by (2.20) we have

$$\langle \partial G(u_f), u_f - u_g \rangle \geq G(u_f) - G(u_g),$$

and

$$\langle \partial G(u_g), u_f - u_g \rangle \leq G(u_f) - G(u_g).$$

where ∂G is a subgradient of G. It follows that

$$\langle \partial G(u_f) - \partial G(u_g), u_f - u_g \rangle \geq 0. \tag{2.22}$$

The minimizers of $I(u, f)$ and $I(u, g)$ are characterized by the Euler-Lagrangue equations

$$\partial G(u_f) = \frac{f - u_f}{\lambda},$$

and

$$\partial G(u_g) = \frac{g - u_g}{\lambda}$$

respectively. It follows that

$$\partial G(u_f) - \partial G(u_g) + \frac{u_f - u_g}{\lambda} = \frac{f-g}{\lambda}.$$

Then taking the inner product with $u_f - u_g$ on both sides, we have

$$\langle \partial G(u_f) - \partial G(u_g), u_f - u_g \rangle + \frac{1}{\lambda}\|u_f - u_g\|_2^2 = \frac{1}{\lambda}\langle f - g, u_f - u_g \rangle.$$

Recall that the first term on the left hand-side above is non-negative, therefore we have

$$\frac{1}{\lambda}\|u_f - u_g\|_2^2 \leq \frac{1}{\lambda}\langle f - g, u_f - u_g \rangle \leq \frac{1}{\lambda}\|f - g\|_2 \|u_f - u_g\|_2.$$

That is

$$\|u_f - u_g\|_2 \leq \|f - g\|.$$

■

This shows that if g is very close to f, the minimizer u_g is very close to the minimizer u_f.

2.6 Inequalities

In this work, we will use the following inequalities.

Cauchy-Schwarz ineqaulity: $\|xy\| \leq \|x\|\|y\|$.

Hölder's inequality: Assume $1 \leq p, q \leq \infty$, $\frac{1}{p} + \frac{1}{q} = 1$. Then if $u \in L^p\Omega$, $v \in L^q(\Omega)$, we have

$$\int_\Omega |uv| dx \leq \|u\|_{L^p(\Omega)} \|v\|_{L^q(\Omega)}.$$

Jensen's inequality: Assume that $f : \mathbb{R} \to \mathbb{R}$ is convex, and $\Omega \subset \mathbb{R}^N$ is open and bounded. Let $u : \Omega \to \mathbb{R}$ be integrable. Then

$$f\left(\fint_\Omega u dx\right) \leq \left(\fint_\Omega f(u) dx\right),$$

where $\fint_\Omega u dx$ denotes the mean value of u over Ω.

Minkowski's inequality: Assume $1 \leq p < \infty$ and $u, v \in L^p(\Omega)$. Then

$$\|u + v\|_{L^p(\Omega)} \leq \|u\|_{L^p(\Omega)} + \|v\|_{L^p(\Omega)}.$$

Young's inequality: Assume $1 < p, q < \infty$, $\dfrac{1}{p} + \dfrac{1}{q} = 1$. Then:

$$ab \leq \frac{a^p}{p} + \frac{b^q}{q} \ (a, b > 0).$$

Chapter 3

Bivariate Spline Approximation for the ROF Model

In this chapter we use the bivariate spline approach to approximate the minimizer of the well-known ROF model:

$$\min_{u\in \mathrm{BV}(\Omega)} |u|_{BV} + \frac{1}{2\lambda}\int_\Omega |u-f|^2, \tag{3.1}$$

where $\mathrm{BV}(\Omega)$ is the space of all functions of bounded variation over Ω, $|u|_{BV}$ denotes the BV semi-norm, and f is a given function. As a by-product, we propose a new spline method for scattered data fitting by approximating the minimizer above based on discrete image values.

The minimization in (4.1) has been studied for about twenty years. See [48], [1], [13], [5], [11], [24], and many references in [51]. Many numerical methods have been proposed to approximate the minimizer. Typically, one first regularizes the minimization by considering the following ϵ-version of the ROF model:

$$\min_{u\in \mathrm{BV}(\Omega)} \int_\Omega \sqrt{\epsilon + |\nabla u|^2} + \frac{1}{2\lambda}\int_\Omega |u-f|^2, \tag{3.2}$$

where ∇u is the standard gradient of u, and A_Ω is the area of Ω. Here the first integral is well defined for $u \in W^{1,1}(\Omega)$ which is dense in $\mathrm{BV}(\Omega)$ with respect to the L^1 topology. But for $u \in \mathrm{BV}(\Omega)\backslash W^{1,1}(\Omega)$, we use Acar and Vogel's definition (2.16). The Prime-Dual algorithm (cf. [11]), the projected gradient algorithm (cf. [24]) and finite element methods have been used to find the numerical solution of (3.2) by solving its Euler-Lagrange equation

$$\mathrm{div}\ \left(\frac{\nabla u}{\sqrt{\epsilon + |\nabla u|^2}}\right) - \frac{1}{\lambda}(u-f) = 0 \tag{3.3}$$

or its time dependent version

$$u_t = \mathrm{div}\ \left(\frac{\nabla u}{\sqrt{\epsilon + |\nabla u|^2}}\right) - \frac{1}{\lambda}(u-f) \tag{3.4}$$

starting with $u(x, y, 0) = u_0$ together with Dirichlet or Neumann boundary condition. We refer to [54], [20], [28], and [29] for theoretical studies of finite difference and finite element methods.

To the best knowledge of Dr. Lai and myself, bivariate splines have not been used to solve the nonlinear PDE (3.3) nor time dependent PDE (3.4) in the literature so far. For convenience, let $\epsilon = 1$. It is known (cf. [1]) that the following minimization

$$\min\{E(u), \quad u \in \mathrm{BV}(\Omega)\}, \tag{3.5}$$

where the energy functional $E(u)$ is defined by

$$E(u) = \int_\Omega \sqrt{1 + |\nabla u|^2} dx + \frac{1}{2\lambda} \frac{1}{A_\Omega} \int_\Omega |u - f|^2 dx \tag{3.6}$$

has a unique solution, where A_Ω is the area of the polygonal domain Ω. We use u_f to denote the minimizer. The discussion of the existence and uniqueness of the minimizer of (3.5) can be found in [1] and [13]. In this dissertation, we will show that

$$\min\{E(u), \quad u \in S_d^r(\triangle)\}, \tag{3.7}$$

also has a unique solution. We shall denote by S_f the minimizer of (3.7). Finally, in practice, we only observe discrete corrupted image intensity values over Ω. That is, we have $\{(x_i, f_i), i = 1, \cdots, n\}$ with $x_i \in \Omega$ and corrupted pixel values f_i for $i = 1, \cdots, n$. Let

$$E_d(u) = \int_\Omega \sqrt{1 + |\nabla u(x)|^2} dx + \frac{1}{2\lambda} \frac{1}{n} \sum_{i=1}^n |u(x_i) - f_i|^2 \tag{3.8}$$

be an energy functional. We use bivariate splines to solve the following minimization problem:

$$\min\{E_d(u), \quad u \in S_d^r(\Omega)\}, \tag{3.9}$$

and denote the solution by s_f. Here we suppose the data locations satisfy conditions (2.5) and (2.6).

One of our main results in this chapter is to show

Theorem 3.0.1 *Suppose Ω is a bounded domain with Lipschitz boundary and $\triangle$ is a β-quasi-uniform triangulation of Ω. If $u_f \in W^{1,1}(\Omega)$, then S_f converges to u_f in $L^2(\Omega)$ norm as the size $|\triangle|$ of triangulation $\triangle$ goes to zero. More precisely,*

$$\|S_f - u_f\|_{L^2(\Omega)} \to 0, \quad \textit{when } |\triangle| \to 0.$$

When $u_f \in W^{1,1}(\Omega)$,

$$\|S_f - u_f\|_{L^2(\Omega)} \leq C\sqrt{|\triangle|}$$

for a positive constant C independent of $\triangle$.

We also discuss how to compute the minimizer S_f of (3.7). First the minimizer S_f satisfies the following nonlinear equations: let $\{\phi_1, \cdots, \phi_N\}$ be a basis for $S_d^r(\triangle)$,

$$\frac{\partial}{\partial t} E(S_f + t\phi_j, f)\big|_{t=0} = \int_\Omega \frac{\nabla S_f \cdot \nabla \phi_j}{\sqrt{1 + |\nabla S_f|^2}} dx + \frac{1}{\lambda}\frac{1}{A_\Omega}\int_\Omega (S_f - f)\phi_j dx = 0 \tag{3.10}$$

for all basis functions $\phi_j, j = 1, \cdots, N$. As these are nonlinear equations, we will use a fixed point iterative algorithm as in [20]. Our next result is to show the convergence of the iterative algorithm. Our analysis is completely different from the one given in [20].

3.1 Existence and Uniqueness of Solutions S_f in $S_d^r(\triangle)$

In this section we will talk about the existence, the uniqueness and the stablity of the bivariate spline solution S_f to (3.7). We begin with the following lemma

Lemma 3.1.1 *Assume that the triangulation $\triangle$ is β-quasi-uniform. The minimization problem (3.7) has one and only one solution in the Bivariate spline space $S_d^r(\triangle)$.*

Proof. Let $s_0 \in S_d^r(\triangle)$ be a spline approximation of f, i.e., s_0 satisfies

$$\int_\Omega |s_0 - f|^2 = \min_{s \in S_d^r(\triangle)} \int_\Omega |s - f|^2. \tag{3.11}$$

Let $\mathcal{U}$ be a subset of $S_d^r(\triangle)$ defined by

$$\mathcal{U} = \{u \in S_d^r(\triangle), \quad E(u) \leq E(s_0) + 1\}. \tag{3.12}$$

Clearly, $s_0 \in \mathcal{U}$, so $\mathcal{U}$ is not an empty set. We now show that $\mathcal{U}$ is bounded in $L^2(\Omega)$ norm. For convenience, define

$$\|f\|_{L^2(\Omega)} := \left(\frac{1}{A_\Omega}\int_\Omega |f(x)|^2 dx\right)^{1/2}$$

to be the norm for $L^2(\Omega)$. For any $u \in \mathcal{U}$,

$$\begin{aligned} \|u-f\|^2_{L^2(\Omega)} &\leq 2\lambda\left(\frac{1}{2\lambda}\|u-f\|^2_{L^2(\Omega)} + \int_\Omega \sqrt{1+|\nabla u|^2}dx\right) \\ &= 2\lambda E(u) \leq 2\lambda(E(s_0)+1). \end{aligned} \tag{3.13}$$

Thus we have

$$\|u\|_{L^2(\Omega)} \leq \|u-f\|_{L^2(\Omega)} + \|f\|_{L^2(\Omega)} \leq (2\lambda(E(s_0)+1))^{1/2} + \|f\|_{L^2(\Omega)}. \tag{3.14}$$

That is, $\mathcal{U}$ is a bounded set. Since $\mathcal{U}$ is a closed bounded subset of a finite dimensional space, $\mathcal{U}$ is compact. Let $\{u_j\} \in \mathcal{U}$ be a sequence such that,

$$\lim_{j\to+\infty} E(u_j) = \inf_{u\in S^r_d(\triangle)} E(u).$$

By the compactness for $\mathcal{U}$, there exists a subsequence, say u_j again and $\tilde{u}$ s.t. u_j converges to $\tilde{u}$ in $L^2(\Omega)$ norm.

Next we claim $E(\tilde{u}) = \inf_{u\in S^r_d(\triangle)} E(u)$. It is sufficient to prove that

$$\lim_{j\to\infty}\int_\Omega \sqrt{1+|\nabla u_j|^2}dx = \int_\Omega \sqrt{1+|\nabla \tilde{u}|^2}dx \tag{3.15}$$

Indeed, for any w and fixed $v \in S^r_d(\triangle)$, we have

$$\begin{aligned} & \left|\int_\Omega \sqrt{1+|\nabla w|^2}dx - \int_\Omega \sqrt{1+|\nabla v|^2}dx\right| \\ = & \left|\int_\Omega \frac{(1+|\nabla w|^2)-(1+|\nabla v|^2)}{\sqrt{1+|\nabla w|^2}+\sqrt{1+|\nabla u|^2}}dx\right| \\ \leq & \frac{1}{2}\int_\Omega |\nabla w - \nabla v|\,|\nabla w + \nabla v|dx \\ \leq & \frac{1}{2}\left(\int_\Omega |\nabla(w-v)|^2 dx\right)^{\frac{1}{2}}\left(\int_\Omega |\nabla(w+v)|^2 dx\right)^{\frac{1}{2}} \\ = & \frac{A_\Omega}{2}\|\nabla(w-v)\|_{L^2(\Omega)}\,\|\nabla(w+v)\|_{L^2(\Omega)}. \end{aligned}$$

That is, we have

$$\begin{aligned} &\left|\int_\Omega \sqrt{1+|\nabla w|^2}dx - \int_\Omega \sqrt{1+|\nabla v|^2}dx\right| \qquad (3.16)\\ \leq\ & \frac{A_\Omega}{2}\|\nabla(w-v)\|_{L^2(\Omega)}\left(\|\nabla w\|_{L^2(\Omega)}+\|\nabla v\|_{L^2(\Omega)}\right). \end{aligned}$$

Now we need to use Markov's inequality (cf. Theorem 2.1.5) to show that for any spline $s = w, v, w - v \in S_d^r(\triangle)$,

$$\int_\Omega |\nabla s|^2 dx \leq \frac{C\beta^2}{|\triangle|^2}\int_\Omega |s|^2 dx.$$

It follows from (3.16) that

$$\left|\int_\Omega \sqrt{1+|\nabla u_j|^2}dx - \int_\Omega \sqrt{1+|\nabla \tilde{u}|^2}dx\right| \ \leq\ \frac{C}{2}\frac{\beta^2}{|\triangle|^2}\|u_j-\tilde{u}\|_{L^2(\Omega)}\left(\|u_j\|_{L^2(\Omega)}+\|\tilde{u}\|_{L^2(\Omega)}\right).$$

The convergence of u_j to $\tilde{u}$ in L^2 implies claim (3.15).

The uniqueness follows directly from the strict convexity of the functional $E(u)$. These complete the proof. ■

Lemma 3.1.2 *Assume that the triangulation $\triangle$ is β-quasi-uniform and suppose that the data sites $x_i, i = 1, \cdots, n$ satisfy the condition (2.5). Then the minimization problem (3.9) has one and only one solution.*

Proof. The proof is almost the same as in the proof of Lemma 3.1.1, where $\frac{1}{A_\Omega}\int_\Omega |u-f|^2dx$ has to be replaced by $\frac{1}{n}\sum_{i=1}^n |u(x_i)-f_i|^2$. But we are not able to show that u is bounded in L^2 unless we use the condition in (2.5). Indeed, similar to the proof in Lemma 3.1.1, we have $\sum_{i=1}^n |u(x_i)|^2$ is bounded. Since $u \in S_d^r(\triangle)$, we use (2.5) to have

$$\|u\|_{L^\infty(\Omega)} \leq \frac{1}{F_1}\left(\sum_{i=1}^n |u(x_i)|^2\right)^{1/2}$$

and hence, $\int_\Omega |u|^2dx$ is bounded. The remainder of the proof is again similar to the corresponding part of the proof of Lemma 3.1.1. We may leave the details to the interested reader.

Once we have the existence, the solution is unique due to the strict convexity of $E_d(u)$.

■

3.2 Properties of Minimizer of Continuous Functional

In this section we discuss the properties of the minimizer of the continuous functional (3.7). Since $\int_\Omega \sqrt{1+|\nabla u|^2}dx$ is a convex functional of u, by Theorem 2.5.1, we have the well-known non-expansive property for the minimizer of a convex functional.

Lemma 3.2.1 *[Non-expansive] Suppose $f, g \in L^2(\Omega)$. Let $S_f, S_g \in S_d^\tau(\triangle)$ be the minimizers of (3.7) associated with f and g respectively. Then the norm of the difference of S_f and S_g is bounded by the norm of the difference of f and g, i.e.*

$$\|S_f - S_g\|_{L^2(\Omega)} \leq \|f-g\|_{L^2(\Omega)}. \tag{3.17}$$

Also we can calculate the extreme value the energy functionals $E(S_f)$ in the following lemma.

Lemma 3.2.2 *Let S_f be the minimizer of (3.7). Then we have the following equation for $E(S_f)$,*

$$E(S_f) = \frac{1}{2\lambda A_\Omega}(\|f\|^2_{L^2(\Omega)} - \|S_f\|^2_{L^2(\Omega)}) + \int_\Omega \frac{1}{\sqrt{1+|\nabla S_f|^2}}dx. \tag{3.18}$$

Proof. By using (3.10), S_f satisfies

$$\int_\Omega \frac{\nabla S_f \cdot \nabla S_f}{\sqrt{1+|\nabla S_f|^2}}dx = \frac{1}{\lambda}\frac{1}{A_\Omega}\int_\Omega (f-S_f)S_f dx$$

Adding $\frac{1}{2\lambda A_\Omega}\|f-S_f\|^2_{L^2(\Omega)}$ to both sides above, we get

$$\begin{aligned} E(S_f) - \int_\Omega \frac{1}{\sqrt{1+|\nabla S_f|^2}}dx &= \frac{1}{2\lambda A_\Omega}\|f-S_f\|^2_{L^2(\Omega)} + \frac{1}{\lambda}\frac{1}{A_\Omega}\int_\Omega (f-S_f)S_f dx \\ &= \frac{1}{2\lambda A_\Omega}(\|f\|^2_{L^2(\Omega)} - \|S_f\|^2_{L^2(\Omega)}). \end{aligned}$$

This proves the result in the lemma. ■

3.3 Approximation of S_f and s_f to u_f

In this section, we show that S_f and s_f approximate u_f. We first extend the arguments in [18] to show the convergence of S_f and s_f to u_f, the analysis will require $u_f \in W^{2,\infty}(\Omega)$.

As an image function may not have such high regularity, next we use the ideas from [57] to show the convergence which only require $u_f \in W^{1,1}(\Omega)$ (the case of u_f in $\mathrm{BV}(\Omega)$, if Ω is a rectangular region, will be discussed in Chapter 4).

Let $S_d^r(\triangle)$ be an N-dimensional space, s_N be an approximation of u_f in $S_d^r(\triangle)$, and S_f be the minimizer of (3.7) in $S_d^r(\triangle)$. Define the error term between u_f and S_f by

$$E_N = \int_\Omega \frac{|\nabla(u_f - S_f)|^2}{\sqrt{1+|\nabla S_f|^2}} dx + \frac{1}{2\lambda}\frac{1}{A_\Omega}\int_\Omega |u_f - S_f|^2 dx. \tag{3.19}$$

then we have the following approximation property of S_f and u_f.

Lemma 3.3.1 *Suppose that u_f can be approximated by s_N well in the following sense that*

$$\int_\Omega |\nabla(u_f - s_N)|^2 dx + \frac{1}{\lambda}\frac{1}{A_\Omega}\int_\Omega |u_f - s_N|^2 dx \to 0, \quad N \to \infty. \tag{3.20}$$

Then S_f can also approximate u_f in the sense that $E_N \to 0$, as $N \to \infty$.

Proof. Recall the minimizers u_f of (3.5) and S_f of (3.7) satisfies the following equations:

$$\int_\Omega \frac{\nabla u_f}{\sqrt{1+|\nabla u_f|^2}} \nabla\phi_j dx + \frac{1}{\lambda}\frac{1}{A_\Omega}\int_\Omega (u_f - f)\phi_j dx = 0, \tag{3.21}$$

and

$$\int_\Omega \frac{\nabla S_f \cdot \nabla\phi_j}{\sqrt{1+|\nabla S_f|^2}} dx + \frac{1}{\lambda}\frac{1}{A_\Omega}\int_\Omega (S_f - f)\phi_j dx = 0, \tag{3.22}$$

for every $\phi_j,\ j = 1, ..., N$. Subtracting (3.22) from (3.21) yields

$$\int_\Omega \left(\frac{\nabla u_f}{\sqrt{1+|\nabla u_f|^2}} - \frac{\nabla S_f}{\sqrt{1+|\nabla S_f|^2}} \right) \cdot \nabla\phi_j + \frac{1}{\lambda}\frac{1}{A_\Omega}\int_\Omega (u_f - S_f)\phi_j = 0. \tag{3.23}$$

For convenience, we introduce the following notation for the first term of E_N:

$$\widetilde{E}_N = \int_\Omega \frac{|\nabla(u_f - S_f)|^2}{\sqrt{1+|S_f|^2}} dx. \tag{3.24}$$

It is easy to see

$$\widetilde{E}_N = \int_\Omega \frac{\nabla(u_f - S_f)\cdot\nabla(u_f - s_N)}{\sqrt{1+|\nabla S_f|^2}} dx + \int_\Omega \frac{\nabla(u_f - S_f)\cdot\nabla(s_N - S_f)}{\sqrt{1+|\nabla S_f|^2}} dx, \tag{3.25}$$

where s_N is an approximation of u_f in $S_d^r(\triangle)$. The first term gives

$$\int_\Omega \frac{1}{\sqrt{1+|\nabla S_f|^2}}\nabla(u_f - S_f)\cdot\nabla(u_f - s_N)dx \le \left(\int_\Omega \frac{|\nabla(u_f - s_N)|^2}{\sqrt{1+|\nabla S_f|^2}}\right)^{\frac{1}{2}} \widetilde{E}_N^{\frac{1}{2}}. \tag{3.26}$$

The second term of (3.25) can be written as the sum of two items:

$$\begin{aligned} & \int_\Omega \frac{\nabla(u_f - S_f)\cdot\nabla(s_N - S_f)}{\sqrt{1+|\nabla S_f|^2}}dx \\ = & \int_\Omega \left(\frac{\nabla u_f}{\sqrt{1+|\nabla u_f|^2}} - \frac{\nabla S_f}{\sqrt{1+|\nabla S_f|^2}}\right)\cdot\nabla(s_N - S_f)dx \\ & + \int_\Omega \left(\frac{\nabla u_f}{\sqrt{1+|\nabla S_f|^2}} - \frac{\nabla u_f}{\sqrt{1+|\nabla u_f|^2}}\right)\cdot\nabla(s_N - S_f)dx. \end{aligned} \tag{3.27}$$

By the equation in (3.23) with ϕ_j replaced by $s_N - S_f$, the first term in (3.27) equals

$$\begin{aligned} & \int_\Omega \left(\frac{\nabla u_f}{\sqrt{1+|\nabla u_f|^2}} - \frac{\nabla S_f}{\sqrt{1+|\nabla S_f|^2}}\right)\cdot\nabla(s_N - S_f)dx \\ = & -\frac{1}{\lambda}\int_\Omega (u_f - S_f)(s_N - S_f)dx \\ = & -\frac{1}{\lambda}\int_\Omega (u_f - S_f)^2 dx - \frac{1}{\lambda}\int_\Omega (u_f - S_f)(s_N - u_f)dx \\ \le & -\frac{1}{\lambda}\int_\Omega (u_f - S_f)^2 dx + \frac{1}{\lambda}\|u_f - S_f\|_{L^2(\Omega)}\|u_f - s_N\|_{L^2(\Omega)}. \end{aligned} \tag{3.28}$$

The second term in (3.27) satisfies

$$\begin{aligned} & \int_\Omega \left(\frac{\nabla u_f}{\sqrt{1+|\nabla S_f|^2}} - \frac{\nabla u_f}{\sqrt{1+|\nabla u_f|^2}}\right)\nabla(s_N - S_f)dx \\ \le & \int_\Omega \frac{|\nabla u_f|\,|\nabla(u_f - S_f)|}{\sqrt{1+|\nabla u_f|^2}\sqrt{1+|\nabla S_f|^2}}|\nabla(s_N - S_f)|dx. \end{aligned} \tag{3.29}$$

Let

$$\gamma(u) = \max_{x\in\Omega}\frac{|\nabla u|}{\sqrt{1+|\nabla u|^2}} < 1,$$

the inequality in (3.29) can be rewritten as

$$\begin{aligned}
&\int_\Omega \left(\frac{\nabla u_f}{\sqrt{1+|\nabla S_f|^2}} - \frac{\nabla u_f}{\sqrt{1+|\nabla u_f|^2}} \right) \nabla(s_N - S_f) dx \qquad (3.30)\\
\leq\ & \gamma(u_f) \int_\Omega \frac{|\nabla(u_f - S_f)||\nabla(s_N - S_f)|}{\sqrt{1+|\nabla S_f|^2}} dx \\
\leq\ & \gamma(u_f) \left(\int_\Omega \frac{|\nabla(u_f - S_f)|^2}{\sqrt{1+|\nabla S_f|^2}} dx + \int_\Omega \frac{|\nabla(u_f - S_f)||\nabla(u_f - s_N)|}{\sqrt{1+|\nabla S_f|^2}} \right) \\
\leq\ & \gamma(u_f) \left(\widetilde{E}_N + \widetilde{E}_N^{1/2} \left(\int_\Omega \frac{|\nabla(u_f - s_N)|^2}{\sqrt{1+|\nabla S_f|^2}} \right)^{1/2} \right).
\end{aligned}$$

Now let us consider the whole error term (3.19). By the discussion above, we have

$$\begin{aligned}
E_N &= \widetilde{E}_N + \frac{1}{2\lambda} \|u_f - S_f\|^2_{L^2(\Omega)} \\
&\leq \widetilde{E}_N^{1/2} \left(\int_\Omega \frac{|\nabla(u_f - s_N)|^2}{\sqrt{1+|\nabla S_f|^2}} dx \right)^{1/2} + \frac{1}{2\lambda} \|u_f - S_f\|_{L^2(\Omega)} \|u_f - s_N\|_{L^2(\Omega)} \\
&\quad + \gamma(u_f) \left(\widetilde{E}_N + \widetilde{E}_N^{1/2} \left(\int_\Omega \frac{|\nabla(u_f - s_N)|^2}{\sqrt{1+|\nabla S_f|^2}} dx \right)^{1/2} \right) \\
&\leq (1+\gamma(u_f)) \widetilde{E}_N^{1/2} \left(\int_\Omega \frac{|\nabla(u_f - s_N)|^2}{\sqrt{1+|\nabla S_f|^2}} dx \right)^{1/2} \\
&\quad + \frac{1}{2\lambda} \|u_f - S_f\|_{2,\Omega} \|u_f - s_N\|_{2,\Omega} + \gamma(u_f) \widetilde{E}_N \\
&\leq 2(\widetilde{E}_N + \frac{1}{2\lambda} \|u_f - S_f\|^2_{L^2(\Omega)})^{\frac{1}{2}} \left(\int_\Omega \frac{|\nabla(u_f - s_N)|}{\sqrt{1+|\nabla S_f|^2}} dx + \frac{1}{2\lambda} \|u_f - s_N\|^2 \right)^{\frac{1}{2}} + \gamma(u_f) \widetilde{E}_N \\
&= 2E_N^{\frac{1}{2}} \left(\int_\Omega \frac{|\nabla(u_f - s_N)|}{\sqrt{1+|\nabla S_f|^2}} dx + \frac{1}{2\lambda} \|u_f - s_N\|^2 \right)^{\frac{1}{2}} + \gamma(u_f) \widetilde{E}_N.
\end{aligned}$$

Since $\widetilde{E}_N \leq E_N$, we can rewrite the above inequality as follows.

$$(1 - \gamma(u_f)) E_N \leq E_N^{\frac{1}{2}} \left(4 \int_\Omega |\nabla(u_f - s_N)|^2 dx + \frac{2}{\lambda} \|u_f - s_N\|^2_{L^2(\Omega)} \right)^{\frac{1}{2}}.$$

That is, we have

$$E_N^{\frac{1}{2}} \leq \frac{2}{1 - \gamma(u_f)} \left(\int_\Omega |\nabla(u_f - s_N)|^2 dx + \frac{1}{2\lambda} \frac{1}{A_\Omega} \int_\Omega (u_f - s_N)^2 \right)^{\frac{1}{2}}.$$

Therefore, if u_f can be approximated by s_N in the sense of (3.20), then $E_N \to 0$. That is, S_f approximates u_f. This completes the proof. ■

Similarly, we can prove

Lemma 3.3.2 *Suppose that u_f can be approximated by s_N in the following sense that*

$$\int_\Omega |\nabla(u_f - s_N)|^2 dx + \frac{1}{\lambda}\frac{1}{n}\sum_{i=1}^{n}(u_f(x_i) - s_N(x_i))^2 \to 0, \quad n, N \to \infty. \tag{3.31}$$

Then the minimizer s_f of (3.9) can approximates u_f also very well in the following sense:

$$\int_\Omega \frac{|\nabla(u_f - s_f)|^2}{\sqrt{1+|\nabla s_f|^2}} dx + \frac{1}{2\lambda}\frac{1}{n}\sum_{i=1}^{n}|u_f(x_i) - s_f(x_i)|^2 \to 0 \tag{3.32}$$

as n and N go to ∞.

Finally, we get the approximation property in the following theorem.

Theorem 3.3.1 *Suppose $u_f \in W^{2,\infty}(\Omega)$. Then S_f and s_f approximate u_f, in the sense of (3.20) and (3.32) respectively.*

Proof. We just need to prove conditions (3.20) and (3.31) hold. First take $s_N = Qf$ in Theorem 2.1.6, then

$$\|\nabla(u_f - s_N)\|_{L^2(\Omega)} \le C|\triangle||u_f|_{W^{2,2}(\Omega)},$$

and

$$\|u_f - s_N\|_{L^2(\Omega)} \le C|\triangle|^2|u_f|_{W^{2,2}(\Omega)}.$$

By embedding of Lebesgue Spaces, we have $|u_f|_{W^{2,2}(\Omega)} \le C\|u_f\|_{W^{2,\infty}(\Omega)}$. Therefore the condition (3.20) holds. Similarly we can also find $s_N \in S_d^\tau(\Omega)$ such that

$$\|\nabla(u_f - s_N)\|_{L^\infty(\Omega)} \le C|\triangle||u_f|_{W^{2,\infty}(\Omega)},$$

and

$$\|u_f - s_N\|_{L^\infty(\Omega)} \le C|\triangle|^2|u_f|_{W^{2,\infty}(\Omega)}.$$

Since $\|\nabla(u_f - s_N)\|_{L^2(\Omega)} \le C\|\nabla(u_f - s_N)\|_{L^\infty(\Omega)}$, and $\frac{1}{n}\sum_{i=1}^{n}(u_f(x_i) - s_N(x_i))^2 \le C\|u_f - s_N\|_{L^\infty(\Omega)}$, the condition (3.31) holds also. ■

In general, u_f may not be in $W^{2,\infty}(\Omega)$, e.g,.most image intensive values do not have such a high smoothness. Therefore it is of interest to study the approximation of S_f and u_f in spaces of lower regularity, e.g., $W^{1,1}(\Omega)$ or $\mathrm{BV}(\Omega)$. Next we discuss the approximation of S_f and $u_f \in W^{1,1}(\Omega)$, starting with the following lemma.

Lemma 3.3.3 *Let u_f be the solution to (3.5). For any $u \in BV(\Omega)$,*

$$\|u - u_f\|^2_{L^2(\Omega)} \leq 2\lambda A_\Omega (E(u) - E(u_f)). \tag{3.33}$$

In particular, we have

$$\|S_f - u_f\|^2_{L^2(\Omega)} \leq 2\lambda A_\Omega (E(S_f) - E(u_f)). \tag{3.34}$$

Proof. Using the concept of subdifferential and its basic property (see, e.g. [25]), we have

$$0 = \partial E(u_f) = \partial J(u_f) - \frac{1}{\lambda A_\Omega}(f - u_f) \text{ and } \langle \partial J(u_f), u - u_f \rangle \leq J(u) - J(u_f),$$

where $J(u) = \displaystyle\int_\Omega \sqrt{1 + |\nabla u|^2} dx$. From the above equations, it follows that

$$\frac{1}{\lambda A_\Omega} \int_\Omega (f - u_f)(u - u_f) dx \leq \int_\Omega \sqrt{1 + |\nabla u|^2} - \sqrt{1 + |\nabla u_f|^2} dx. \tag{3.35}$$

We can write

$$\begin{aligned}
& E(u) - E(u_f) \\
= & \int_\Omega \sqrt{1 + |\nabla u|^2} - \sqrt{1 + |\nabla u_f|^2} dx + \frac{1}{2\lambda |A_\Omega|} \left(\int_\Omega |u - f|^2 dx - \int_\Omega |u_f - f|^2 dx \right) \\
= & \int_\Omega \sqrt{1 + |\nabla u|^2} - \sqrt{1 + |\nabla u_f|^2} dx + \frac{1}{2\lambda |A_\Omega|} \left(\int_\Omega (u - u_f + u_f - f)^2 dx - \int_\Omega |u_f - f|^2 dx \right) \\
= & \int_\Omega \sqrt{1 + |\nabla u|^2} - \sqrt{1 + |\nabla u_f|^2} dx + \frac{1}{\lambda |A_\Omega|} \int_\Omega (u - u_f)(u_f - f) dx + \frac{1}{2\lambda |A_\Omega|} \int_\Omega |u - u_f|^2 dx \\
\geq & \frac{1}{2\lambda |A_\Omega|} \int_\Omega |u - u_f|^2 dx
\end{aligned}$$

by (3.35). Therefore the inequality (3.33) holds. ■

Next we show that $E(S_f) - E(u_f) \to 0$. To this end, we recall two standard concepts: extension theorem and mollification. Since $\Omega \subset \mathbb{R}^2$ is a region with piecewise smooth

boundary $\partial\Omega$ and u_f is assumed to be in $W^{1,1}(\Omega)$, using the extension theorem from E.M.Stein in [49], there exists a linear operator $\mathfrak{E} : W^{1,1}(\Omega) \to W^{1,1}(\mathbb{R}^2)$ such that,

(i)$\mathfrak{E}(u_f)|_\Omega = u_f$,

(ii)$\mathfrak{E}$ maps $W^{1,1}(\Omega)$ continuously into $W^{1,1}(\mathbb{R}^2)$:

$$\|\mathfrak{E}(u_f)\|_{W^{1,1}(\mathbb{R}^2)} \leq C\|u_f\|_{W^{1,1}(\Omega)}. \tag{3.36}$$

Note that $\mathfrak{E}(u_f)$ is a compactly supported function in $W^{1,1}(\mathbb{R}^2)$. Thus, without loss of generality we may assume $u_f \in W^{1,1}(\mathbb{R}^2)$.

Let u_f^ϵ be the mollification of u_f defined by

$$u_f^\epsilon(x) = \int_{\Omega_\epsilon} \eta_\epsilon(x-y)u_f(y)dy = \int_{B(x,\epsilon)} \eta_\epsilon(x-y)u_f(y)dy,$$

where $\Omega_\epsilon := \{x \in \mathbb{R}^2 \mid \text{dist}(x,\Omega) < \epsilon\}$. It is known that $\|u_f^\epsilon - u_f\|_{L^2(\Omega)} \to 0$ as $\epsilon \to 0$ and $u_f^\epsilon \in C_0^\infty(\Omega_\epsilon)$. See, e.g. [26].

Our general plan to show $E(S_f) - E(u_f) \to 0$ is to establish the following sequence of inequalities:

$$E(u_f) \leq E(S_f) \leq E(Qu_f^\epsilon) \leq E(u_f^\epsilon) + \text{err}(|\triangle|,\epsilon) \leq E(u_f) + \text{err}_\epsilon + \text{err}(|\triangle|,\epsilon),$$

where Qu_f^ϵ is a spline approximation of u_f^ϵ as in Theorem 2.2, $\text{err}(|\triangle|,\epsilon)$ and err_ϵ are error terms which will go to zero when ϵ and $|\triangle|$ go to zero.

We first show $E(u_f^\epsilon)$ approximates $E(u_f)$.

Lemma 3.3.4 *Let u_f^ϵ be the mollification of u_f defined above. Then $E(u_f^\epsilon)$ approximates $E(u_f)$, when $\epsilon \to 0$. In particular, when $u_f \in W^{1,\infty}(\Omega), E(u_f^\epsilon) - E(u_f) \leq C\epsilon$ for a positive constant dependent on u_f.*

Proof. First we claim that

$$E(u_f^\epsilon) \leq E(u_f) + err_\epsilon$$

for an error term err_ϵ

$$err_\epsilon = \int_{\Omega_\epsilon \setminus \Omega} \sqrt{1 + |\nabla u_f(x)|^2}dx + \frac{1}{2\lambda}\left(\|u_f^\epsilon - u_f\|_{L^2(\Omega)}^2 + 2\|u_f^\epsilon - u_f\|_{L^2(\Omega)}\|u_f - f\|_{L^2(\Omega)}\right). \tag{3.37}$$

Moreover err_ϵ goes to zero when $\epsilon \to 0$.

By the convexity of $\sqrt{1+|t|^2}$ and the property of the mollifier, we have

$$\sqrt{1+|\nabla u_f^\epsilon(x)|^2} = \sqrt{1+\left|\int_{B(0,\epsilon)} \eta_\epsilon(x-y)\nabla u_f(y)dy\right|^2} \le \int_{B(x,\epsilon)} \eta_\epsilon(x-y)\sqrt{1+|\nabla u_f(y)|^2}dy.$$

It follows that

$$\begin{aligned}
\int_\Omega \sqrt{1+|u_f^\epsilon(x)|^2}dx &\le \int_\Omega \int_{B(x,\epsilon)} \eta_\epsilon(x-y)\sqrt{1+|\nabla u_f(y)|^2}dydx. \\
&\le \int_{\Omega_\epsilon} \sqrt{1+|\nabla u_f(y)|^2} \int_{B(y,\epsilon)} \eta_\epsilon(x-y)dxdy \\
&= \int_{\Omega_\epsilon} \sqrt{1+|\nabla u_f(y)|^2}dy. \\
&= \int_\Omega \sqrt{1+|\nabla u_f(y)|^2}dy + \int_{\Omega_\epsilon\setminus\Omega} \sqrt{1+|\nabla u_f(y)|^2}dy.
\end{aligned}$$

By the fact that $u_f \in W^{1,1}(\mathbb{R}^2)$ and (3.36), it follows that

$$\int_{\Omega_\epsilon\setminus\Omega} \sqrt{1+|\nabla u_f(y)|^2}dy \le \int_{\Omega_\epsilon\setminus\Omega} (1+|\nabla u_f(y)|)\,dy \to 0, \quad as\ \epsilon \to 0.$$

Next we have

$$\frac{1}{2\lambda}\|u_f^\epsilon - f\|^2_{L^2(\Omega)} \le \frac{1}{2\lambda}\left(\|u_f^\epsilon - u_f\|^2_{L^2(\Omega)} + 2\|u_f^\epsilon - u_f\|_{L^2(\Omega)}\|u_f - f\|_{L^2(\Omega)} + \|u_f - f\|^2_{L^2(\Omega)}\right).$$

Since $\|u_f^\epsilon - u_f\|_{L^2(\Omega)} \to 0$ as explained above and $\|u_f - f\|_{L^2(\Omega)}$ is bounded because $\frac{1}{2\lambda}\|u_f - f\|^2 \le E(0)$,

$$\frac{1}{2\lambda}\left(\|u_f^\epsilon - u_f\|^2_{L^2(\Omega)} + 2\|u_f^\epsilon - u_f\|_{L^2(\Omega)}\|u_f - f\|_{L^2(\Omega)}\right) \to 0, \quad as\ \epsilon \to 0.$$

This finished the proof of our claim.

Clearly, $u_f^\epsilon \in W^{1,1}(\Omega) \subset \mathrm{BV}(\Omega)$. As u_f is the minimizer in $\mathrm{BV}(\Omega)$, it follows that

$$E(u_f) \le E(u_f^\epsilon) \le E(u_f) + err_\epsilon,$$

which implies $E(u_f^\epsilon)$ approximates $E(u_f)$ when $\epsilon \to 0$.

When $u_f \in W^{1,\infty}(\Omega)$, the above analysis applies. We use (3.37) and Lemma 2.4.3 to conclude

$$err_\epsilon \le C|u_f|_{W^{1,\infty}(\Omega)} \cdot \epsilon.$$

■

We next estimate $E(Qu_f^\epsilon) - E(u_f^\epsilon)$. To do so, we need semi-norm $|u_f^\epsilon|_{W^{2,1}(\Omega_\epsilon)}$.

Lemma 3.3.5 *For any fixed $\epsilon > 0$, $u_f^\epsilon \in W^{2,1}(\Omega_\epsilon)$ and*

$$|u_f^\epsilon|_{W^{2,1}(\Omega_\epsilon)} \leq \frac{C}{\epsilon}|u_f|_{W^{1,1}(\Omega)} \tag{3.38}$$

for a constant $C > 0$.

Proof. Due to the mollification, $u_f^\epsilon \in W^{2,1}(\Omega_\epsilon)$. Letting D_1 denote the partial derivative with respect to the first variable, we consider $\|D_1 D_1 u_f^\epsilon\|_{L^1(\Omega_\epsilon)}$. Recall that $u_f^\epsilon(x) = \int_{B(x,\epsilon)} \eta_\epsilon(x - y)u_f(y)dy$. We have

$$D_1 D_1 u_f^\epsilon = -\int_{B(x,\epsilon)} D_1 u_f(y) D_1 \eta_\epsilon(x - y)dy.$$

It follows that

$$\begin{aligned}
|D_1 D_1 u_f^\epsilon|_{L^1(\Omega_\epsilon)} &= \int_{\Omega_\epsilon} \left| \int_{B(x,\epsilon)} D_1 u_f(y) D_1 \eta_\epsilon(x - y)dy \right| dx \\
&\leq \int_{\Omega} \int_{B(x,\epsilon)} |D_1 u_f(y)||D_1 \eta_\epsilon(x - y)|dydx \\
&\leq \int_{\Omega_\epsilon} |D_1 u_f(y)| \int_{B(y,\epsilon)} |D_1 \eta_\epsilon(x - y)|dxdy, \quad \text{change the order of integration} \\
&= \int_{\Omega_\epsilon} |D_1 u_f(y)|dy \int_{B(0,\epsilon)} |D_1 \eta_\epsilon(z)|dz, \quad z = x - y.
\end{aligned}$$

By Lemma 2.4.2, we have

$$|D_1 \eta_\epsilon(z)| \leq \frac{C}{\epsilon^3},$$

therefore

$$|D_1 D_1 u_f^\epsilon|_{L^1(\Omega_\epsilon)} \leq \|D_1 u_f\|_{L^1(\Omega)} \frac{C}{\epsilon^3} \int_{B(0,\epsilon)} dz \leq |u_f|_{W^{1,1}(\Omega)} \frac{C'}{\epsilon} \tag{3.39}$$

for a positive constant C'. Using the similar arguments, we can show that $\|D_1 D_2 u_f^\epsilon\|_{L^1(\Omega_\epsilon)}$ and $\|D_2 D_2 u_f^\epsilon\|_{L^1(\Omega_\epsilon)}$ have the same upper bound as in (3.39). And thus, we proved that

$$|u_f^\epsilon|_{W^{2,1}(\Omega_\epsilon)} \leq \frac{C}{\epsilon}|u_f|_{W^{1,1}(\Omega)}$$

for some positive constant $C > 0$. ■

Recall $\triangle$ is a triangulation of Ω. Let $\triangle' = \{t_i\}$ be a new triangulation of Ω_ϵ with $\triangle \subset \triangle'$ and $|\triangle'| = |\triangle|$.

Using Theorem 2.1.6, we can choose $Qu_f^\epsilon \in S_d^r(\triangle')$ such that

$$\|D_1^\alpha D_2^\beta (Q(u_f^\epsilon) - u_f^\epsilon)\|_{L^1(\Omega_\epsilon)} \leq C|\triangle|^{2-\alpha-\beta}|u_f^\epsilon|_{W^{2,1}(\Omega_\epsilon)} \tag{3.40}$$

for all $\alpha + \beta = 1$.

Lemma 3.3.6 *Let $\tilde{s} := Qu_f^\epsilon|_\Omega$ be the restriction of $Qu_f^\epsilon \in S_d^r(\triangle)$ on Ω. Then $E(\tilde{s})$ approximates $E(u_f^\epsilon)$, when $\frac{|\triangle|}{\epsilon} \to 0$.*

Proof. We first bound the difference between $|E(\tilde{s}) - E(u_f^\epsilon)|$ by

$$\begin{aligned}
& |E(\tilde{s}) - E(u_f^\epsilon)| \\
\leq\ & \left| \int_\Omega \sqrt{1+|\nabla \tilde{s}|^2} - \sqrt{1+|\nabla u_f^\epsilon|^2} dx \right| + \frac{1}{2\lambda} \left| \|\tilde{s} - f\|_{L^2(\Omega)}^2 - \|u_f^\epsilon - f\|_{L^2(\Omega)}^2 \right| \\
\leq\ & \left| \int_\Omega \sqrt{1+|\nabla \tilde{s}|^2} - \sqrt{1+|\nabla u_f^\epsilon|^2} dx \right| + \frac{1}{2\lambda} \left(\|\tilde{s} - u_f^\epsilon\|_{L^2(\Omega)}^2 + 2\|\tilde{s} - u_f^\epsilon\|_{L^2(\Omega)} \|u_f^\epsilon - f\|_{L^2(\Omega)} \right).
\end{aligned}$$

Denote the right-hand side of the inequality above by $err(|\triangle|, \epsilon)$. Next we will show that $err(|\triangle|, \epsilon) \to 0$, as $|\triangle|/\epsilon \to 0$. Note that the support of $Q(u_f^\epsilon)$ is in Ω_ϵ. Using the inequality in (3.40) with $\alpha + \beta = 1$, we have

$$\|\nabla(\tilde{s} - u_f^\epsilon)\|_{L^1(\Omega)} \leq \|\nabla(Q(u_f^\epsilon) - u_f^\epsilon)\|_{L^1(\Omega_\epsilon)} \leq C|\triangle'||u_f^\epsilon|_{W^{2,1}(\Omega_\epsilon)} \leq \frac{C|\triangle|}{\epsilon}|u_f|_{W^{1,1}(\Omega)} \tag{3.41}$$

Therefore,

$$\begin{aligned}
& \left| \int_\Omega \sqrt{1+|\nabla \tilde{s}|^2} - \sqrt{1+|\nabla u_f^\epsilon|^2} dx \right| = \left| \int_\Omega \frac{|\nabla \tilde{s}|^2 - |\nabla u_f^\epsilon|^2}{\sqrt{1+|\nabla \tilde{s}|^2} + \sqrt{1+|\nabla u^{\epsilon_f}|^2}} dx \right| \\
\leq\ & \int_\Omega \frac{|\nabla \tilde{s} - \nabla u_f^\epsilon||\nabla \tilde{s} + \nabla u_f^\epsilon|}{\sqrt{1+|\nabla \tilde{s}|^2} + \sqrt{1+|\nabla u_f^\epsilon|^2}} dx \\
\leq\ & \|\nabla(\tilde{s} - u_f^\epsilon)\|_{L^1(\Omega)} \\
\leq\ & C\frac{|\triangle|}{\epsilon}|u_f|_{W^{1,1}(\Omega)}.
\end{aligned}$$

It is straightforward that the quantity $\|u_f^\epsilon - f\|_{L^2(\Omega)}$ is bounded because

$$\|u_f^\epsilon - f\|_{L^2(\Omega)} \leq \|u_f^\epsilon - u_f\|_{L^2(\Omega)} + \|u_f - f\|_{L^2(\Omega)} \leq 1 + \sqrt{2\lambda A_\Omega}\|f\|_{L^2(\Omega)}$$

where $\|u_f^\epsilon - u_f\|_{L^2(\Omega)} \leq 1$ if ϵ is small enough, the bound of the second term comes from the property of the minimizer u_f. Using (3.41) and the well-known Sobolev inequality: for any function $g \in W^{1,1}(\Omega_\epsilon)$,

$$\|g\|_{L^2(\Omega_\epsilon)} \leq C|\nabla g|_{L^1(\Omega_\epsilon)}$$

for Ω_ϵ with C^1 boundary (cf. [26]), we have,

$$\|\tilde{s} - u_f^\epsilon\|_{L^2(\Omega)} \leq \|\tilde{s} - u_f^\epsilon\|_{L^2(\Omega_\epsilon)} \leq C\|\nabla(\tilde{s} - u_f^\epsilon)\|_{L^1(\Omega_\epsilon)} \leq \frac{C|\triangle|}{\epsilon}|u_f|_{W^{1,1}(\Omega)}.$$

Therefore, we conclude that $err(|\triangle|, \epsilon) \to 0$, as $|\triangle|/\epsilon \to 0$, and thus $E(\tilde{s})$ approximates $E(u_f^\epsilon)$. ■

Summarizing the discussion above, we have

Theorem 3.3.2 *Suppose that $u_f \in W^{1,1}(\Omega)$. S_f approximates u_f in $L^2(\Omega)$ when $|\triangle| \to 0$. In particular, when $u_f \in W^{1,\infty}(\Omega)$,*

$$\|S_f - u_f\|_{L^2(\Omega)} \leq C|u_f|_{W^{1,\infty}(\Omega)}\sqrt{|\triangle|}$$

for a positive constant C independent of $|\triangle|$.

Proof. Since $S_d^r(\triangle) \subset W^{1,1}(\Omega)$, we have $E(u_f) \leq E(S_f)$. Also $\tilde{s} \in S_d^r(\triangle)$ implies $E(S_f) \leq E(\tilde{s})$. By Lemmas 3.3.4 and 3.3.6, we have

$$E(u_f) \leq E(S_f) \leq E(\tilde{s}) \leq E(u_f^\epsilon) + err(|\triangle|, \epsilon) \leq E(u_f) + err_\epsilon + err(|\triangle|, \epsilon).$$

For each triangulation $\triangle$, we choose $\epsilon = \sqrt{|\triangle|}$ which ensures $|\triangle|/\epsilon \to 0$. Thus, the above error terms go to zero as $|\triangle| \to 0$. By Lemma 3.3.3, S_f converges to u_f in L^2.

When $u_f \in W^{1,\infty}(\Omega)$, we have $err_\epsilon \leq C|u_f|_{W^{1,\infty}(\Omega)} \cdot \epsilon$ and $err(|\triangle|, \epsilon) \leq C\sqrt{|\triangle|}|u_f|_{W^{1,\infty}(\Omega)}$ as we trivially have $|u_f|_{W^{1,1}(\Omega)} \leq C|u_f|_{W^{1,\infty}(\Omega)}$ with positive constant C dependent only on A_Ω. These complete the proof. ■

3.4 A Fixed Point Algorithm and its Convergence

Denote $\{\phi_i\}_{i=1}^N$ the basis of of the spline space $S_d^r(\Omega)$. The following iterations will be used to approximate S_f.

Algorithm 3.4.1 *Given $u^{(k)}$, we find $u^{(k+1)} \in S_d^r(\triangle)$ such that*

$$\int_\Omega \frac{\nabla u^{(k+1)} \cdot \nabla \phi_j}{\sqrt{1+|\nabla u^{(k)}|^2}} dx + \frac{1}{\lambda A_\Omega} \int_\Omega u^{(k+1)} \phi_j dx = \frac{1}{\lambda A_\Omega} \int_\Omega f \phi_j dx, \quad \text{for all } j = 1, ..., n. \quad (3.42)$$

We first show that the above iteration is well defined. Since $u^{(k+1)} \in S_d^r(\triangle)$, it can be written as $u^{(k+1)} = \sum_i^n c_i^{(k+1)} \phi_i$. Plugging it in (3.42), we have

$$\sum_i^n c_i^{(k+1)} \left(\int_\Omega \frac{\nabla \phi_i \cdot \nabla \phi_j}{\sqrt{1+|\nabla u^{(k)}|^2}} dx + \frac{1}{\lambda A_\Omega} \int_\Omega \phi_i \phi_j dx \right) = \frac{1}{\lambda A_\Omega} \int_\Omega f \phi_j dx, \quad j = 1, ..., n. \quad (3.43)$$

Denote by

$$\begin{aligned} D^{(k)} &:= (d_{i,j}^{(k)})_{N\times N} \text{ with } d_{i,j}^{(k)} = \lambda \int_\Omega \frac{\nabla \phi_i \cdot \nabla \phi_j}{\sqrt{1+|\nabla u^{(k)}|^2}} dx, \\ M &:= (m_{i,j})_{N\times N} \text{ with } m_{i,j} = \frac{1}{A_\Omega} \int_\Omega \phi_i \phi_j dx, \\ \mathbf{v} &:= (v_j, j = 1, \cdots, N) \text{ with } v_j = \frac{1}{A_\Omega} \int_\Omega f \phi_j dx. \end{aligned}$$

To solve equation of (3.43) is equivalent to solving the equation

$$(D^{(k)} + M)\mathbf{c}^{(k+1)} = \mathbf{v}, \quad (3.44)$$

where $\mathbf{c}^{(k+1)} = [c_1^{(k+1)}, c_2^{(k+1)}, ..., c_n^{(k+1)}]$. Furthermore, if imposing the smoothness conditions $H\mathbf{c}^{(k+1)} = 0$ in Theorem 2.1.2, we solve the following linear system

$$\begin{pmatrix} H' & D^{(k)} + M \\ 0 & H \end{pmatrix} \begin{pmatrix} \alpha \\ \mathbf{c}^{(k+1)} \end{pmatrix} = \begin{pmatrix} \mathbf{v} \\ 0 \end{pmatrix}. \quad (3.45)$$

Lemma 3.4.1 *(3.44) has a unique solution $\mathbf{c}^{(k+1)}$.*

Proof. It is easy to prove $D^{(k)}$ is semi-positive definite and M is positive definite because for any nonzero $\mathbf{c} = [c_1, c_2, ..., c_n]$,

$$\mathbf{c}^\top D^{(k)} \mathbf{c} = \lambda \int_\Omega \frac{|\sum_i^n c_i \nabla \phi_i|^2}{\sqrt{1+|\nabla u^{(k)}|^2}} dx \geq 0,$$

and

$$\mathbf{c}^\top \ M \ \mathbf{c} = \frac{1}{A_\Omega} \int_\Omega |\sum_i^n c_i \phi_i|^2 dx > 0.$$

Moreover $(D^{(k)} + M)$ is also positive definite, and consequently invertible. So (3.44) has a unique solution. ■

Lemma 3.4.2 *$\{u^{(k)}, k = 1, 2, \cdots\}$ are bounded in L^2 by $\|f\|_{L^2(\Omega)}$ for all $k > 0$, i.e.,*

$$\|u^{(k+1)}\|_{L^2(\Omega)} \leq \|f\|_{L^2(\Omega)}. \tag{3.46}$$

Also, there exists a positive constant C dependent on β and $|\triangle|$ such that

$$\|\nabla u^{(k+1)}\|_{L^2(\Omega)} \leq C\|f\|_{L^2(\Omega)}.$$

Proof. Multiply $(\mathbf{c}^{(k+1)})^\top$ to both sides of (3.44) to get

$$\lambda \int_\Omega \frac{|\nabla u^{(k+1)}|^2}{\sqrt{1 + |\nabla u^{(k)}|^2}} dx + \frac{1}{A_\Omega} \int_\Omega |u^{(k+1)}|^2 dx = \frac{1}{A_\Omega} \int_\Omega f u^{(k+1)} dx. \tag{3.47}$$

Since the first term of (3.47) is nonnegative, we have

$$\|u^{(k+1)}\|^2_{L^2(\Omega)} \leq \frac{1}{A_\Omega} \int_\Omega f u^{(k+1)} \leq \|f\|_{L^2(\Omega)} \|u^{(k+1)}\|_{L^2(\Omega)} \tag{3.48}$$

which yields

$$\|u^{(k+1)}\|_{L^2(\Omega)} \leq \|f\|_{L^2(\Omega)},$$

and hence $\|u^{(k+1)}\|_{L^2(\Omega)}$ is bounded if $f \in L^2(\Omega)$.

Let λ_{min} is the smallest eigenvalue of M, then $\lambda_{min} > 0$ by the positivity of M. Since

$$\|u^{(k)}\|^2_{L^2(\Omega)} = (\mathbf{c}^{(k)})^\top M \mathbf{c}^{(k)},$$

then

$$\lambda_{min} \|\mathbf{c}^{(k)}\|^2_{l^2} \leq \|u^{(k)}\|^2_{L^2(\Omega)} \leq \|f\|^2_{L^2(\Omega)},$$

which implies

$$\|\mathbf{c}^{(k)}\|^2_{l^2} \leq \frac{1}{\lambda_{min}} \|f\|^2_{L^2(\Omega)}$$

Consider the matrix $P = (p_{i,j})_{n\times n}$, where $p_{i,j} = \int_\Omega \nabla\phi_i \cdot \nabla\phi_j dx$. Then $\|\nabla u^{(k)}\|^2_{L^2(\Omega)} = (\mathbf{c}^{(k)})^\top P \mathbf{c}^{(k)}$. It is easy to see that P is also semi-positive definite . Suppose π_{max} is the largest eigenvalue of P, then $\pi_{max} \geq 0$, and

$$\|\nabla u^{(k)}\|^2_{L^2(\Omega)} = (\mathbf{c}^{(k)})^\top P \mathbf{c}^{(k)} \leq \pi_{max} \|\mathbf{c}^{(k)}\|^2_{l^2} \leq \frac{\pi_{max}}{\lambda_{min}} \|f\|^2_{L^2(\Omega)}$$

or

$$\|\nabla u^{(k)}\|_{L^2(\Omega)} \leq \sqrt{\frac{\pi_{max}}{\lambda_{min}}}\|f\|_{L^2(\Omega)} \tag{3.49}$$

which finishes the proof. The second part of the results of Lemma 3.4.2 follows straightforwardly by using Markov's inequality in Theorem 2.1.5. ■

Next we need to show that the iterative algorithm above converges. We need the following inequality. Note that the proof of the inequality is different from the one in Lemma 3.3.3. The reason is that $u^{(k+1)}$ is not a minimizer of $E(u)$ in $S_d^r(\triangle)$. Thus the technique of the sub-differentiation can not be applied here. We have to give a different proof.

Lemma 3.4.3 *If $u^{(k+1)}$ is the solution of our Algorithm 3.4.1, then the following inequality holds*

$$\|u^{(k)} - u^{(k+1)}\|^2_{L^2(\Omega)} \leq 2\lambda A_\Omega (E(u^{(k)}) - E(u^{(k+1)})). \tag{3.50}$$

Proof. First of all we use (3.42) to have

$$\frac{1}{\lambda A_\Omega}\int_\Omega (f - u^{(k+1)})(u^{(k)} - u^{(k+1)})dx = \int_\Omega \frac{\nabla u^{(k)} \cdot \nabla u^{(k+1)}}{\sqrt{1+|\nabla u^{(k)}|^2}}dx - \int_\Omega \frac{|\nabla u^{(k+1)}|^2}{\sqrt{1+|\nabla u^{(k)}|^2}}dx$$

since $u^{(k)} - u^{(k+1)}$ is a linear combination of $\phi_j, j = 1, \cdots, n$. Then the following inequality follows.

$$\frac{1}{\lambda A_\Omega}\int_\Omega (f - u^{(k+1)})(u^{(k)} - u^{(k+1)})dx \leq \int_\Omega \frac{|\nabla u^{(k)}|^2}{2\sqrt{1+|\nabla u^{(k)}|^2}}dx - \int_\Omega \frac{|\nabla u^{(k+1)}|^2}{2\sqrt{1+|\nabla u^{(k)}|^2}}dx. \tag{3.51}$$

Now we are ready to prove (3.50). The difference between $E(u^{(k)})$ and $E(u^{(k+1)})$ is

$$\begin{aligned}
& E(u^{(k)}) - E(u^{(k+1)}) \\
= & \int_\Omega \sqrt{1+|\nabla u^{(k)}|} - \sqrt{1+|\nabla u^{(k+1)}|^2}dx + \frac{1}{2\lambda A_\Omega}\int_\Omega |u^{(k)} - f|^2 - |u^{(k+1)} - f|^2 dx \\
= & \int_\Omega \sqrt{1+|\nabla u^{(k)}|} - \sqrt{1+|\nabla u^{(k+1)}|^2}dx + \frac{1}{2\lambda A_\Omega}\int_\Omega (u^{(k)} - u^{(k+1)})(u^{(k)} + u^{(k+1)} - 2f)dx \\
= & \int_\Omega \sqrt{1+|\nabla u^{(k)}|} - \sqrt{1+|\nabla u^{(k+1)}|^2}dx + \int_\Omega \frac{1}{\lambda A_\Omega}(u^{(k+1)} - f)(u^{(k)} - u^{(k+1)}) \\
& + \frac{1}{2\lambda A_\Omega}\int_\Omega |u^{(k)} - u^{(k+1)}|^2 dx \\
\geq & = 0.
\end{aligned}$$

The last inequality holds because by applying (3.51), we have

$$\begin{aligned}
&\int_\Omega \sqrt{1+|\nabla u^{(k)}|} - \sqrt{1+|\nabla u^{(k+1)}|^2}dx + \frac{1}{\lambda A_\Omega}\int_\Omega (u^{(k+1)}-f)(u^{(k)}-u^{(k+1)}) \\
\geq\ & \int_\Omega \sqrt{1+|\nabla u^{(k)}|^2} - \sqrt{1+|\nabla u^{(k+1)}|^2}dx - \int_\Omega \frac{|\nabla u^{(k)}|^2}{2\sqrt{1+|\nabla u^{(k)}|^2}}dx + \int_\Omega \frac{|\nabla u^{(k+1)}|^2}{2\sqrt{1+|\nabla u^{(k)}|^2}}dx \\
=\ & \int_\Omega \frac{2+|\nabla u^{(k)}|^2+|\nabla u^{(k+1)}|^2}{2\sqrt{1+|\nabla u^{(k)}|^2}} - \sqrt{1+|\nabla u^{(k+1)}|^2}dx \\
\geq\ & \int_\Omega \frac{\sqrt{1+|\nabla u^{(k)}|^2}\sqrt{1+|\nabla u^{(k+1)}|^2}}{\sqrt{1+|\nabla u^{(k)}|^2}} - \sqrt{1+|\nabla u^{(k+1)}|^2}dx = 0.
\end{aligned}$$

We have thus established the proof. ■

We are now ready to show the convergence of $u^{(k)}$ to the minimizer S_f.

Theorem 3.4.1 *The sequence $\{u^{(k)}, k = 1, 2, \cdots, \}$ obtained from Algorithm 3.4.1 converges to the true minimizer S_f.*

Proof. By Lemma 3.4.2, the sequence $\{u^{(k)}, k = 1, \cdots, \}$ is bounded. Actually, we know $\|u^{(k)}\|_{L^2(\Omega)} \leq \|f\|_{L^2(\Omega)}$. So there must be a convergent subsequence $\{u^{(n_j)}\}$. Suppose $u^{(n_j)} \to \bar{u}$. By Lemma 3.4.3, we see $\{E(u^{(k)}), k = 1, 2, \cdots, \}$ is a decreasing sequence and bounded below, so $\{E(u^{(k)})\}$ is convergent as well as any subsequence of it. We use Lemma 3.4.3 to have

$$\begin{aligned}
\|u^{(n_j+1)} - \bar{u}\|^2_{L^2(\Omega)} &\leq 2\|u^{(n_j+1)} - u^{(n_j)}\|^2_{L^2(\Omega)} + 2\|u^{(n_j)} - \bar{u}\|^2_{L^2(\Omega)} \\
&\leq 4\lambda A_\Omega (E(u^{(n_j)}) - E(u^{(n_j+1)})) + 2\|u^{(n_j)} - \bar{u}\|^2_{L^2(\Omega)} \to 0,
\end{aligned}$$

which implies $u^{(n_j+1)} \to \bar{u}$.

According to Markov's inequality, i.e. Theorem 2.1.5, we have

$$\int_\Omega |\nabla u^{(n_j)} - \nabla \bar{u}|^2 dx \leq \frac{\beta^2}{|\triangle|^2}\int_\Omega |u^{(n_j)} - \bar{u}|^2 dx.$$

It follows from the convergence of $u^{(n_j)} \to \bar{u}$ that $\nabla u^{(n_j)} \to \nabla \bar{u}$ in L^2 as well. Replacing $u^{(n_j)}$ by $u^{(n_j+1)}$ above, we have $\nabla u^{(n_j+1)} \to \nabla \bar{u}$ too by the convergence of $u^{(n_j+1)} \to \bar{u}$. As $u^{(n_j)}$, $u^{(n_j+1)}$ and $\bar{u}$ are spline functions in $S^r_d(\triangle)$. The convergence of $u^{(n_j)}$ and $u^{(n_j+1)}$ to

$\bar{u}$, respectively implies the coefficients of $u^{(n_j)}$ and $u^{(n_j+1)}$ in terms of the basis functions $\phi_j, j = 1, \cdots, N$ are convergent to the coefficients of $\bar{u}$, respectively.

Since $u^{(n_j+1)}$ solves the equations (3.42), we have

$$\int_\Omega \frac{\nabla u^{(n_j+1)} \cdot \nabla \phi_j}{\sqrt{1+|\nabla u^{(n_j)}|^2}} dx = \int_\Omega \frac{f - u^{(n_j+1)}}{\lambda A_\Omega} \phi_i dx$$

for all $\phi_i, i = 1, \cdots, N$. Letting $j \to \infty$, we obtain

$$\int_\Omega \frac{\nabla \bar{u} \cdot \nabla \phi_i}{\sqrt{1+|\nabla \bar{u}|^2}} dx = \int_\Omega \frac{f - \bar{u}}{\lambda A_\Omega} \phi_i dx$$

for all $i = 1, \cdots, N$. That is, $\bar{u}$ is a local minimizer. Since the functional is convex, a local minimizer is the global minimizer and hence, $\bar{u} = S_f$. Thus all convergent subsequences of $\{u^{(k)}\}$ converge to S_f, which implies $\{u^{(k)}\}$ itself converges to S_f. ■

3.5 Numerical Results

We have implemented our bivariate spline approach in MATLAB and performed several image enhancement experiments: image inpainting, image resizing and wrinkle removal. We shall briefly explain how to triangulate a polygonal domain and how to use a bivariate spline space. After these, we report our numerical results.

First of all, let us briefly explain how to choose a polygonal domain. For image inpainting and wrinkle reduction, we simply choose a polygonal domain of interest by hand. For image resizing, the polygonal domain is the image domain. For image denoising, we use the Chan-Vese active contour method proposed in [16] to choose polygonal domains. We will explain this method in detail in Chapter 4.

We mainly use the standard Delaunay triangulation algorithm to find a triangulation of a polygon. A key ingredient is to choose boundary points as equally-spaced as possible and points inside the polygon as evenly-distributed as possible. If some points are clustered near the boundary of the polygon, we have to thin a few point off. Thus, the triangulation is β quasi-uniform. In addition, we check the triangles from the Delaunay triangulation

method to see which ones are outside of the domain and delete such triangles. Triangles in triangulation from our MATLAB code are almost uniform in size and in area. In our computation we mainly use bivariate spline spaces $S_3^1(\Omega)$, $S_5^1(\Omega)$ and $S_7^1(\Omega)$.

Let us explain how to implement the bivariate splines as locally supported basis functions are hard to construct. We mainly use the ideas in [8]. That is, fixed $r \geq 0$ and $d > 0$, we express the polynomial piece of each spline function s over a triangle $T \in \triangle$ in B-form. That is, $s = \sum_{T\in\triangle} \sum_{i+j+k=d} c_{T,ijk} B_{T,ijk}$ is expressed in a discontinuous function over $\triangle$, i.e., $s \in S_d^{-1}(\Omega)$. Then we add smoothness conditions including continuous conditions as side constrains, i.e., let H be the smoothness matrix such that $H\mathbf{c} = 0$ for $\mathbf{c} = (c_{T,ijk}, T \in \triangle, i+j+k = d)^T$ if and only if $s \in S_d^r(\triangle)$. See [38] and [8] for B-form and constructing H. We iteratively solve S_f in the following system of nonlinear equations:

$$\int_\Omega \frac{\nabla S_f \cdot \nabla \phi_m}{\sqrt{1+|\nabla S_f|^2}} dx + \frac{1}{\lambda}\frac{1}{A_\Omega}\int_\Omega (S_f - f)\phi_m dx = 0 \tag{3.52}$$

subject to the smoothness constrains $S_f \in S_d^r(\triangle)$, where ϕ_m is one of discontinuous functions $B_{T,ijk}$ which is defined only on T and $i+j+k = d$. This system can be solved by using the iterative algorithm in [9].

Example 3.5.1 (Image Inpainting) *In Fig. 3.1, we show an example of the application of our minimal surface area fitting spline in image inpainting. A corrupted image, the recovered image and the triangulation are shown. Assume that we can find the locations of corrupted parts, we use the known image values to recover the lost image data values. Fig 3.2 and Fig 3.3 demonstrate two examples of our approach to recover specified regions of corrupted images which have* 50% *lost and* 60% *data lost respectively. However, if there are a large number of triangles in our triangulation, such as the case in Fig.3.1, then the size of the linear system (3.45) is pretty large. The size of* $D^{(k)}$ *is* $R\binom{d+2}{2}$*-by-*$R\binom{d+2}{2}$*, where* R *is the number of triangles, and* d *is the degree of polynomial of the bivariate splines we use. This might cause the out-of-memory problem in some computers. To solve this problem, we use the domain decomposition technique developed in [39], which can transform the problem into solving a set of linear systems of small size.*

Figure 3.1: Example of inpainting by our fitting spline. We use the domain decomposition technique in our computation.

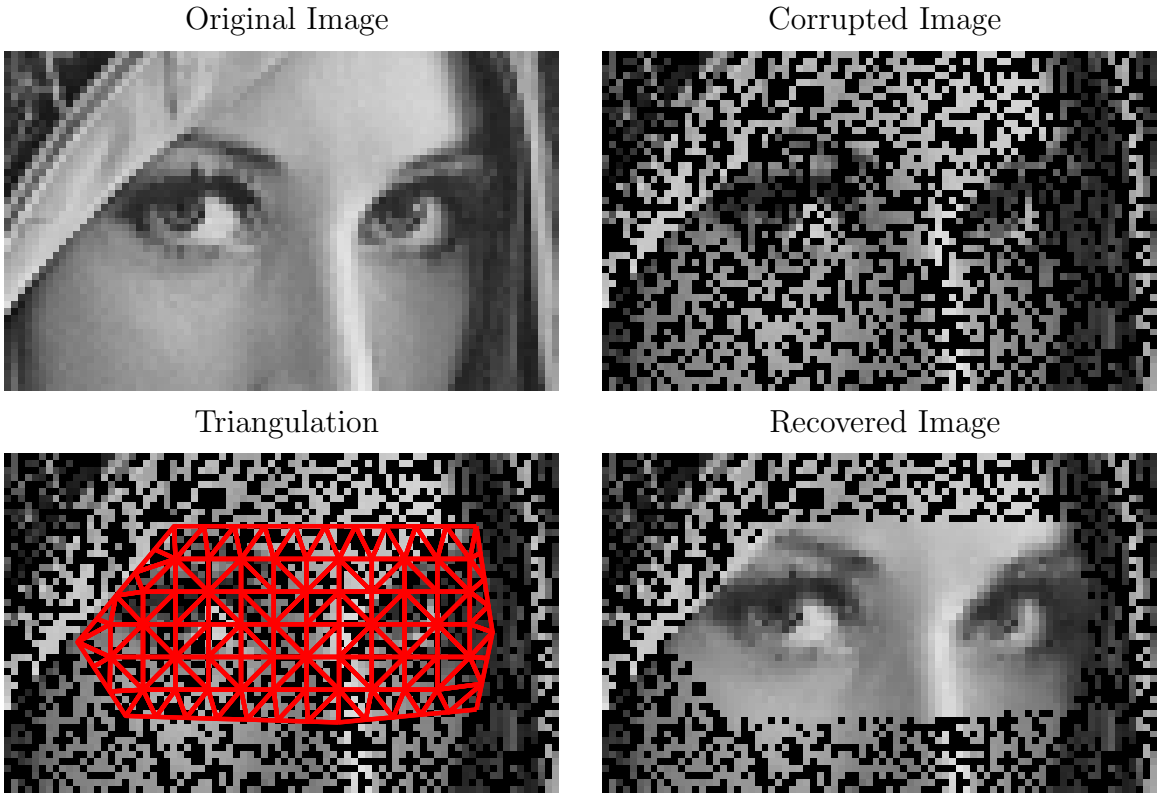

Figure 3.2: Example of inpainting by our fitting spline. A specified region of a 50% data-corrupted image is recovered.

Example 3.5.2 (Image Resizing) *Due to the accuracy of evaluation of spline functions, we can apply the minimum surface area fitting splines to image resizing. We compare our method to the bicubic and bilinear interpolation methods provided by MATLAB function "imresize". In Fig. 3.4, the two images showed in both column (not in actual size) are enlarged by 10. One can notice that compared to our approach, both the bicubic and the bilinear interpolation cause the Gibbs discontinuity on the edges, such as the edge of the hat of Laura. In Fig. 3.5, Fig. 3.6 and Fig. 3.6, our bivariate spline method is compared to the bicubic interpolation and bilinear interpolation method on the effect of enlarging non-rectangular region. To interpolate values on the boundary, the bilinear and bicubic interpolation methods use a simple symmetric extension to extend the boundary. However on non-rectangular regions,*

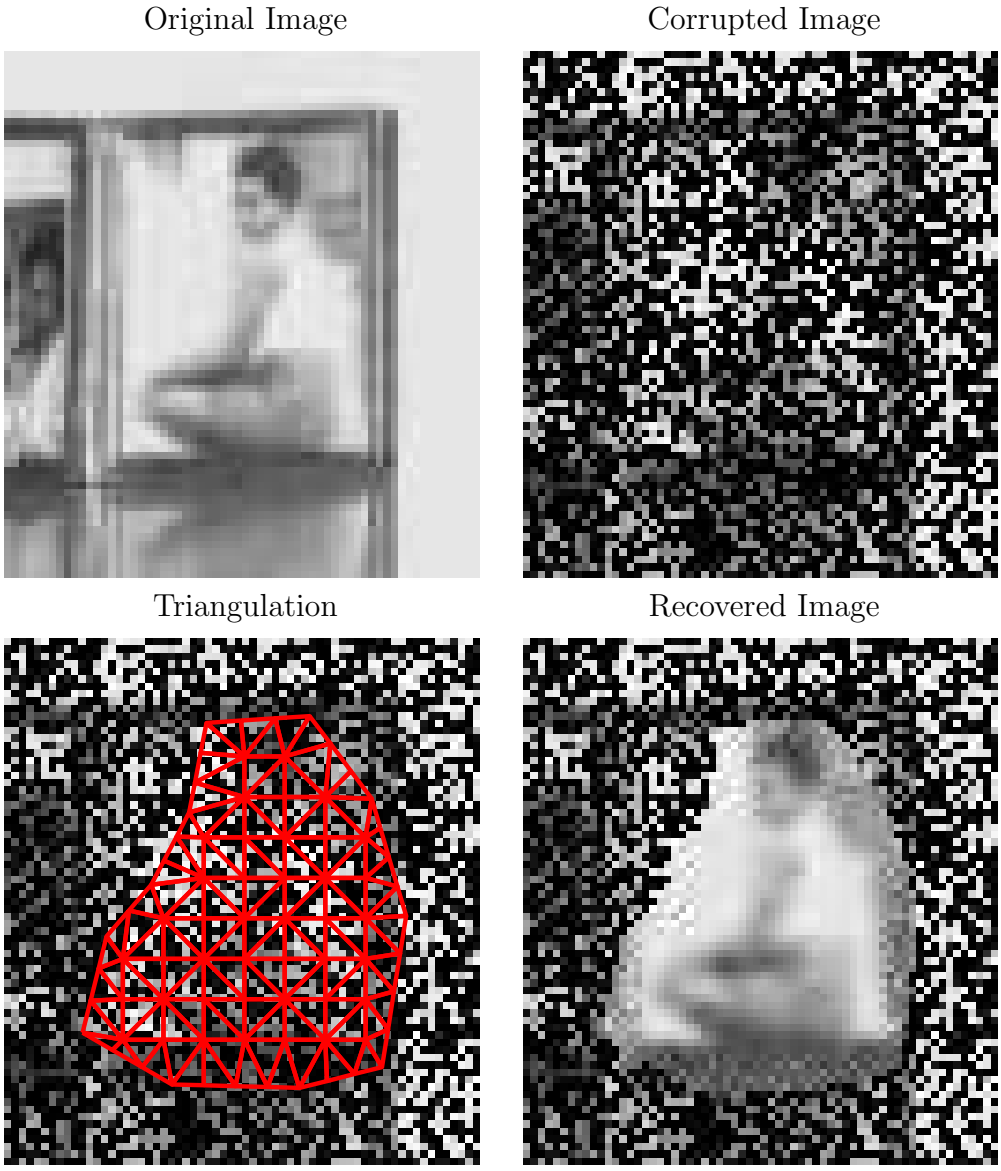

Figure 3.3: Example of inpainting by our fitting spline. A specified region of a 60% data-corrupted image is recovered.

this symmetric extension does not work. In this case, as shown in the examples, the bilinear and bicubic interpolation method can not interpolate values on the boundary. This problem is more obvious in the bicubic interpolation than the bilinear interpolation, because as a higher order interpolation, the bicubic interpolation requires a longer extension. On the other hand

we can avoid this problem by using our minimal surface fitting splines due to their capability to approximate functions on a flexible polygon domain, and the fact that the Euler-Lagrange equation we solve has no boundary condition.

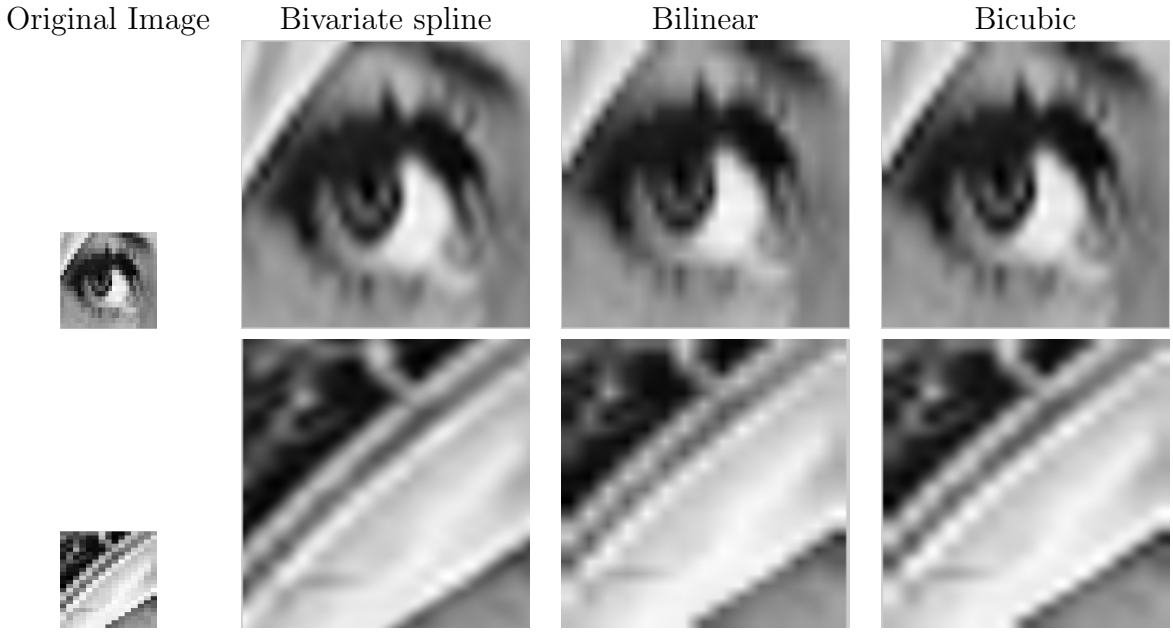

Figure 3.4: Images are scaled by 10 times by using our spline method, bilinear and bicubic interpolation respectively.

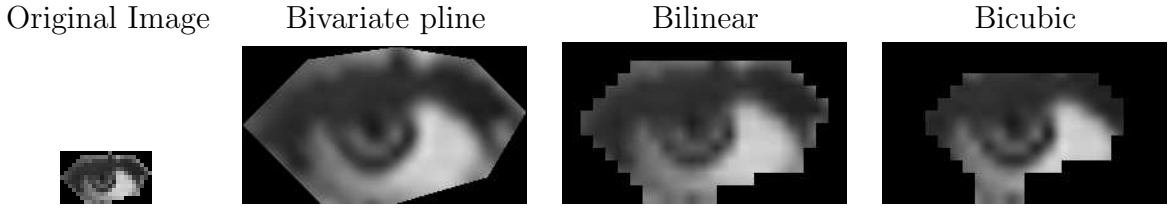

Figure 3.5: Images are enlarged by 10 times by using our spline method, Bicubic and Bilinear interpolation respectively.

Example 3.5.3 (Wrinkle Removal) *Finally we present a wrinkle removal experiment. We are interested in reducing some wrinkles from a human face. We identify a couple of regions of interest near eyes and cheeks and apply our bivariate spline approach over each region. In Fig. 3.8, we reduce some wrinkles around the lady's eyes. The logo "cobis" at the top left corner is also removed. The modified locations and the corresponding triangulation*

Figure 3.6: Images are enlarged by 10 times by using our spline method, bilinear and bicubic interpolation respectively.

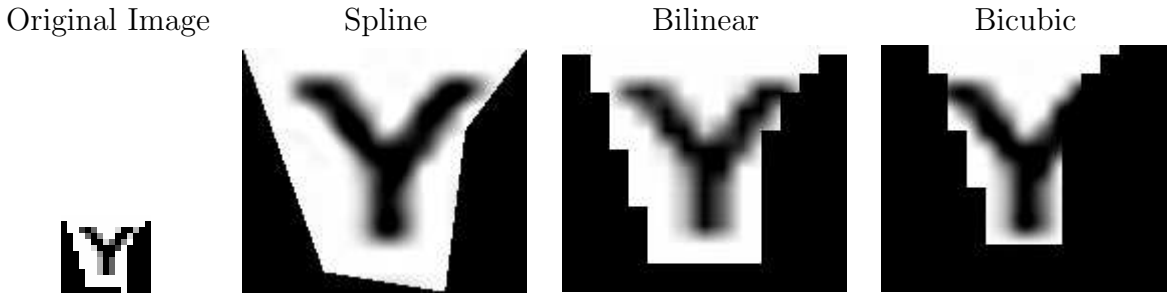

Figure 3.7: Images are scaled by 10 times by using our spline method, bilinear and bicubic interpolation respectively.

are also shown. In Fig. 3.9, two images are shown. The human face on the right is clearly enhanced in the areas near eyes and cheeks. The enlarged pictures of the 4 positions where wrinkles are removed are shown in Fig. 3.10.

Example 3.5.4 *The convergence of our numerical algorithm and the effectiveness of our approach on image denoising are examined in Chapter 4.*

(a):Original Image

(b):Triangulation

(c):Wrinkle-removed Image

Figure 3.8: Wrinkles around the eyes and the logo “corbis” are removed.

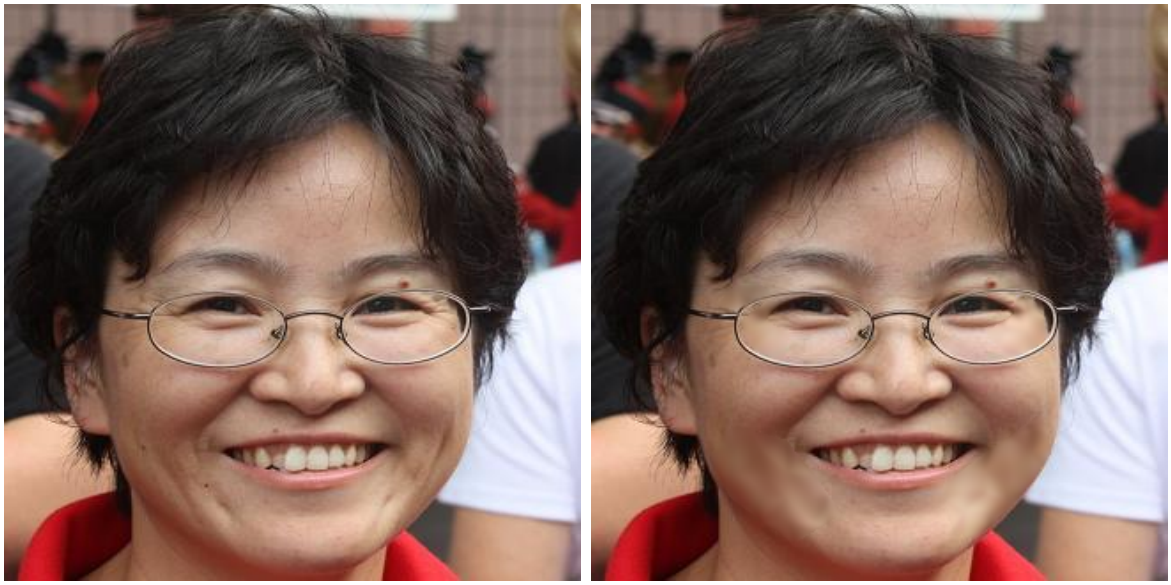

Figure 3.9: A face with wrinkles on the left and the face with reduced wrinkles on the right. We use $d = 3$ and $r = 1$ in our computation.

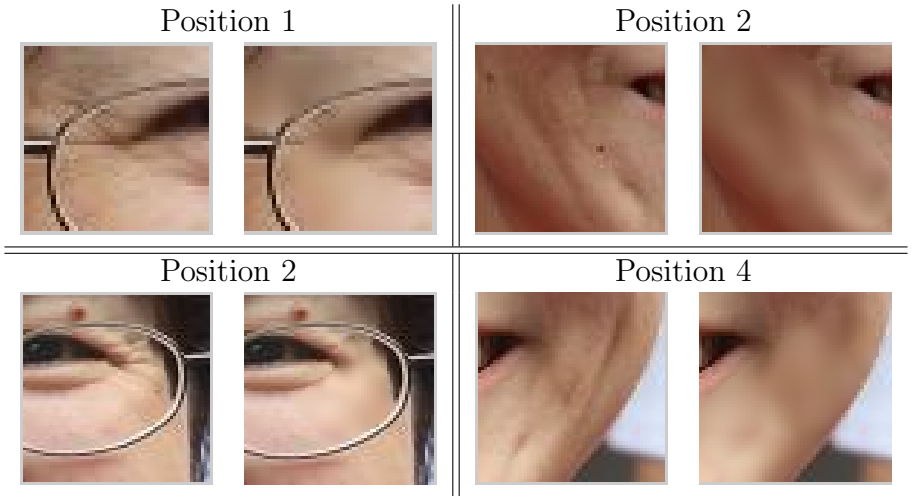

Figure 3.10: Enlarged details of 4 positions where wrinkles are removed.

Chapter 4

Bivariate Spline Approximation to a TV-L^p Model

Recall that the ROF model can be given in the following equivalent form:

$$\min_{u\in \mathrm{BV}(\Omega)} |u|_{\mathrm{BV}(\Omega)} + \frac{1}{2\lambda}\int_\Omega |u-f|^2 dx. \tag{4.1}$$

Many extensions of the ROF model can be found in the literature [2], [3], and [4], [41], [42], [15], [58], [59], and [23]. For example, the following TV-L^1 model is closely related to the original ROF model:

$$\min_{u\in \mathrm{BV}(\Omega)} |u|_{\mathrm{BV}(\Omega)} + \frac{1}{\lambda}\int_\Omega |u-f| dx. \tag{4.2}$$

The above TV-L^1 model was studied in the context of image denoising and deblurring by many researchers as mentioned in the literature above. As the energy functional

$$\mathcal{E}(u) = |u|_{\mathrm{BV}(\Omega)} + \frac{1}{\lambda}\int_\Omega |u-f| dx$$

is convex lower semi-continuous and BV-coercive, it is easy to see the existence of minimizers. However, due the fact that the energy functional is not strictly convex, the minimizers are not unique. Many results related to the set of minimizers have been obtained. For example, properties of maximum principle, monotonicity, commutation with constants, affine invariance and contract invariance are studied. See [15], [59], and [23].

In addition to the TV-L^1 model, the following TV-L^p model has been proposed in the literature:

$$\min_{u\in \mathrm{BV}(\Omega)} |u|_{\mathrm{BV}(\Omega)} + \frac{1}{p\lambda}\int_\Omega |u-f|^p dx \tag{4.3}$$

for $p \geq 1$. Besides $p = 1$ and $p = 2$, it is not clear in the literature that if this TV-L^p model makes sense. We shall present a statistical explanation together with numerical examples to

show when the noise of an image is from a random variable of p-exponential distribution with $p \neq 2$, the TV-L^p model will be useful. Thus we shall discuss some properties of the minimizers of the TV-L^p model. To compute the minimizers, we shall use the following (ϵ, η)-version of TV-L^p model for $p \geq 1$.

$$\min_{u \in \mathrm{BV}(\Omega)} \int_\Omega \sqrt{\epsilon + |\nabla u|^2} dx + \frac{1}{p\lambda} \int_\Omega (\eta + |u - f|^2)^{p/2} dx. \tag{4.4}$$

for $\epsilon, \eta > 0$.

It is shown that when $\epsilon \to 0$,

$$J_\epsilon(u) := \int_\Omega \sqrt{\epsilon + |\nabla u|^2} dx.$$

converges to $|u|_{\mathrm{BV}(\Omega)}$ (cf. [1]). Similarly when $\eta \to 0$, the second term in the minimization (4.4) converges to $\|f - u\|^p_{L^p(\Omega)}$. Hence, the (ϵ, η) version of TV-L^p model gives an approximation of the standard TV-L^p model (4.3).

When $\epsilon, \eta > 0$, the energy functional $E_{\epsilon,\eta}$ associated with (4.4) is strictly convex and hence, the minimizer $u_f := u_{f,\epsilon,\eta}$ is unique in $\mathrm{BV}(\Omega)$. We shall show that the minimizer of the (ϵ, η)-version of the TV-L^p model has the stable and continuous properties. It is clear that we can find the minimizer of the TV-L^p model in a finite dimensional space, e.g. finite element space, or more generally bivariate spline space, $S^r_d(\triangle)$. The key point is that the minimizer in the finite dimensional space converge to the minimizer in the $\mathrm{BV}(\Omega)$. The main result in this chapter is the following

Theorem 4.0.1 *Fix $p \geq 1$ $\eta > 0$ and $\epsilon > 0$. Suppose f is bounded and u_f is the minimizer of (4.4). $S^r_d(\triangle)$ is a bivariate spline space of a degree $d \geq 3r + 2$. Let S_f be the minimizer of*

$$\min_{u \in S^r_d(\triangle)} \int_\Omega \sqrt{\epsilon + |\nabla u|^2} dx + \frac{1}{p\lambda} \int_\Omega |u - f|^p dx \tag{4.5}$$

in $S^r_d(\triangle)$. Then

$$\|S_f - u_f\|_{L^2(\Omega)} \leq C\lambda\sqrt{|\triangle|}, \tag{4.6}$$

where C is a positive constant independent of $|\triangle|$, the size of triangulation $\triangle$.

This study leads to a numerical approach to compute an approximation of the minimizer of the (ϵ, η)-version of the TV-L^p model for $p \geq 1$. An iterative algorithm will be derived to solve the associated nonlinear problem in the bivariate spline space. We shall show that the numerical algorithm converges. Several numerical examples will be shown to demonstrate the effectiveness and convenience for image denoising.

This chapter is organized as follows. First, we shall give a statistic explanation of the TV-L^p model in §4.1. We then study the properties of the minimizer in §4.2. With this preparation, we discuss how to approximate the minimizer of the TV-L^p model using spline spaces in §4.3 and present an iterative algorithm and show that the iterative algorithm is convergent in §5. Finally we should demonstrate in our numerical examples that the TV-L^p model is indeed useful to denoise images which contain some non-Gaussian noise.

4.1 A Statistical Explanation of the TV-L^p Model

Recall that the classic Rudin-Osher-Fetami (ROF) model for image denoising is the following minimization:

$$\min_{u \in BV(\Omega)} \{|u|_{\mathrm{BV}(\Omega)}, \text{ subject to } \mathrm{var}(u - f) \leq \sigma_0^2\} \tag{4.7}$$

where $f = u_0 + \xi$ is a given noised image, u_0 is the original image, and $\mathrm{var}(\cdot)$ stands for the standard variance. The minimizer u is supposed to be the clean image which is expected to be close to the original image u_0. Thus it is expected that $u - f$ is very close to ξ, i.e.,

$$u - f \simeq \xi. \tag{4.8}$$

In the discrete setting, suppose that $f = \{f_i, \cdots, f_n\}$ is a given image with $f_i = u_i + \xi_i$, where u_i are pixel values of grayscale and ξ_i are noise values. Suppose that ξ_i are independent identically distributed (i.i.d.) random variable whose mean is zero and variance σ^2. A standard method to estimate σ^2 is by using the sample deviation s^2 defined by

$$s^2 = \frac{1}{n-1} \sum_{i=1}^{n} (\xi_i - \bar{\xi})^2,$$

where $\bar{\xi} = \frac{1}{n}\sum_{i=1}^{n}\xi_i$. It is known that s^2 is an unbiased estimator. That is, $E(s^2) = \sigma^2$. Note that $\bar{\xi} \approx 0$. Thus, by (4.8),

$$s^2 \simeq \frac{1}{n-1}\sum_{i=1}^{n}(\xi_i)^2 = \frac{1}{n-1}\sum_{i=1}^{n}(u_i - f_i)^2 \simeq \frac{1}{A_\Omega}\int_\Omega |u-f|^2 dx$$

where A_Ω stands for the area of Ω. Hence, the ROF model can be rewritten as

$$\min_{u\in BV(\Omega)}\{|u|_{\mathrm{BV}(\Omega)},\ \text{subject to } \frac{1}{A_\Omega}\textstyle\int_\Omega |u-f|^2 dx \le \sigma_0^2\}. \tag{4.9}$$

By the Chambolle-Lions theorem [13], the minimization is equivalent to the following unconstrained problem

$$\min_{u\in BV(\Omega)} |u|_{\mathrm{BV}(\Omega)} + \frac{1}{2\lambda}\int_\Omega |u-f|^2 dx \tag{4.10}$$

for some λ dependent on σ_0 if $\sigma_0 \in (0, \frac{1}{A_\Omega}\int_\Omega |u_0|^2 dx]$.

Furthermore, suppose that we have an *a priori* knowledge of the distribution of ξ_i. For example, ξ_i's are independent identically distributed random (i.i.d.) variables with probability density function:

$$g_p(x) = \frac{C_p}{b}\exp\left(-\left|\frac{x}{b}\right|^p\right), p \ge 1 \tag{4.11}$$

with $C_p = \dfrac{p}{2\Gamma(1/p)}$ and b being an fixed parameter. Such a distribution is called the Laplacian distribution, or p-exponential distribution. It can be calculated that the mean $E(\xi_i) = 0$ and the variance

$$\sigma^2 = \mathrm{var}(\xi_i) = \frac{\Gamma(3/p)}{\Gamma(1/p)}b^2. \tag{4.12}$$

One of the standard methods to estimate the parameter b in statistic is the maximum likelihood method. Let us use the discrete setting to explain it again. For the given image $f = \{f_1, \cdots, f_n\}$, with the random variables $\xi_i, i = 1, \cdots, n$ which are i.i.d. with probability density function g_p, we assume that the event $\xi_i, i = 1, \cdots, n$ happens when the joint probability

$$L(\xi_1, \xi_2, \cdots, \xi_{n-1}, \xi_n |\, b) = \left(\frac{C_p}{b}\right)^n \exp\left(-\frac{\sum_i^n |\xi_i|^p}{b^p}\right)$$

is maximized as a function of b. Under this assumption, we get an estimation of the parameter b. To compute the maximizer it is equivalent to find the maximizer of the logarithm of the

above maximum likelihood function

$$\log L = n\log(C_p) - n\log(b) - \frac{\sum_i^n |\xi_i|^p}{b^p}.$$

We solve

$$\frac{d\log(L)}{db} = -\frac{n}{b} + \frac{p\sum_i^n |\xi_i|^p}{b^{(p+1)}} = 0.$$

It follows that the maximum likelihood estimator $\hat{b}$ for b is $\hat{b} = \left(\frac{p}{n}\sum_{i=1}^{n} |\xi_i|^p\right)^{1/p}$.

Therefore, by (4.12) and (4.8), when $n \to \infty$ the variance

$$\begin{aligned} \mathrm{var}(u-f) &= \sigma^2 = \frac{\Gamma(3/p)}{\Gamma(1/p)} b^2 \simeq \frac{\Gamma(3/p)}{\Gamma(1/p)} \left(\frac{p}{n}\sum_{i}^{n} |\xi_i|^p\right)^{2/p} \\ &= \frac{\Gamma(3/p)}{\Gamma(1/p)} \left(\frac{p}{n}\sum_{i}^{n} |u_i - f_i|^p\right)^{2/p} \approx \frac{\Gamma(3/p)}{\Gamma(1/p)} \left(\frac{p}{A_\Omega}\int_\Omega |u-f|^p\right)^{2/p}. \end{aligned}$$

The ROF model in this case is

$$\min_{u\in BV(\Omega)} \{|u|_{\mathrm{BV}(\Omega)}, \text{ subject to } \frac{\Gamma(3/p)}{\Gamma(1/p)} \left(\frac{p}{A_\Omega}\int_\Omega |u-f|^p\right)^{2/p} \le \sigma_0^2\} \tag{4.13}$$

Similar to the proof of the Chambolle-Lions theorem [13], the minimization is equivalent to the following

$$\min_{u\in BV(\Omega)} |u|_{\mathrm{BV}(\Omega)} + \frac{p}{2\lambda}\left(\int_\Omega |u-f|^p\right)^{2/p} \tag{4.14}$$

for some λ dependent on σ_0.

Lemma 4.1.1 *The estimate $\widehat{b^p} := \frac{p}{n}\sum_i^n |\xi_i|^p$ is an unbiased estimator for b^p. However, when $p<2$, $\widehat{b^2} = \left(\frac{p}{n}\sum_i^n |\xi_i|^p\right)^{2/p}$ is a biased estimator of b^2 and hence the $\widehat{var}(u-f) := \frac{\Gamma(3/p)}{\Gamma(1/p)}\widehat{b^2}$ is a biased estimator of $var(u-f)$.*

Proof. Since ξ_i's are i.i.d., by using integration by parts,

$$\begin{aligned} E(\widehat{b^p}) &= E\left(\frac{p}{n}\sum_i^n |\xi_i|^p\right) = pE(|\xi_1|^p) = 2pC_p\int_0^\infty \frac{|x|^p}{b}\exp\left(-\left|\frac{x}{b}\right|^p\right)dx \\ &= 2C_p b^p p\int_0^\infty y^p\exp(-y^p)dy = b^p. \end{aligned}$$

On the other hand, as $y = x^{2/p}$ is a strict convex function when $p < 2$, by Jensen's inequality,

$$E(\widehat{b^2}) = E((\widehat{b^p})^{2/p}) > (E(\widehat{b^p}))^{2/p} = (b^p)^{2/p} = b^2.$$

That is, $\widehat{b^2}$ is a biased estimator of b^2. Since $\mathrm{var}(u-f) = \dfrac{\Gamma(3/p)}{\Gamma(1/p)} b^2$, $\widehat{\mathrm{var}}(u-f)$ is also a biased estimator of $\mathrm{var}(u-f)$. ■

Next let us point out that $\widehat{b^p}$ is a sufficient statistic in the sense that it summarizes all relevant information the entire random sample can provide about b^p.

Lemma 4.1.2 *The estimator $\widehat{b^p}$ in Lemma 4.1.1 is a sufficient estimator of b^p.*

Proof. Let $u = \sum_i^n |\xi_i|^p$ be a random variable. Then the likelihood function of b is

$$L(\xi_1, ..., \xi_n | b) = \left(\frac{C_p}{b}\right)^n \exp\left(-\frac{u}{b^p}\right).$$

By Fisher-Neyman factorization theorem (cf. [55]), u is a sufficient statistic of b. Therefore $\widehat{b^p}$ is a sufficient estimator of b^p. ■

Finally, since $\widehat{b^p}$ is unbiased and sufficient, by the Rao-Blackwell theorem (cf. [55]), it is the minimum-variance unbiased estimator among all unbiased estimators of b^p. That is,

$$E((\widehat{b^p} - b^p)^2) = \min\{E((\beta - b^p)^2),\ \beta \text{ is an unbiased estimator of } b^p\}.$$

Such a minimizer is unique.

Therefore it is better to use the unbiased estimator $\widehat{b^p}$ rather than $\widehat{b^2}$ in the model. Therefore we consider the following model

$$\min_{u \in BV(\Omega)} |u|_{\mathrm{BV}(\Omega)} + \frac{1}{p\lambda} \int_\Omega |u - f|^p dx.$$

This justifies the TV-L^p.

We shall explain how to generate such a random variable ξ_i subject to the probability density function g_p in §4.5 to demonstrate the performance of TV-L^p model for p-exponential distributions.

4.2 Basic Properties of the (ϵ, η)-version TV-L^p Model

We first rewrite the (ϵ, η)-version of the TV-L^p model as follows:

$$\min_{u \in \mathrm{BV}(\Omega)} E_{\epsilon,\eta}(u) \tag{4.15}$$

with energy functional

$$E_{\epsilon,\eta}(u) := J_\epsilon(u) + \frac{1}{p\lambda} \int_\Omega (\eta + (u-f)^2)^{p/2}. \tag{4.16}$$

It is easy to see that when $p \geq 1$ and $\eta > 0$, the minimization functional $E_{\epsilon,\eta}$ is strictly convex , weakly lower semi-continuous, and BV-coercive. Therefore according to Theorem 2.3.7, there exists a unique minimizer $u_f \in \mathrm{BV}(\Omega)$ for any $\epsilon \geq 0$. Similarly, when $p > 1$, $\eta = 0$ and $\epsilon \geq 0$ or when $p = 1$, $\eta = 0$ and $\epsilon > 0$, $E_{\epsilon,\eta}$ is also strictly convex and lower semi-continuous. Thus, the minimizer u_f is unique. Only when $p = 1$ and $\eta = 0$ and $\epsilon = 0$, the functional $E_{\epsilon,\eta}(u)$ is not strictly convex. The minimizers are not unique for certain $\lambda > 0$. See the discussion in [15].

We shall further study other properties of u_f in this section. We begin with the following

Lemma 4.2.1 *Let u_f be the minimizer of problem (4.15) for input f. Consider the setting (p, ϵ, η) such that the minimizer u_f is unique. If f is bounded, then u_f is also bounded and*

$$\inf_{x \in \Omega} f(x) \leq u_f(x) \leq \sup_{x \in \Omega} f(x). \tag{4.17}$$

Proof. Let $\bar{u}_f$ be the truncation of u_f by $\sup_{x\in\Omega} f(x)$ and $\inf_{x\in\Omega} f(x)$, i.e.,

$$\bar{u}_f(y) = \begin{cases} \sup_{x\in\Omega} f(x), & \text{if } u_f(y) > \sup_{x\in\Omega} f(x) \\ u_f(y), & \text{if } \inf_{x\in\Omega} f(x) < u_f(y) < \sup_{x\in\Omega} f(x) \\ \inf_{x\in\Omega} f(x), & \text{if } \inf_{x\in\Omega} f(x) > u_f(y). \end{cases}$$

It is easy to verify if $u_f \in W^{1,1}(\Omega)$,

$$|\bar{u}_f(y) - f(y)| \leq |u_f(y) - f(y)|, \quad \forall y \in \Omega$$

and

$$\int_\Omega \sqrt{\epsilon + |\nabla \bar{u}_f|^2} \leq \int_\Omega \sqrt{\epsilon + |\nabla u_f|^2}.$$

According to Theorem 2.3.1, for $u_f \in \mathrm{BV}(\Omega)$, we can find a sequence $\{u_n\}$ in $W^{1,1}(\Omega)$ that converges to u_f in $L^1(\Omega)$ and

$$\lim_{n\to\infty} \int_\Omega \sqrt{\epsilon + |\nabla u_n|^2} = \int_\Omega \sqrt{\epsilon + |\nabla u_f|^2}.$$

We also have $\bar{u}_n$ converge to $\bar{u}_f$ in $L^1(\Omega)$ as n tends to infinity, where $\bar{u}_n$ is the truncation of u_n. Note that the functional $J_\epsilon(u)$ is lower semi-continuous (cf. [1]). Then

$$\begin{aligned}\int_\Omega \sqrt{\epsilon + |\nabla \bar{u}_f|^2} &\leq \varliminf_{n\to\infty} \int_\Omega \sqrt{\epsilon + |\nabla \bar{u}_n|^2} \\ &\leq \lim_{n\to\infty} \int_\Omega \sqrt{\epsilon + |\nabla u_n|^2} = \int_\Omega \sqrt{\epsilon + |\nabla u_f|^2}.\end{aligned}$$

Then

$$E_{\epsilon,\eta}(\bar{u}_f) \leq E_{\epsilon,\eta}(u_f)$$

which implies $\bar{u}_f = u_f$ because of the uniqueness of the solution. ■

With a similar argument we can show Lemma 4.2.1 also holds if u_f is the solution of the problem (4.4) in the spline space $S_d^r(\triangle)$. We next present the continuous property of the minimizers.

Theorem 4.2.1 *Fix $p \geq 1$ and $\eta > 0$. Suppose u_f is the solution of problem (4.4) with f bounded. Then for any bounded function u with* $\sup|u| \leq \sup|f|$,

$$\|u - u_f\|_{L^2(\Omega)} \leq C\lambda(E_{\epsilon,\eta}(u) - E_{\epsilon,\eta}(u_f))$$

for all $\epsilon \geq 0$, where C depends on $\sup|f|$ *and η. In particular, if S_f is the solution of the problem (4.4) in the spline space $S_d^r(\Omega)$, $d \geq 3r+2$, then according to Lemma 4.2.1,* $\sup|S_f| \leq \sup|f|$. *Therefore,*

$$\|S_f - u_f\|_{L^2(\Omega)} \leq C\lambda(E_{\epsilon,\eta}(S_f) - E_{\epsilon,\eta}(u_f)).$$

Proof. We first give the Euler-Lagrange equation for the minimizer u_f of (4.15)

$$\partial J_\epsilon(u) + \frac{1}{\lambda}\frac{u_f - f}{(\eta + (u_f - f)^2)^{1-p/2}} = 0 \tag{4.18}$$

Its equivalent inequality is

$$J_\epsilon(u) - J_\epsilon(u_f) \geq \left\langle -\frac{1}{\lambda}\frac{u_f - f}{(\eta + (u_f - f)^2)^{1-p/2}}, u - u_f \right\rangle, \tag{4.19}$$

where $\langle f, g\rangle$ is the standard inner product in $L^2(\Omega)$.

Following this calculation, we continue to compute the difference between two energies. Assume u_f is the minimizer for an input function f, u is a $L^p(\Omega)$ function

$$\begin{aligned} &E_{\epsilon,\eta}(u) - E_{\epsilon,\eta}(u_f) \\ =& \frac{1}{\lambda p}\int_\Omega (\eta + (u-f)^2)^{p/2} - (\eta + (u_f - f)^2)^{p/2}\, dx + J_\epsilon(u) - J_\epsilon(u_f). \end{aligned}$$

Using (4.19), we have

$$\begin{aligned} &E_{\epsilon,\eta}(u) - E_{\epsilon,\eta}(u_f) \\ \geq& \frac{1}{\lambda p}\int_\Omega (\eta + (u-f)^2)^{p/2} - (\eta + (u_f - f)^2)^{p/2}\, dx \\ &+ \left\langle -\frac{1}{\lambda p}\frac{u_f - f}{(\eta + (u_f - f)^2)^{1-p/2}}, u - u_f \right\rangle \end{aligned}$$

For simplicity we let

$$\phi_\eta(x) = \frac{1}{p}(\eta + x^2)^{p/2} \tag{4.20}$$

which is convex and infinitely differentiable for all x when $\eta > 0$. Then

$$\begin{aligned} &\lambda(E_{\epsilon,\eta}(u) - E_{\epsilon,\eta}(u_f)) \\ \geq& \int_\Omega \phi_\eta(u-f) - \phi_\eta(u_f - f)\, dx - \langle \phi_\eta'(u_f - f), u - u_f\rangle \\ =& \int_\Omega \phi_\eta''(\zeta)(u - u_f)^2\, dx \end{aligned} \tag{4.21}$$

where ζ is a function between $u - f$ and $u_f - f$. Direct calculation shows

$$\phi_\eta''(y) = \frac{(\eta + (p-1)y^2)}{(\eta + y^2)^{2-p/2}} \tag{4.22}$$

is a positive decreasing function which goes to zero when $y \to \infty$.

Lemma 4.2.1 and the assumption imply that both $u - f$ and $u_f - f$ are bounded by $2\sup|f|$ and hence,

$$\phi''(\zeta) \geq \frac{1}{C}$$

with C depending on $\sup|f|$ and η. Hence, the result follows. ■

With similar argument, we can show that

Theorem 4.2.2 *Fix $p \geq 1$ and $\eta > 0$. Suppose that f and g are bounded. Let u_f and u_g be the minimizers of TV-L^p model (4.15) associated with images f and g, respectively. Then*

$$\|u_f - u_g\|_{L^2(\Omega)} \leq C\|f - g\|_{L^2(\Omega)}$$

for all $\epsilon \geq 0$, where $C > 0$ depends on the bound of f and g as well as η.

Proof. Assume u_f is the minimizer for f and u_g is the minimizer for g, by the definition, we have

$$\langle \partial J_\epsilon(u_f), u_g - u_f \rangle \leq J(u_g) - J(u_f),$$
$$\langle \partial J_\epsilon(u_g), u_f - u_g \rangle \leq J(u_f) - J(u_g).$$

Adding these two inequalities, and using (4.18) we have

$$\langle \phi'_\eta(u_g - g) - \phi'_\eta(u_f - f), u_g - u_f \rangle \leq 0.$$

Note that

$$\phi'_\eta(u_g - g) - \phi'_\eta(u_f - f) = \phi''_\eta(\xi)(u_g - u_f + f - g). \tag{4.23}$$

Therefore, by Cauchy-Schwarz inequality

$$\begin{aligned}
&\langle \phi''_\eta(\xi)(u_g - u_f), u_g - u_f \rangle \\
\leq\ &\langle \phi''_\eta(\xi)(g - f), u_g - u_f \rangle \\
\leq\ &(\langle \phi''_\eta(\xi)(g - f), g - f \rangle)^{1/2} (\langle \phi''_\eta(\xi)(u_g - u_f), u_g - u_f \rangle)^{1/2}.
\end{aligned}$$

It thus follows

$$\langle \phi''_\eta(\xi)(u_g - u_f), u_g - u_f\rangle \le \langle \phi''_\eta(\xi)(g-f), g-f\rangle. \tag{4.24}$$

As $\phi''_\eta(\xi)$ is bounded from below and from above when u_g and u_f are bounded, the desired inequality follows. ■

4.3 Bivariate Spline Approximation of the TV-L^p Model

To find the minimizers of the TV-L^p minimization, we consider the minimization problem in a finite dimensional space, e.g., we can use bivariate spline space $S^r_d(\triangle)$.

The minimization problem in the spline space is formulated as

$$\min\{E_{\epsilon,\delta}(u), \quad u \in S^r_d(\triangle)\}. \tag{4.25}$$

We shall study the relationship between the minimizer of (4.25) and the minimizer of the original problem (4.15). Assuming S_f is the minimizer of (4.25), we shall prove that $E_{\epsilon,\eta}(S_f) - E_{\epsilon,\eta}(u_f) \to 0$ as the size $|\triangle|$ of the triangulation tends to zero, where $|\triangle|$ is the largest of the lengths of edges in $\triangle$.

We first introduce the notation of the extension of functions on $\Omega = [0,1]\times[0,1]$: for any function u defined on Ω, let $\operatorname{Ext} u$ be the extension of u defined on $\mathbb{R}^2$ by first reflecting u about the boundary of Ω and then periodically extending the resulting function to the whole plane $\mathbb{R}^2$. For details, see [57]. Let ψ be a standard symmetric non-negative mollifier and define

$$u^\delta(x) = \int_{R^2} \operatorname{Ext} u(x-y)\psi(\frac{y}{\delta})\frac{dy}{\delta^2}.$$

Lemma 4.3.1 *Suppose f is bounded. Then*

$$E_{\epsilon,\eta}(u^\delta_f) \le E_{\epsilon,\eta}(u_f) + C\delta|u_f|_{\mathrm{BV}(\Omega)}$$

where $C > 0$ is a constant dependent on $\|f\|_\infty$ and p.

Proof. First we claim that

$$\int_\Omega \sqrt{\epsilon + |\nabla u_f^\delta|^2} \leq \int_\Omega \sqrt{\epsilon + |\nabla u_f|^2}$$

for δ small enough. Indeed, it is straightforward to verify that this inequality holds for $u_f \in W^{1,1}(\Omega)$ by using the convexity of $J_\epsilon(u)$ and the property of the mollifier for any $\delta > 0$. For $u_f \in \mathrm{BV}(\Omega)$, the inequality still holds due to the fact that any BV function can be approximated by $W^{1,1}$ functions in the sense of Theorem 2.3.1.

Next we have

$$\left| \int_\Omega (\eta + (u_f^\delta - f)^2)^{p/2} - (\eta + (u_f - f)^2)^{p/2} \right| \leq \int_\Omega \left| \phi_\eta'(\xi)(u_f^\delta - u_f) \right|,$$

where $\phi_\eta(x)$ is the function defined in (4.20), and ξ is a function between $u_f^\delta - f$ and $u_f - f$. Since f is bounded , we have u_f is also bounded by Lemma 4.2.1. The following calculation shows that u_f^δ is also bounded.

$$\begin{aligned} |u_f^\delta(x)| &= \left| \int_{\mathbb{R}^2} \mathrm{Ext}\, u_f(x-y)\psi(\frac{y}{\delta})\frac{dy}{\delta^2} \right| \\ &\leq \max|f| \int_{\mathbb{R}^2} \psi(\frac{y}{\delta})\frac{dy}{\delta^2} = \max|f|. \end{aligned}$$

Therefore,

$$\begin{aligned} &\left| \int_\Omega (\epsilon + (u_f^\delta - f)^2)^{p/2} - (\epsilon + (u_f - f)^2)^{p/2} \right| \\ &\leq C\|u_f^\delta - u_f\|_{L^1(\Omega)} \leq C\delta |u_f|_{\mathrm{BV}(\Omega)}. \end{aligned}$$

The last inequality holds for $|u_f|_{W^{1,1}(\Omega)}$ according to Lemma 2.4.3. Then using a density argument in Theorem 2.3.1, we can extend it to $|u_f|_{\mathrm{BV}(\Omega)}$. ■

We need to use the following standard result.

Lemma 4.3.2 *If $u \in \mathrm{BV}(\Omega)$,*

$$|u^\delta|_{W^{2,1}(\Omega)} \leq \frac{C}{\delta}|u|_{\mathrm{BV}(\Omega)} \tag{4.26}$$

Proof. According to Theorem 2.3.1, we can pick a sequence $\{u_n\} \in W^{1,1}(\Omega)$ such that when $n \to \infty$,

$$\|u_n - u\|_{L^1(\Omega)} \to 0,$$

and

$$|u_n|_{\mathrm{BV}(\Omega)} \to |u|_{\mathrm{BV}(\Omega)}.$$

By Lemma 3.3.5 the inequality (4.26) holds for all $u_n \in W^{1,1}(\Omega)$. To finish the proof, we just need to show

$$|u_n^\delta|_{W^{2,1}(\Omega)} \to |u^\delta|_{W^{2,1}(\Omega)}, \quad n \to \infty,$$

which needs the following inequality:

$$\begin{aligned}
\|D_1^2(u_n^\delta - u^\delta)\|_{L^1(\Omega)} &= \int_\Omega \left| \int_{B(x,\delta)} (u_n(y) - u(y)) D_1^2 \psi_\delta(x-y) dy \right| dx \\
&\leq \int_\Omega \int_{B(x,\delta)} |u_n(y) - u(y)||D_1^2 \psi_\delta(x-y)| dy dx \\
&\leq \int_{\Omega_\delta} |u_n(y) - u(y)| \int_{B(y,\delta)} |D_1^2 \psi_\delta(x-y)| dx dy \\
&= \int_{\Omega_\delta} |u_n(y) - u(y)| dy \int_{B(0,\delta)} |D_1^2 \psi_\delta(z)| dz \quad z = x - y \\
&\leq \|u_n - u\|_{L^1(\Omega)} \int_{B(0,\delta)} \frac{C}{\delta^4} dz \qquad \text{(by Lemma 2.4.2 and extension theorem)} \\
&= \|u_n - u\|_{L^1(\Omega)} \frac{C}{\delta^2},
\end{aligned}$$

where $\psi_\delta(x) = \psi(\frac{x}{\delta})$. ■

We now prove that the energy of the spline approximation is close to the energy of the smoothed function.

Lemma 4.3.3 *Suppose f is bounded. Suppose that $S_d^r(\triangle)$ contains a spline space $S_d^r(\triangle)$ for a degree $d \geq 3r + 2$. Let $Qu_f^\delta \in S_d^r(\triangle)$ be the quasi-interpolatory spline mentioned in Theorem 2.1.6. Then*

$$E_{\epsilon,\eta}(Qu_f^\delta) \leq E_{\epsilon,\eta}(u_f^\delta) + C(\frac{|\Delta|}{\delta} + |\Delta|)|u_f|_{\mathrm{BV}(\Omega)}.$$

Proof. We bound the difference between $|E_{\epsilon,\eta}(Qu_f^\delta) - E_{\epsilon,\eta}(u_f^\delta)|$ by

$$\begin{aligned}
&|E_{\epsilon,\eta}(Qu_f^\delta) - E_{\epsilon,\eta}(u_f^\delta)| \\
\leq &\left| \int_\Omega \sqrt{1+|\nabla Qu_f^\delta|^2} - \sqrt{1+|\nabla u_f^\epsilon|^2} dx \right| \\
&+ \frac{1}{\lambda} \left| \int_\Omega (\epsilon + (Qu_f^\delta - f)^2)^{p/2} - (\epsilon + (u_f^\delta - f)^2)^{p/2} \right|.
\end{aligned}$$

For the first term on the right side of the inequality

$$\begin{aligned}
&\left| \int_\Omega \sqrt{\epsilon+|\nabla Qu_f^\delta|^2} - \sqrt{\epsilon+|\nabla u_f^\delta|^2} dx \right| \\
&= \left| \int_\Omega \frac{|\nabla Qu_f^\delta|^2 - |\nabla u_f^\delta|^2}{\sqrt{1+|\nabla Qu_f^\delta|^2} + \sqrt{\epsilon+|\nabla \tilde{u_f^\delta}|^2}} dx \right| \\
&\leq \int_\Omega \frac{|\nabla Qu_f^\delta - \nabla u_f^\delta||\nabla Qu_f^\delta + \nabla u_f^\delta|}{\sqrt{\epsilon+|\nabla Qu_f^\delta|^2} + \sqrt{\epsilon+|\nabla \tilde{u_f^\delta}|^2}} dx \\
&\leq \|\nabla(Qu_f^\delta - u_f^\delta)\|_{L^1(\Omega)}.
\end{aligned}$$

By Theorem 2.1.6 (with $m = 1$) and Lemma 4.3.2,

$$\|\nabla(Qu_f^\delta - u_f^\delta)\|_{L^1(\Omega)} \leq C|\Delta||u_f^\delta|_{W^{2,1}(\Omega)} \leq C\frac{|\Delta|}{\delta}|u_f|_{\mathrm{BV}(\Omega)}.$$

For the second term, since f is bounded, u_f, u_f^δ and Qu_f^δ are also bounded. We apply Theorem 2.1.6 to get

$$\begin{aligned}
&\left| \int_\Omega (\eta + (Qu_f^\delta - f)^2)^{p/2} - (\eta + (u_f^\delta - f)^2)^{p/2} \right| \\
&\leq \int_\Omega \left| \phi_\eta'(\xi)(Qu_f^\delta - u_f^\delta) \right| \\
&\leq C \int_\Omega |(Qu_f^\delta - u_f^\delta)| \, dx \\
&\leq C|\Delta||u_f^\delta|_{W^{1,1}(\Omega)} \leq C|\Delta||u_f|_{\mathrm{BV}(\Omega)}.
\end{aligned}$$

The last inequality uses Lemma 2.4.1 which claims that for any function $u \in \mathrm{BV}(\Omega)$,

$$|u^\delta|_{W^{1,1}(\Omega)} \leq |u|_{\mathrm{BV}(\Omega)}.$$

Summarizing the discussion above, we have completed the proof. ■

Finally we are ready to prove the main result in this section.

Theorem 4.3.1 *Fix $p \geq 1$ and $\eta > 0$. Suppose f is bounded. Let $\delta = \sqrt{|\triangle|}$. Then*

$$E_{\epsilon,\eta}(S_f) - E_{\epsilon,\eta}(u_f) \leq C\sqrt{|\Delta|}\, E_{\epsilon,\eta}(0) \tag{4.27}$$

for all $\epsilon \geq 0$, where C is a constant dependent on f, p, and the smallest angle $\theta_\triangle$ of triangulation $\triangle$. By Theorem 4.2.1,

$$\|S_f - u_f\|_{L^2(\Omega)} \leq C\lambda\sqrt{|\triangle|}, \tag{4.28}$$

where C is another positive constant independent of $|\triangle|$.

Proof. Combine Lemma 4.3.1 and Lemma 4.3.3. We have

$$E_{\epsilon,\eta}(u_f) \leq E_{\epsilon,\eta}(S_f) \leq E_{\epsilon,\eta}(Qu_f^\delta) \leq E_{\epsilon,\eta}(u_f) + C(\frac{|\Delta|}{\delta} + |\Delta| + \delta)|u_f|_{\mathrm{BV}(\Omega)}.$$

For $\delta = \sqrt{|\Delta|}$, we have

$$E_{\epsilon,\eta}(S_f) - E_{\epsilon,\eta}(u_f) \leq C\sqrt{|\Delta|}\,|u_f|_{\mathrm{BV}(\Omega)} \leq C\sqrt{|\Delta|}E_{\epsilon,\eta}(0).$$

The inequality (4.28) follows from (4.27) and Theorem 4.2.1 directly. ■

4.4 A Numerical Algorithm

In this section, we shall derive an iterative algorithm to compute the minimizers of the (ϵ, η) version TV-L^p model and show that the iterative algorithm converges. The discussion is similar to the one in [35] where the minimizer of the TV-L^p model was considered. The proof has to be carefully modified when $p < 2$. Thus, we present a detailed discussion here. Recall

$$E_{\epsilon,\eta}(u) := \int_\Omega \sqrt{\epsilon + |\nabla u|^2}dx + \frac{1}{p\lambda}\int_\Omega (\eta + |u - f|^2)^{p/2}dx \tag{4.29}$$

for $\epsilon \geq 0$ and $\eta \geq 0$. Note that it is also defined for $p > 0$. We first have

Theorem 4.4.1 *Fix $p > 0, \epsilon \geq 0$ and $\eta > 0$. There exists a solution of the following minimization problem*

$$\min\{E_{\epsilon,\eta}(s),\ s \in S_d^r(\triangle)\}, \tag{4.30}$$

where $S_d^r(\triangle)$ is a spline space introduced in the previous section. When $p > 1$ or when $p = 1$ and $\eta > 0$, the minimizer is unique.

Proof. Let $D := \{E_{\epsilon,\eta}(s) \leq E_{\epsilon,\eta}(0), s \in S_d^r(\triangle)\}$. It is not hard to see $D \subset S_d^r(\triangle)$ is bounded compact. Note that $E_{\epsilon,\eta}(u)$ is a continuous functional for any fixed $p > 0, \eta \geq 0, \eta > 0$. Therefore there exists a spline $S_f \in D$ which achieves the minimum, i.e., $E_{\epsilon,\eta}(S_f) \leq E_k(s), s \in D$.

When $p > 1$ or when $p = 1$ and $\eta > 0$, the minimization functional $E_{\epsilon,\eta}$ is strictly convex and has a unique minimizer. ■

Let $\phi_1, ..., \phi_n$ be a basis for spline space $S_d^r(\triangle)$. The following iterative algorithm will be used to approximate S_f

Algorithm 4.4.1 *Given $u^{(k)}$, we find $u^{(k+1)} \in S_d^r(\triangle)$ such that*

$$\begin{aligned}\int_\Omega \frac{\nabla u^{(k+1)} \cdot \nabla \phi_j}{\sqrt{\epsilon + |\nabla u^{(k)}|^2}} dx + \frac{1}{\lambda} \int_\Omega \frac{u^{(k+1)} \phi_j}{(\eta + |u^{(k)} - f|^2)^{1-p/2}} dx \\ = \frac{1}{\lambda} \int_\Omega \frac{f \phi_j}{(\eta + |u^{(k)} - f|^2)^{1-p/2}} dx, \quad \forall j = 1, ..., n.\end{aligned} \tag{4.31}$$

We first show that the above iteration is well defined. Since $u^{(k+1)} \in S_d^r(\triangle)$, it can be written as $u^{(k+1)} = \sum_i^n c_i^{(k+1)} \phi_i$. Plugging it in (4.31), we have

$$\begin{aligned}\sum_i^n c_i^{(k+1)} \left(\int_\Omega \frac{\nabla \phi_i \cdot \nabla \phi_j}{\sqrt{\epsilon + |\nabla u^{(k)}|^2}} dx + \frac{1}{\lambda} \int_\Omega \frac{\phi_i \phi_j}{(\eta + |u^{(k)} - f|^2)^{1-p/2}} dx \right) \\ = \frac{1}{\lambda} \int_\Omega \frac{f \phi_j}{(\eta + |u^{(k)} - f|^2)^{1-p/2}} dx.\end{aligned} \tag{4.32}$$

Denote by

$$\begin{aligned} D^{(k)} &:= (d_{i,j}^{(k)})_{N \times N} \text{ with } d_{i,j}^{(k)} = \lambda \int_\Omega \frac{\nabla \phi_i \cdot \nabla \phi_j}{\sqrt{\epsilon + |\nabla u^{(k)}|^2}} dx \\ M^{(k)} &:= (m_{i,j}^{(k)})_{N \times N} \text{ with } m_{i,j} = \int_\Omega \frac{\phi_i \phi_j}{(\eta + |u^{(k)} - f|^2)^{1-p/2}} dx, \end{aligned}$$

$$\mathbf{v}^{(k)} \;:=\; (v_j^{(k)}, j = 1, \cdots, N) \text{ with } v_j = \int_\Omega \frac{f\phi_j}{(\eta + |u^{(k)} - f|^2)^{1-p/2}} dx.$$

Then to solve (4.32) is equivalent to solving the equation

$$(D^{(k)} + M^{(k)})\mathbf{c}^{(k+1)} = \mathbf{v}^{(\mathbf{k})}, \tag{4.33}$$

where $\mathbf{c}^{(k+1)} = [c_1^{(k+1)}, c_2^{(k+1)}, ..., c_n^{(k+1)}]^T$.

Theorem 4.4.2 *The algorithm 4.4.1 has a unique solution in $S_d^r(\triangle)$.*

Proof. $D^{(k)}$ is semi-positive definite and M is positive definite because, for any nonzero $\mathbf{c} = (c_i)_n$, because

$$\mathbf{c}^T D^{(k)} \mathbf{c} = \lambda \int_\Omega \frac{|\sum_i^n c_i \nabla\phi_i|^2}{\sqrt{\epsilon + |\nabla u^{(k)}|^2}} dx \geq 0,$$

and

$$\mathbf{c}^T \; M^{(k)} \; \mathbf{c} = \int_\Omega \frac{|\sum_i^n c_i \phi_i|^2}{(\eta + |u^{(k)} - f|^2)^{1-p/2}} dx > 0.$$

Therefore $(D^{(k)} + M^{(k)})$ is also positive definite, and hence invertible. So (4.33) has a unique solution and so does (4.31). ■

Next we show the iterative solution converges to the minimizer S_f in $S_d^r(\triangle)$. We need the following lemmas.

Lemma 4.4.1 *For $0 < p \leq 2$, the following inequality holds*

$$\frac{1}{p}\left((\eta + x^2)^{p/2} - (\eta + y^2)^{p/2}\right) \geq \frac{(x-y)^2}{2(\eta + x^2)^{1-p/2}} + \frac{y(x-y)}{(\eta + x^2)^{1-p/2}} \tag{4.34}$$

for all $x, y \geq 0$.

Proof. Since

$$\begin{aligned} & (\eta + x^2)^{p/2} - (\eta + y^2)^{p/2} \\ = \; & \frac{(\eta + x^2) - (\eta + x^2)^{1-p/2}(\eta + y^2)^{p/2}}{(\eta + x^2)^{1-p/2}} \\ = \; & \frac{\eta + x^2 + py^2 - pxy - (\eta + x^2)^{1-p/2}(\eta + y^2)^{p/2}}{(\eta + x^2)^{1-p/2}} + \frac{py(x-y)}{(\eta + x^2)^{1-p/2}} \end{aligned}$$

By Young's inequality which states that if $0 \leq a, b \leq 1$ and $a + b = 1$, then

$$ax + by \geq x^a y^b, \quad \text{where } x, y \geq 0,$$

we have

$$\begin{aligned} & \eta + x^2 + py^2 - pxy - (\eta + x^2)^{1-p/2}(\eta + y^2)^{p/2} - \frac{p}{2}(x-y)^2 \\ = \; & (1 - \frac{p}{2})(\eta + x^2) + \frac{p}{2}(\eta + y^2) - (\eta + x^2)^{1-p/2}(\eta + y^2)^{p/2} \geq 0. \end{aligned}$$

It follows that

$$\frac{1}{p}\left((\eta + x^2)^{p/2} - (\eta + y^2)^{p/2}\right) \geq \frac{(x-y)^2}{2(\eta + x^2)^{1-p/2}} + \frac{y(x-y)}{(\eta + x^2)^{1-p/2}}$$

■

Lemma 4.4.2 *Let $u^{(k+1)}$ be the solution of our Algorithm 4.4.1. Suppose that $0 < p \leq 2$. Then the following inequality holds*

$$E_{\epsilon,\eta}(u^{(k)}) - E_{\epsilon,\eta}(u^{(k+1)}) \geq \frac{1}{\lambda}\int_\Omega \frac{(u^{(k)} - u^{(k+1)})^2}{2(\eta + |u^{(k)} - f|^2)^{1-p/2}} dx \tag{4.35}$$

where $E_{\epsilon,\eta}(\cdot)$ is the energy functional given in (4.15).

Proof. $K(u) := \displaystyle\int_\Omega \frac{|\nabla u|^2}{2\sqrt{\epsilon + |\nabla u^{(k)}|^2}} dx$ is a convex functional, direct calculation shows

$$\frac{d}{dt} K(u^{(k+1)} + t\phi) = \int_\Omega \frac{\nabla u^{(k+1)} \cdot \nabla \phi}{\sqrt{\epsilon + |\nabla u^{(k)}|^2}},$$

or in another words,

$$\langle \partial K(u^{(k+1)}, \phi \rangle = \int_\Omega \frac{\nabla u^{(k+1)} \cdot \nabla \phi}{\sqrt{\epsilon + |\nabla u^{(k)}|^2}},$$

where ∂K is the subdifferential of K. It follows from (4.31) that

$$-\frac{1}{\lambda}\frac{u^{(k+1)} - f}{(\eta + |u^{(k)} - f|^2)^{1-p/2}} \in \partial K(u^{(k+1)}).$$

By the properties of subdifferential, we have

$$\langle \partial K(u^{(k+1)}), u^{(k)} - u^{(k+1)} \rangle \leq K(u^{(k)}) - K(u^{(k+1)}),$$

or equivalently,

$$\frac{1}{\lambda}\int_\Omega \frac{(f-u^{(k+1)})(u^{(k)}-u^{(k+1)})}{(\eta+|u^{(k)}-f|^2)^{1-p/2}}dx \le \int_\Omega \frac{|\nabla u^{(k)}|^2}{2\sqrt{\epsilon+|\nabla u^{(k)}|^2}}dx - \int_\Omega \frac{|\nabla u^{(k+1)}|^2}{2\sqrt{\epsilon+|\nabla u^{(k)}|^2}}dx.$$

Denoting $u^{(k)}-f$ by $w^{(k)}$, the above inequality can be rewritten as:

$$\frac{1}{\lambda}\int_\Omega \frac{(-w^{(k+1)})(w^{(k)}-w^{(k+1)})}{(\eta+|w^{(k)}|^2)^{1-p/2}}dx \le \int_\Omega \frac{|\nabla u^{(k)}|^2}{2\sqrt{\epsilon+|\nabla u^{(k)}|^2}}dx - \int_\Omega \frac{|\nabla u^{(k+1)}|^2}{2\sqrt{\epsilon+|\nabla u^{(k)}|^2}}dx. \quad (4.36)$$

Using (4.36), we have

$$\begin{aligned}
& \int_\Omega \sqrt{\epsilon+|\nabla u^{(k)}|}-\sqrt{\epsilon+|\nabla u^{(k+1)}|^2}dx + \frac{1}{\lambda}\int_\Omega \frac{(w^{(k+1)})(w^{(k)}-w^{(k+1)})}{(\eta+|w^{(k)}|^2)^{1-p/2}}dx \quad (4.37)\\
\ge\ & \int_\Omega \sqrt{\epsilon+|\nabla u^{(k)}|^2}-\sqrt{\epsilon+|\nabla u^{(k+1)}|^2}dx\\
& -\int_\Omega \frac{|\nabla u^{(k)}|^2}{2\sqrt{\epsilon+|\nabla u^{(k)}|^2}}dx + \int_\Omega \frac{|\nabla u^{(k+1)}|^2}{2\sqrt{\epsilon+|\nabla u^{(k)}|^2}}dx\\
=\ & \int_\Omega \frac{2\epsilon+|\nabla u^{(k)}|^2+|\nabla u^{(k+1)}|^2}{2\sqrt{\epsilon+|\nabla u^{(k)}|^2}}-\sqrt{\epsilon+|\nabla u^{(k+1)}|^2}dx\\
\ge\ & \int_\Omega \frac{\sqrt{\epsilon+|\nabla u^{(k)}|^2}\sqrt{\epsilon+|\nabla u^{(k+1)}|^2}}{\sqrt{\epsilon+|\nabla u^{(k)}|^2}}-\sqrt{\epsilon+|\nabla u^{(k+1)}|^2}dx = 0.
\end{aligned}$$

By Lemma 4.4.1, we have

$$\begin{aligned}
& \frac{1}{p}\left((\eta+(w^{(k)})^2)^{p/2}-(\eta+(w^{(k+1)})^2)^{p/2}\right)\\
\ge & \frac{(w^{(k)}-w^{(k+1)})^2}{2(\eta+(w^{(k)})^2)^{1-p/2}} + \frac{w^{(k+1)}(w^{(k)}-w^{(k+1)})}{(\eta+(w^{(k)})^2)^{1-p/2}} \quad (4.38)
\end{aligned}$$

Using (4.37) and (4.38), the difference between $E_{\epsilon,\eta}(u^{(k)})$ and $E_{\epsilon,\eta}(u^{(k+1)})$ is

$$\begin{aligned}
& E_{\epsilon,\eta}(u^{(k)})-E_{\epsilon,\eta}(u^{(k+1)})\\
=\ & \int_\Omega \left(\sqrt{\epsilon+|\nabla u^{(k)}|}-\sqrt{\epsilon+|\nabla u^{(k+1)}|^2}\right)dx + \frac{1}{p\lambda}\int_\Omega \left((\eta+|w^{(k)}|^2)^{p/2}-(\eta+|w^{(k+1)}|^2)^{p/2}\right)dx\\
\ge\ & \underbrace{\int_\Omega \sqrt{\epsilon+|\nabla u^{(k)}|}-\sqrt{\epsilon+|\nabla u^{(k+1)}|^2}dx + \frac{1}{\lambda}\int_\Omega \frac{w^{(k+1)}(w^{(k)}-w^{(k+1)})}{(\eta+|w^{(k)}|^2)^{1-p/2}}dx}_{\ge 0}\\
& +\frac{1}{\lambda}\int_\Omega \frac{(w^{(k)}-w^{(k)})^2}{2(\eta+|w^{(k)}|^2)^{1-p/2}}dx.
\end{aligned}$$

Since $w^{(k)}-w^{(k)}=(u^{(k)}-u^{(k)})$, we have thus established the proof. ■

Lemma 4.4.3 *Suppose that $p \in (0, 2]$ and $\eta \geq 0$ and $\epsilon \geq 0$. If $\|f\|_{L^\infty(\Omega)}$ is bounded, then $\|u^{(k)}\|_{L^\infty(\Omega)} \leq C$ for some constant C independent of k.*

Proof. From Theorem 4.4.2, we see that $\{E_{\epsilon,\eta}(u^{(k)})\}$ is a decreasing sequence. Thus,

$$\lambda E_{\epsilon,\eta}(u^{(0)}) \geq \lambda E_{\epsilon,\eta}(u^{(k)}) \geq \int_\Omega (\eta + |u^{(k)} - f|^2)^{p/2} dx \geq \int_\Omega |u^{(k)} - f|^p dx.$$

For $p \geq 1$, we have

$$\|u^{(k)}\|_p \leq \|f\|_{L^p(\Omega)} + \|u^{(k)} - f\|_{L^p(\Omega)} \leq \left(\lambda E_{\epsilon,\eta}(u^{(0)})\right)^{1/p} + A_\Omega^{1/p} \|f\|_{L^\infty(\Omega)}$$

where A_Ω is the area of Ω. It follows that $\|u^{(k)}\|_p$ is bounded. Similarly, when $p \in (0, 1)$, we have

$$\|u^{(k)}\|_p^p \leq \|f\|_{L^p(\Omega)}^p + \|u^{(k)} - f\|_{L^p(\Omega)}^p \leq \lambda E_{\epsilon,\eta}(u^{(0)}) + A_\Omega \|f\|_{L^\infty(\Omega)}^p.$$

In finite dimensional space, $\|\cdot\|_{L^p(\Omega)}$ and $\|\cdot\|_{L^\infty(\Omega)}$ are equivalent. Therefore $\|u^{(k)}\|_{L^\infty(\Omega)}$ is also bounded. ■

Lemma 4.4.4 *If $\|f\|_{L^\infty(\Omega)}$ is bounded, then $\|u^{(k+1)} - u^{(k)}\|_{L^2(\Omega)} \to 0$ as $k \to \infty$.*

Proof. By Lemma 4.4.3 $|u^{(k)}|$ is bounded. Therefore

$$|u^{(k)} - f|^2 \leq (\|u^{(k)}\|_{L^\infty(\Omega)} + \|f\|_{L^\infty(\Omega)})^2 < \infty$$

Let $\|(\eta + |u^{(k)} - f|^2)^{1-p/2}\|_{L^\infty(\Omega)} = M < \infty$. By Lemma 4.4.2, we have

$$\begin{aligned} E_{\epsilon,\eta}(u^{(k)}) - E_{\epsilon,\eta}(u^{(k+1)}) &\geq \frac{1}{\lambda} \int_\Omega \frac{(u^{(k)} - u^{(k+1)})^2}{2(\eta + |u^{(k)} - f|^2)^{1-p/2}} dx \\ &\geq \frac{1}{\lambda M} \int_\Omega (u^{(k)} - u^{(k+1)})^2 dx, \end{aligned}$$

that is,

$$\|u^{(k+1)} - u^{(k)}\|_{L^2(\Omega)} \leq \lambda M \left(E_{\epsilon,\eta}(u^{(k)}) - E_{\epsilon,\eta}(u^{(k+1)})\right).$$

So $\{E_{\epsilon,\eta}(u^{(k)})\}$ is a decreasing sequence and bounded from below, and hence converges. This implies $E_{\epsilon,\eta}(u^{(k)}) - E_{\epsilon,\eta}(u^{(k+1)}) \to 0$ therefore $\|u^{(k+1)} - u^{(k)}\|_{L^2(\Omega)} \to 0$ as $k \to \infty$. ■

Theorem 4.4.3 *For $p \geq 1$ and $\eta > 0$, the sequence $u^{(k)}$ obtained from Algorithm 4.4.1 converges to the true minimizer S_f.*

Proof. By Lemma 4.4.3, the sequence $\{u^{(k)}\}$ is bounded. There must be a convergent subsequence $\{u^{(n_j)}\}$. Suppose $u^{(n_j)} \to \bar{u}$. We use Lemma 4.4.4 to have

$$\|u^{(n_j+1)} - \bar{u}\|_{L^2(\Omega)} \leq \|u^{(n_j+1)} - u^{(n_j)}\|_{L^2(\Omega)} + \|u^{(n_j)} - \bar{u}\|_{L^2(\Omega)} \to 0$$

which implies $u^{(n_j+1)} \to \bar{u}$.

According to Markov's inequality (cf. [38]), we have

$$\int_\Omega |\nabla u^{(n_j)} - \nabla \bar{u}|^2 dx \leq \frac{\beta^2}{|\triangle|^2} \int_\Omega |u^{(n_j)} - \bar{u}|^2 dx, \tag{4.39}$$

where $\beta > 0$ is a constant dependent on the smallest angle $\theta_\triangle$ of $\triangle$. It follows from the convergence of $u^{(n_j)} \to \bar{u}$ that $\nabla u^{(n_j)} \to \nabla \bar{u}$ in L^2 as well. Replacing $u^{(n_j)}$ by $u^{(n_j+1)}$ above, we have $\nabla u^{(n_j+1)} \to \nabla \bar{u}$ too by the convergence of $u^{(n_j+1)} \to \bar{u}$. As $u^{(n_j)}$, $u^{(n_j+1)}$ and $\bar{u}$ are spline functions in $S_d^r(\triangle)$. The convergence of $u^{(n_j)}$ and $u^{(n_j+1)}$ to $\bar{u}$ implies the coefficients of $u^{(n_j)}$ and $u^{(n_j+1)}$ are convergent to the coefficients of $\bar{u}$, respectively.

Since $u^{(n_j+1)}$ solves the equations (4.31), we have

$$\begin{aligned}\int_\Omega \frac{\nabla u^{(n_j+1)} \cdot \nabla \phi_j}{\sqrt{\epsilon + |\nabla u^{(n_j)}|^2}} dx + \frac{1}{\lambda} \int_\Omega \frac{u^{(n_j+1)} \phi_j}{(\eta + |u^{(n_j)} - f|^2)^{1-p/2}} dx \\ = \frac{1}{\lambda} \int_\Omega \frac{f \phi_j}{(\eta + |u^{(n_j)} - f|^2)^{1-p/2}} dx,\end{aligned}$$

for all $\phi_i, i = 1, \cdots, N$. Letting $j \to \infty$, we obtain

$$\int_\Omega \frac{\nabla \bar{u} \cdot \nabla \phi_j}{\sqrt{\epsilon + |\nabla \bar{u}|^2}} dx + \frac{1}{\lambda} \int_\Omega \frac{\bar{u} \phi_j}{(\eta + |\bar{u} - f|^2)^{1-p/2}} dx = \frac{1}{\lambda} \int_\Omega \frac{f \phi_j}{(\eta + |\bar{u} - f|^2)^{1-p/2}} dx,$$

for all $i = 1, \cdots, N$. That is, $\bar{u}$ is a local minimizer. Since the functional is convex when $p > 1$ or when $p = 1$ with $\eta > 0$, a local minimizer is also the global minimizer hence, $\bar{u} = S_f$. Thus all convergent subsequences of $\{u^{(k)}\}$ converge to S_f, which implies $\{u^{(k)}\}$ itself converges to S_f. ■

4.5 Numerical Examples

4.5.1 The Rejection-Sampling Method

In this subsection we discuss a method to generate noises from the p-exponential distribution in (4.11). It is called the rejection sampling, which can be implemented without the knowledge of the cumulated density function of the distribution. It is also commonly called the acceptance-rejection method or accept-reject algorithm. See [43] for more details.

Algorithm 4.5.1 (The Rejection Sampling Algorithm) *Suppose we want to generate random numbers from probability distribution $g(x)$. Let $M > 1$ be a real number and $h(x)$ be an envelope distribution, so that $g(x) \leq Mh(x)$ for some $M > 1$.*

1. *Sample x from $h(x)$, and u from uniform distribution over the unit interval $U(0, 1)$.*
2. *Check weather or not $u \leq \dfrac{g(x)}{Mh(x)}$.*
   - *if this holds, accept x as a realization of $g(x)$.*
   - *if not, reject the value x.*

In this way, we generate random noises subject to the Laplacian distribution(p-exponential distribution). See [46] for more details. Examples of p-exponential random numbers of $p = 1$, $p = 1.5$ and $p = 2$ are shown in Fig. 4.1.

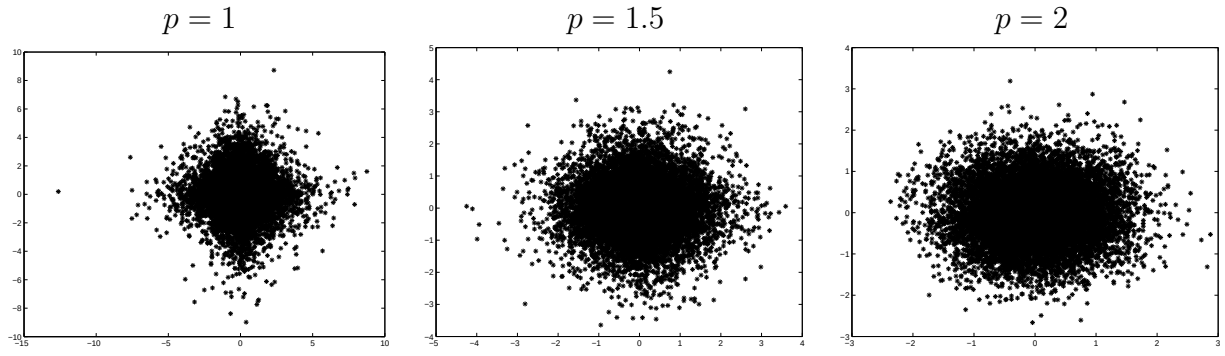

Figure 4.1: Distribution of Laplacian noises of $p = 1$, $p = 1.5$ and $p = 2$.

4.5.2 Numerical Results

Example 4.5.1 *In this example we examine the convergence of our algorithm, i.e., for fixed triangulation* $\triangle$, $\|u^{(k+1)} - u^{(k)}\|_{L^2(\Omega)} \to 0$, *as* $k \to \infty$.

(a) First we try to demonstrate that our algorithm converges regardless the shape of a region. We test our algorithm on seven triangulations of the following figure. The input function f *is a noised image with white noise of* $\sigma = 30$ *and divided into seven patches. We test our iterative numerical algorithm to solve the spline solution of the TV-*L^1 *model on each patch and are able to get a convergent sequence of* $\|u^{(k+1)} - u^{(k)}\|_{L^2(\Omega)}$ *from our numerical algorithm as shown in Fig. 4.3.*

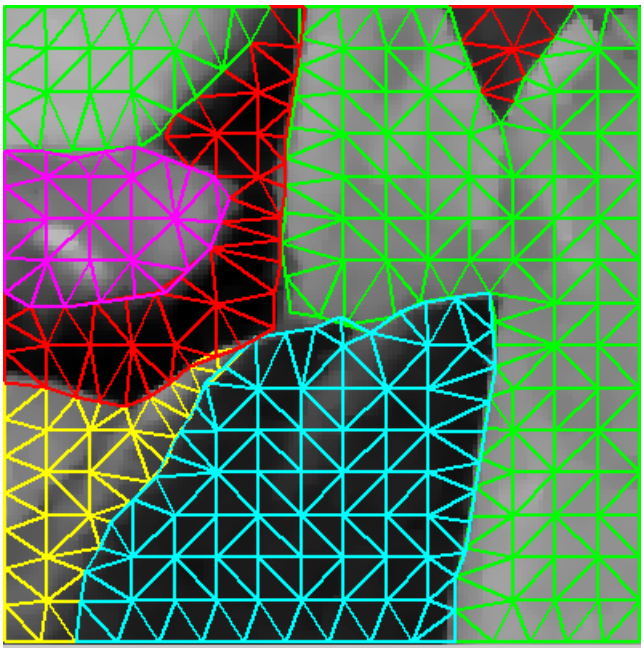

Figure 4.2: Triangulations used to test convergence of the algorithm.

(b)Second, we try to examine that our algorithm converges for variate TV-L^p *models of different* p *values. The input function* f *is a noised image on a circular region with p-exponential noises of* $p = 1$, $\sigma = 30$. *We test the case when* $p = 1$, $p = 1.5$ *and* $p = 2$. *The results are showed in Fig 4.4.*

Example 4.5.2 *It is well-known that for noised image with Gaussian noises, the original ROF model (i.e. TVL*^{2}*) is better than the TV-*L^1 *model. We now present some evidences*

that when an image is corrupted by noises subject to a p-exponential distribution, the noised image is better denoised by the TV-L^p model than by the ROF model for $p < 2$. In this example, we examine the effectiveness of our model in image denoising. We try to give some evidences that the TV-L^p model performs best to the Laplacian noise of the same p value. The input function is a sine function over a circular domain corrupted by p-exponential noises of $p = 1$, $p = 1.5$ and $p = 2$ respectively. In all experiments, $\sigma = 30$. The peak signal-to-noise ratio(PSNR) is used to evaluate the effectiveness of the TV-L^p model. The results are shown in Table 4.1, Table 4.2 and Table 4.3 respectively. The clean figure is shown in Fig. 4.5. And noised images and best recovered image are shown in Fig. 4.6, Fig. 4.7 and Fig. 4.8 respectively. One can see that the TV-L^p model performs consistently better in denoising of the p-exponential noises.

$p = 1$		$p = 1.5$		$p = 2$	
λ	PSNR	λ	PSNR	λ	PSNR
0.05	33.40	0.5	33.17	0.5	32.28
0.1	**33.48**	1	**33.21**	2	32.33
1	31.48	2	33.0591	7	**32.43**
2	27.8108	3	32.7137	10	32.42

Table 4.1: Denoising of p-exponential noises of $p = 1$ by TVL^1, $TVL^{1.5}$ and TVL^2 models

$p = 1$		$p = 1.5$		$p = 2$	
λ	PSNR	λ	PSNR	λ	PSNR
0.05	33.91	0.1	34.21	0.5	34.19
0.1	**33.94**	0.5	**34.22**	1	34.20
0.5	33.58	1	34.19	2	**34.21**
1	32.36	2	33.95	3	34.20

Table 4.2: Denoising of p-exponential noises of $p = 1.5$ by TVL^1, $TVL^{1.5}$ and TVL^2 models

$p = 1$		$p = 1.5$		$p = 2$	
λ	PSNR	λ	PSNR	λ	PSNR
0.05	34.02	0.1	34.45	0.5	34.61
0.1	**34.06**	0.5	**34.50**	1	34.62
0.5	33.91	1	34.49	3	**34.63**
1	32.84	2	34.31	5	34.60

Table 4.3: Denoising of p-exponential noises of $p = 2$ by TVL^1, $TVL^{1.5}$ and TVL^2 models

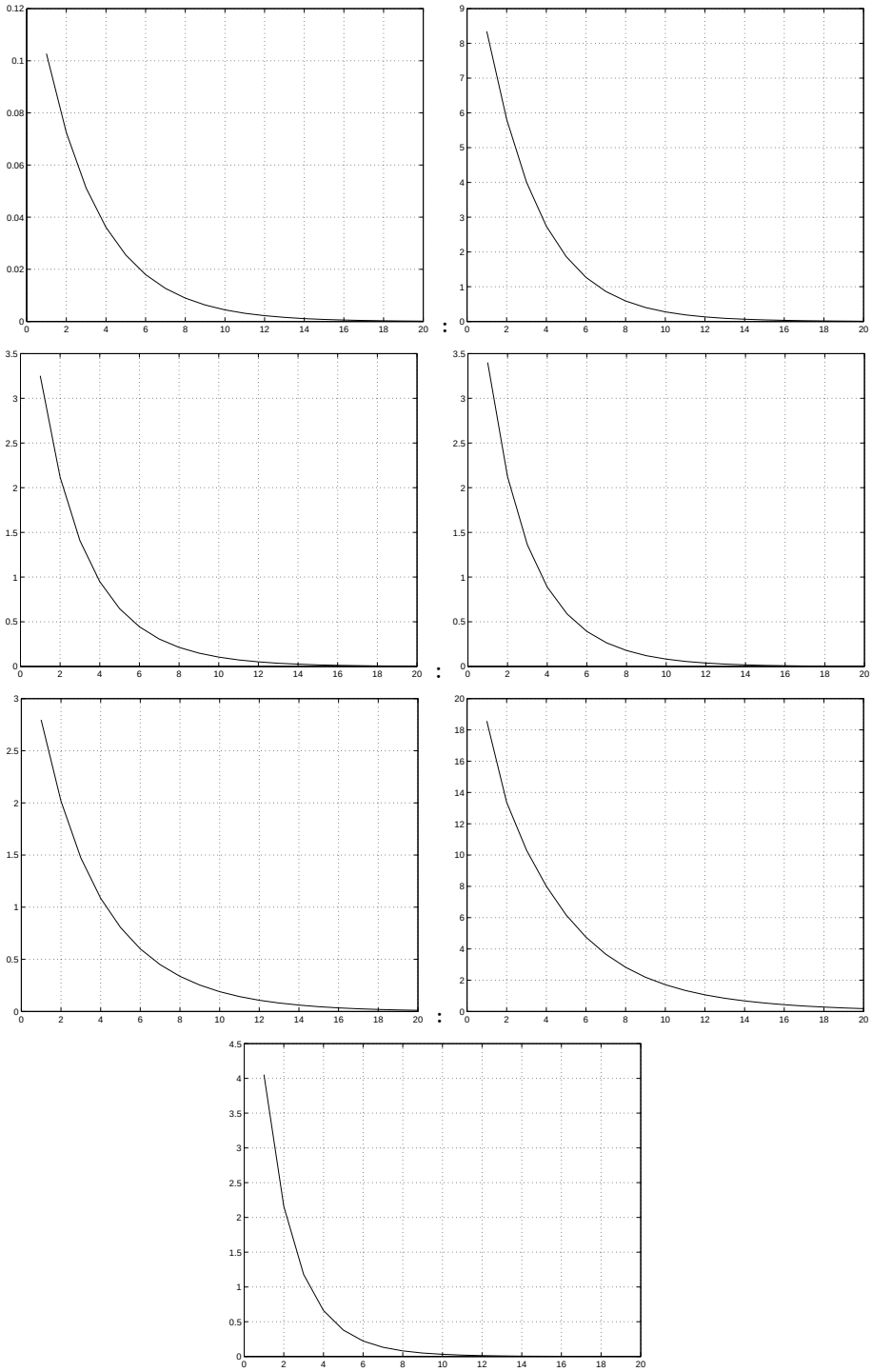

Figure 4.3: Convergency of numerical algorithm on seven different regions. X-axis: number of iterations; Y-axis: $\|u^{(k+1)} - u^{(k)}\|_{L^2(\Omega)}$.

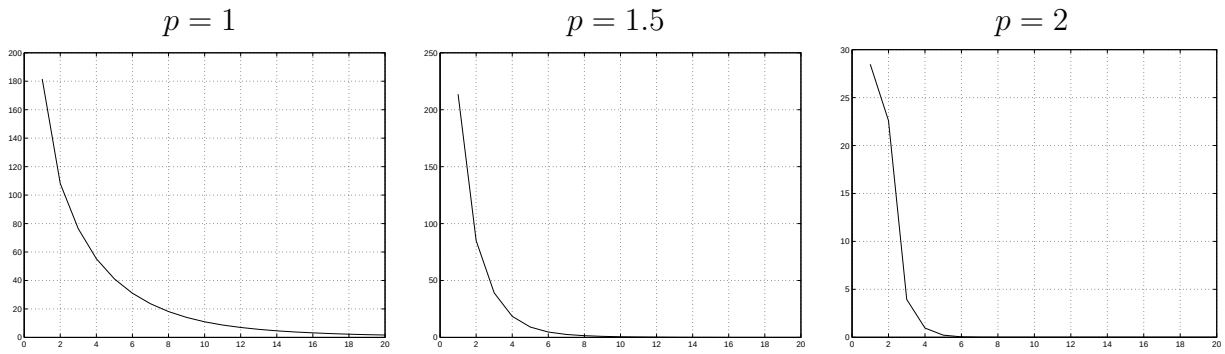

Figure 4.4: Convergency of numerical algorithm in different p values. X-axis: number of iterations; Y-axis: $\|u^{(k+1)} - u^{(k)}\|_{L^2(\Omega)}$.

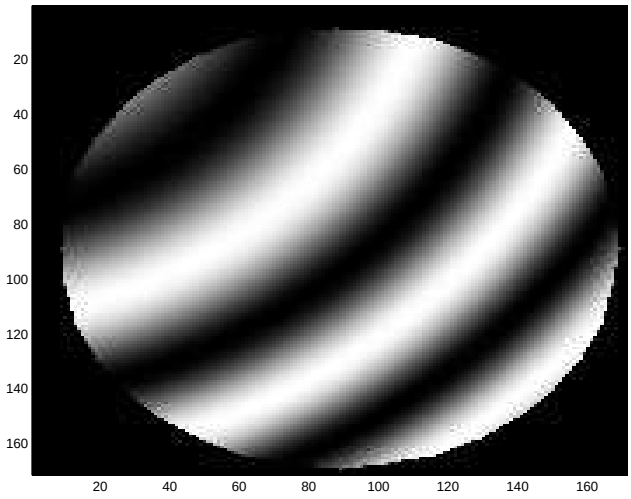

Figure 4.5: Clean image

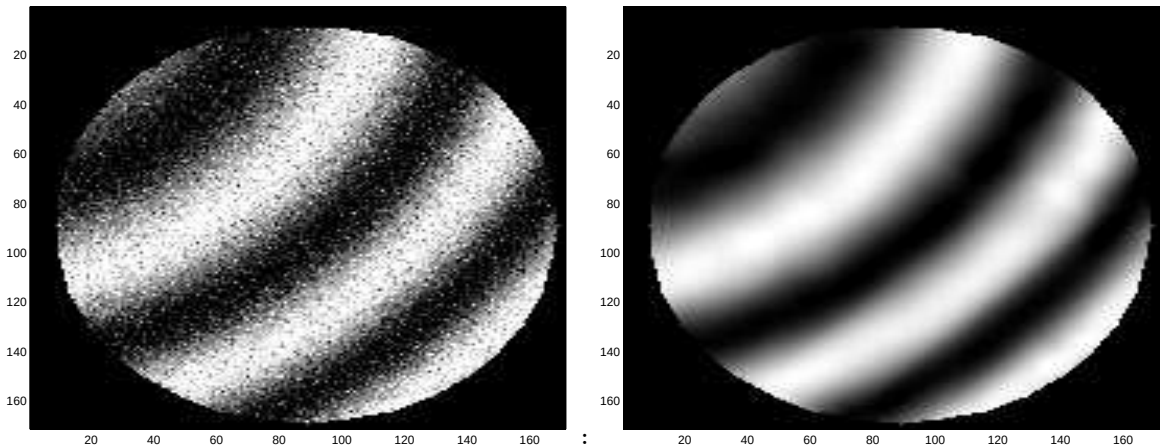

Figure 4.6: Noised image of $p = 1$ and the denoised image with the TV-L^p model of $p = 1$

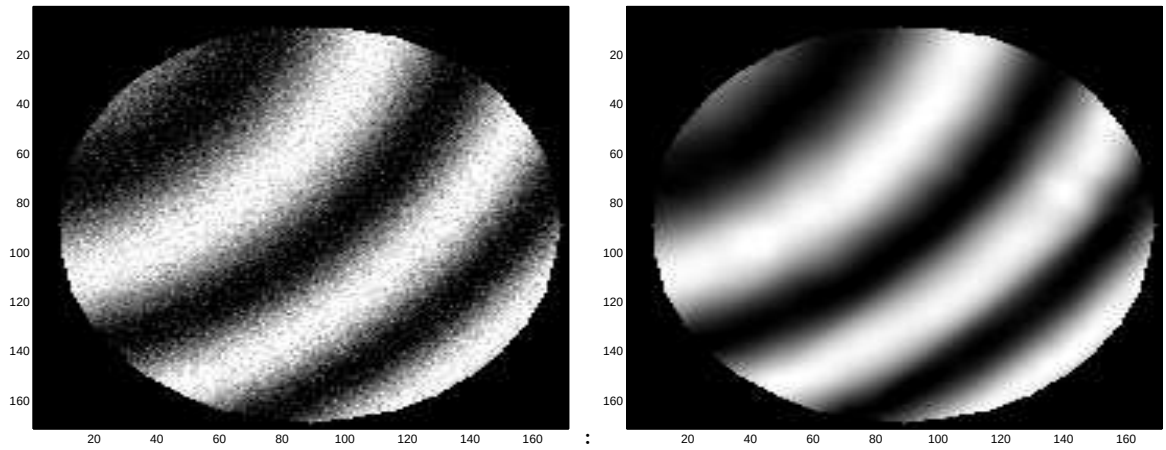

Figure 4.7: Noised image of $p = 1.5$ and the denoised image with the TV-L^p model of $p = 1.5$

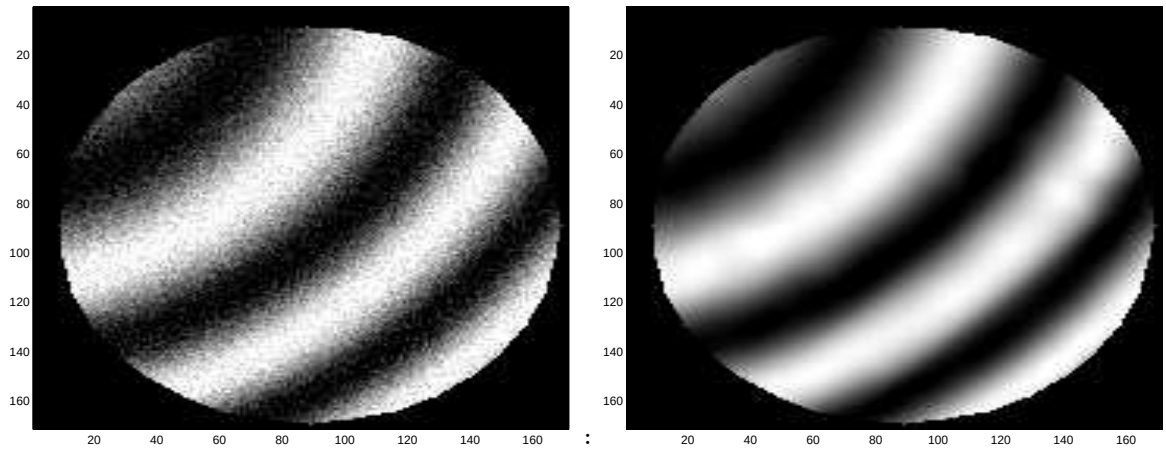

Figure 4.8: Noised image of $p = 2$ and the denoised image with the TV-L^p model of $p = 2$

Chapter 5

Image Segmentation and Triangulation

5.1 Level Set Method

In the application of image segmentation, we can use an interface(a curve) to separate one region from another. To evolve the interface we can assign a force F to control the movement of each point of the interface. The force F is usually given according to some physical mechanisms, for example, gravity, the ratio of the fluid density, and the surface tension between two regions. In the figure 5.1, the interface in red decompose the square region into two regions and it is expanding under a force F.

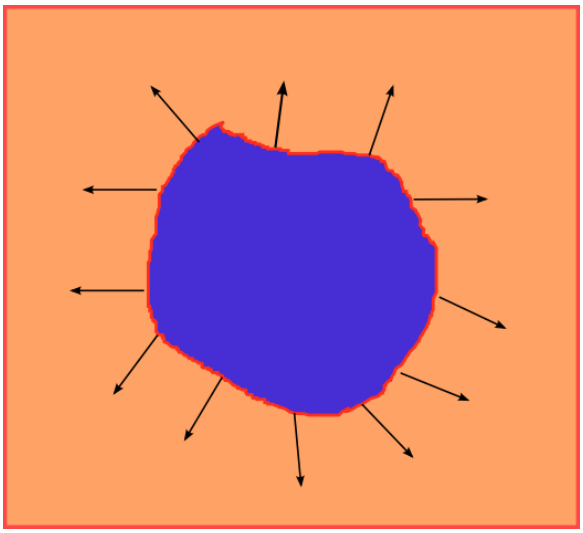

Figure 5.1: Interface involves under forces.

However things get pretty complicated when one interface breaks into two interfaces or when it tries to cross over itself. Therefore, rather than following the interface, the level set method introduced by Osher and Sethian [44] considers an interface as an intersection of

a surface and the x-y plane, or in another words, the zero-level contour of a surface. For example, in two dimensions, the level set method amounts to representing a closed curve Γ in a plane as the zero level set of a two-dimensional auxiliary function ϕ, i.e.,

$$\Gamma = \{(x, y) \,|\, \phi(x, y) = 0\},$$

and manipulating Γ *implicitly* by tracing the surface function $\phi(x, y)$ instead. In figure 5.2, the intersection of red surface ϕ and the blue x-y plane yields the cutting planes in the first row. The boundary of the gray region is the interface Γ. One can see that although the interface breaks into two curves, the topology of the surface remains unchanged. At first

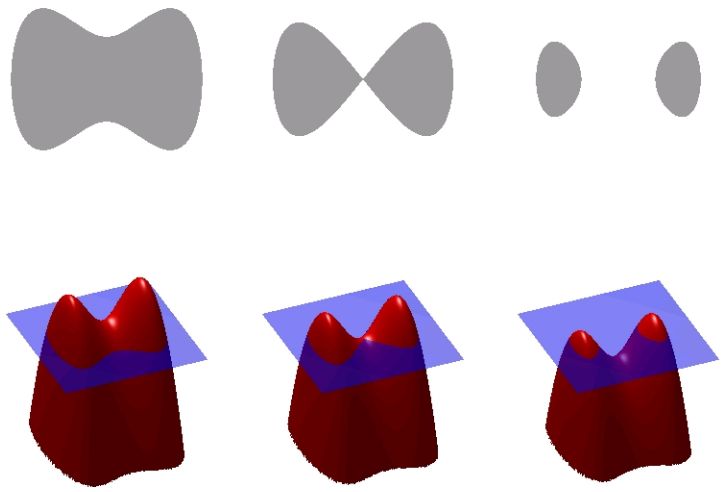

Figure 5.2: Demonstration of the topology's changing of an interface with level set method. Figure is created by Oleg Alexandrov.

glance, it might not be a good idea to trade a problem of a moving curve into a problem of moving surface. Because in this case we need to assign a force to each point on the whole domain, instead of the curve only. It seems it will add to the cost of calculation. However as a tradeoff, the level set method processes some more critical properties, e.g., all the complicated problems of breaking and merging curves.

5.2 Active Contour Model

The active contour method proposed in [16] by Tony F. Chan and Luminita A. Vese originates from the idea of the level set method. Its basic idea is to evolve a closed curve to detect objects in an image, subject to the minimization of an energy defined in (5.1) below. For simplicity, let us assume that the image u is formed by two regions of piecewise-constant intensities of two distinct values u_1 and u_2 and they are separated by a contour $C_0 := \{x : \phi(x) = 0, x \in \Omega\}$. The goal is to find the "fittest" boundary C which best approximates C_0. One numerically computes an approximation C of C_0. Then the image is segmented into two distinguished regions: $\Omega_1 := \{x : \phi(x) > 0\}$ and $\Omega_2 := \{x : \phi(x) < 0\}$. In [16] the research considered the following minimization functional on C:

$$F(C) = \mu \text{Length}(C) + \nu \text{Area}(\Omega_1) + \int_{\Omega_1} |u(x) - u_1|^2 dxdy + \int_{\Omega_2} |u(x) - u_2|^2 dx, \qquad (5.1)$$

where C is a variable curve represented by level set $\{x : \phi(x) = 0, x \in \Omega\}$. Here $u_1 := u_1(\phi)$ and $u_2 := u_2(\phi)$ are the average values of the image in Ω_1 and Ω_2, respectively,

$$u_1 = \int_{\Omega_1} u(x, y)dxdy \text{ and } u_2 = \int_{\Omega_2} u(x, y)dxdy.$$

C_0 is approximated by the minimizer of the fitting term

$$\inf_C F(C). \qquad (5.2)$$

The existence and uniqueness of the problem (5.2) has been proved in [40]. In this chapter we mainly explain how to transform the problem into level set formulation and how to get its Euler-Lagrange equation.

Let $\phi(x, y)$ be the surface function associated to the interface C in the level set method, such that

$$\phi(x, y) := \begin{cases} > 0, & (x, y) \in \Omega_1 \\ = 0, & (x, y) \text{ on } C \\ < 0, & (x, y) \in \Omega_2. \end{cases}$$

Recall that the Heavisible function H and the Dirac Delta function δ are defined by

$$H(z) = \begin{cases} 1, & z \geq 0; \\ 0, & z < 0, \end{cases}$$

and

$$\delta(z) = \frac{d}{dz} H(z).$$

Then we have,

$$H(\phi(x,y)) = \begin{cases} 1, & (x,y) \in \Omega_1; \\ 0, & otherwise, \end{cases}$$

$$|\nabla H(\phi(x,y))| = \begin{cases} 1, & (x,y) \; on \; C; \\ 0, & otherwise, \end{cases}$$

and

$$|\nabla H(\phi(x,y))| = \delta(\phi(x,y))|\nabla\phi(x,y)|.$$

Therefore, the length of C, the areas of Ω_1 and Ω_2 can be written respectively as

$$\text{Length}(\phi = 0) = \int_\Omega \delta(\phi(x,y))|\nabla\phi(x,y)|dxdy,$$

$$\text{Area}(\Omega_1) = \int_\Omega H(\phi(x,y))dxdy,$$

and

$$\text{Area}(\Omega_2) = \int_\Omega 1 - H(\phi(x,y))dxdy.$$

Similarly u_1 and u_2 can be given as:

$$u_1(\phi) = \frac{\int_\Omega u_0(x,y)H(\phi(x,y))dxdy}{\int_\Omega H(\phi(x,y))dxdy}, \tag{5.3}$$

$$u_2(\phi) = \frac{\int_\Omega u_0(x,y)(1 - H(\phi(x,y)))dxdy}{\int_\Omega (1 - H(\phi(x,y)))dxdy}. \tag{5.4}$$

Moreover, we can rewrite the following integrations:

$$\int_{\Omega_1} |u_0(x,y) - u_1|^2 dxdy = \int_\Omega |u_0(x,y) - u_1|^2 H(\phi(x,y))dxdy,$$

$$\int_{\Omega_2} |u_0(x,y) - u_2|^2 dxdy = \int_{\Omega} |u_0(x,y) - u_2|^2 (1 - H(\phi(x,y))|dxdy.$$

However, since the Heavisible function H and Dirac Delta function δ are not differentiable, we use the following regularizations instead,

$$H_\varepsilon(x) = \frac{1}{2}(1 + \frac{2}{\pi} arctan(\frac{x}{\varepsilon})),$$

$$\delta_\varepsilon(x) = \frac{\varepsilon^2}{(\pi(\varepsilon^2 + x^2))}.$$

Now we can rewrite the energy function (5.1) as

$$\begin{aligned} F_\varepsilon(u_1, u_2, \phi) &= \mu \int_\Omega \delta_\varepsilon(\phi)|\nabla\phi| dxdy \\ &+ \nu \int_\Omega H_\varepsilon(\phi) dxdy \\ &+ \lambda_1 \int_\Omega |u_0 - u_1|^2 H_\varepsilon(\phi) dxdy \\ &+ \lambda_2 \int_\Omega |u_0 - u_2|^2 (1 - H_\varepsilon(\phi)) dxdy \end{aligned} \tag{5.5}$$

And the minimization problem (5.2) is transformed to

$$\min_\phi \{F_\varepsilon(\phi)\}. \tag{5.6}$$

Since the energy functional (5.5) is strictly convex, we just to need find a local minimum, which is the solution of the Euler-Lagrange equation. Now we calculate the Euler-Lagrange equation associated to the minimization problem of the energy function (5.5). First, notice that

$$\text{div}\left(\delta_\varepsilon(\phi)\frac{\nabla\phi}{|\nabla\phi|}\right) = \delta'_\varepsilon(\phi)|\nabla\phi| + \delta_\varepsilon(\phi)\text{div}\left(\frac{\nabla\phi}{|\nabla\phi|}\right).$$

Let $\mathbf{n}$ be the normal vector of $\partial\Omega$ and $\psi \in C_0^\infty(\Omega)$ the test function. When $t = 0$, we have

$$\begin{aligned}
& \frac{d}{dt}\int_\Omega \delta_\varepsilon(\phi + t\psi)|\nabla(\phi + t\psi)|dxdy \\
= & \int_\Omega \delta'_\varepsilon(\phi)\psi|\nabla\phi|dxdy + \int_\Omega \delta_\varepsilon(\phi)\frac{\nabla\phi}{|\nabla\phi|}\cdot\nabla\psi \\
= & \int_\Omega \delta'_\varepsilon(\phi)\psi|\nabla\phi|dxdy + \int_{\partial\Omega} \delta_\varepsilon(\phi)\frac{\nabla\phi}{|\nabla\phi|}\cdot\mathbf{n}\,\psi dxdy - \int_\Omega \mathrm{div}\left(\delta_\varepsilon(\phi)\frac{\nabla\phi}{|\nabla\phi|}\right)\psi dxdy \\
= & \int_\Omega \delta'_\varepsilon(\phi)\psi|\nabla\phi|dxdy - \int_\Omega \mathrm{div}\left(\delta_\varepsilon(\phi)\frac{\nabla\phi}{|\nabla\phi|}\right)\psi dxdy \\
= & -\int_\Omega \delta_\varepsilon \mathrm{div}\left(\frac{\nabla\phi}{|\nabla\phi|}\right)\psi dxdy,
\end{aligned}$$

and

$$\frac{d}{dt}H_\varepsilon(\phi + t\psi) = \delta_\varepsilon(\phi)\psi.$$

Assuming $\frac{d}{dt}u_1(\phi + t\psi)|_{t=0} = 0$ and $\frac{d}{dt}u_2(\phi + t\psi)|_{t=0} = 0$, we have the following Euler-Lagrange Equation of (5.6),

$$\begin{cases} 0 = \delta_\varepsilon(\phi)\left(\mu\mathrm{div}\left(\frac{\nabla\phi}{|\nabla\phi|}\right) - \nu - \lambda_1|u_0 - u_1|^2 + \lambda_2|u_0 - u_2|^2\right), & \text{in } \Omega; \\ \frac{\partial\phi}{\partial\mathbf{n}} = \nabla\phi\cdot\mathbf{n} = 0, & \text{on } \partial\Omega. \end{cases} \tag{5.7}$$

Using the method of steepest descent, we can approximate the solution of the Euler-Lagrange equation above by evolving the following time-flow partial differential equation:

$$\begin{cases} \frac{\partial\phi}{\partial t} = \delta_\varepsilon(\phi)\left(\mu\mathrm{div}\left(\frac{\nabla\phi}{|\nabla\phi|}\right) - \nu - \lambda_1|u_0 - u_1|^2 + \lambda_2|u_0 - u_2|^2\right), & \text{in } (0,+\infty)\times\Omega; \\ \frac{\partial\phi}{\partial\mathbf{n}} = 0, & \text{on } (0,+\infty)\times\partial\Omega; \\ \phi(0,x,y) = \phi_0(x,y), & \text{when } t = 0, (x,y)\in\Omega. \end{cases} \tag{5.8}$$

After discretizing the above time flow PDE, in each numerical iteration, we need to update u_1 and u_2 according to (5.3) and (5.4).

To deal with complicated images with more than two distinguished regions, we propose to solve this problem by applying the active contour method iteratively. Figure 5.2 gives an example which shows the process of the iterations. Figure (a) is the original image to be segmented. (b) is the resulting image after the first iteration of the active contour method.

The original images is divided into two regions(black and white), or five separate regions A,B,C,D and E. In figure (c) we go on to divide region A into three separate regions A1,A2 and A4 by one more iteration of active contour method. (d) shows the combination of the results of these two iterations and assigning different colors to each separate region.

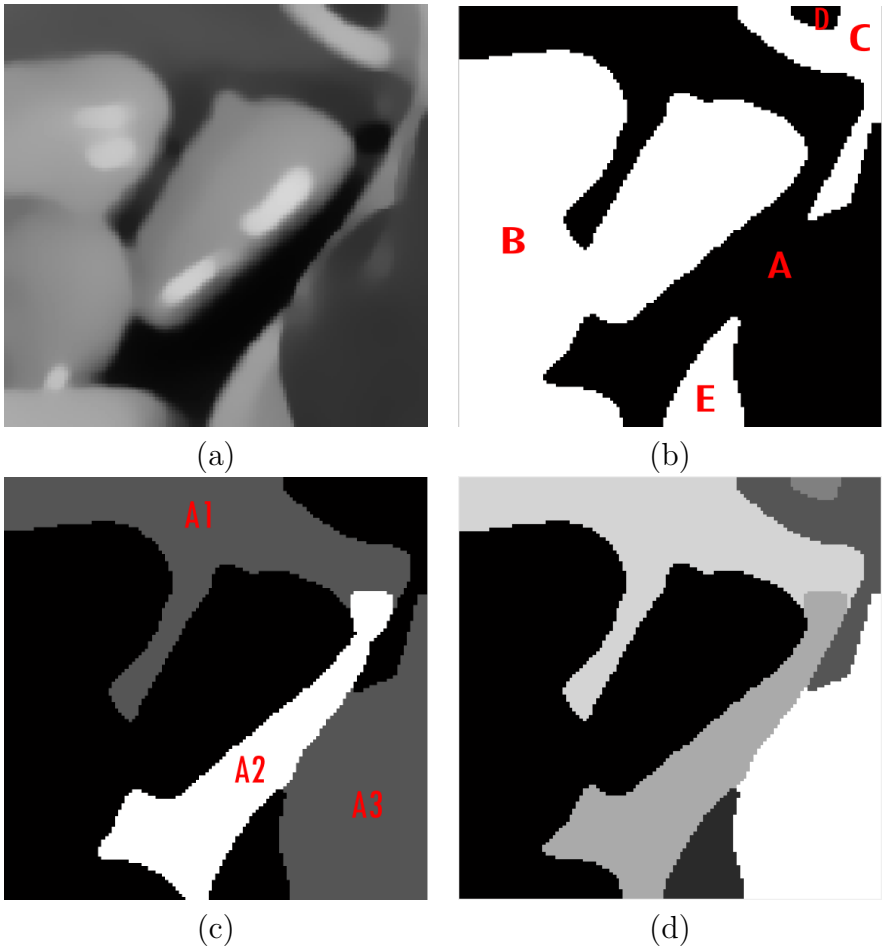

(a) (b) (c) (d)

Figure 5.3: Application of iterative active contours in image segmentation.

5.3 Edge-adaptive Triangulation

Triangulation is a fundamental technique in spline application. The effect of spline function approximation and fitting are known to depend on the shape of the triangulation $\triangle$. For example, as shown in Theorem 2.1.6, the approximation property of spline functions depends on the power of $|\triangle|$, the length of the longest side of all triangles in $\triangle$. Since the running

time of spline function fitting is in direct proportion to the number of triangles, there is a limit to the number of triangles we can use in a triangulation. Therefore when the number is fixed, we would like all triangles have similar area and are as much close to equilateral as possible. Meanwhile the locations of triangles also play a role. For example, if a triangle lies on an edge of an image, to approximate the edge well, we need to use spline functions of high degree, which adds on to the running time. Therefore, we would like to place our triangles at the two sides of an edge, rather than across it. Based on these ideas, we propose the following edge-adaptive triangulation algorithm.

Algorithm 5.3.1 (Edge-adaptive Triangulation) *Suppose we want to generate a triangulation of a given region such that:*

- *Triangles have similar areas.*
- *Triangle are almost equilateral.*
- *Triangles are placed at the two sides of edges.*

Suppose in a pre-step we can attain the edges of the image. Then we generate such a triangulation in the following steps:

1. *Initiate the vertices of the triangulation by using grid points.*
2. *Delete those vertices which are outside the region.*
3. *Delete those vertices which are too close to the edges and the boundary of the region.*
4. *Add vertices on the edges.*
5. *Add vertices on the boundary of the region.*
6. *Use the Delaunay triangulation algorithm to generate triangles based on the vertices.*

The edge-adaptive triangulation algorithm we propose requires a pre-step to generate the a graph of the edges of the given region. In practice, we generate such a graph of the edges by taking the derivative of the solution of the active contour model. The reasons we use active contour model include:

1. Edges generated in such way are closed and continuous.

2. There is no intersection of edges.

3. The areas enclosed in each edge are known.

Reason (1) and (2) make the process to trace edges very handy and precise. Reason (3) makes it possible to group together those triangles belonging to the same region.

Fig. 5.4 gives a demonstration of the six steps to generate the edge-adaptive triangulation.

5.4 Numerical Results

5.4.1 The Finite Difference Scheme

In this section we propose a finite difference scheme to solve the partial differential equation (5.8). Suppose $\Omega = [0,1] \times [0,1]$, $h = \frac{1}{N}$. Given $u_{i,j} = u(ih, jh)$, then the forward difference, backward difference, and central difference are defined by

$$\Delta_x^+ u_{i,j} := u_{i+1,j} - u_{i,j}, \quad \Delta_y^+ u_{i,j} := u_{i,j+1} - u_{i,j};$$

$$\Delta_x^- u_{i,j} := u_{i,j} - u_{i-1,j}, \quad \Delta_y^- u_{i,j} := u_{i,j} - u_{i,j-1};$$

and

$$\Delta_x^c u_{i,j} := u_{i+1,j} - u_{i-1,j}, \quad \Delta_y^c u_{i,j} := u_{i,j+1} - u_{i,j-1}.$$

All the three differences above can be used to approximate the first derivative $\dfrac{\partial}{\partial x}$ and $\dfrac{\partial}{\partial y}$. It is up to the user to decide which discretization to use. For example we can approximate

$$|\nabla u|^2 \simeq \left(\frac{\Delta_x^+ u_{i,j}}{h}\right)^2 + \left(\frac{\Delta_y^c u_{i,j}}{2h}\right)^2.$$

However when we design our scheme, a thumb of rule to follow is the scheme should treat all grid points "fairly", or in another words using all grid points equal times. For example, if we use forward difference Δ_x^+ to approximate the first derivative then we should use backward difference Δ_x^- for the second derivative, e.g.,

$$u_{xx} \simeq \frac{\Delta_x^-(\Delta_x^+ u_{i,j})}{h^2} = \frac{u_{i+1,j} - 2u_{i,j} + u_{i-1,j}}{h^2}.$$

Or in another words, the grid points we use should be symmetrically located around u_{ij}, e.g.,

$$u_{xy} \simeq \frac{\Delta_x^c \Delta_y^c u_{i,j}}{(2h)^2} = \frac{u_{i+1,j+1} - u_{i-1,j+1} - u_{i+1,j-1} + u_{i-1,j-1}}{(2h)^2}.$$

Following the same rule, we use the scheme below to approximate the Laplacian operator,

$$\begin{aligned} \Delta u &= \operatorname{div}(\nabla u) \simeq \frac{\Delta_x^-}{h}\left(\frac{\Delta_x^+ u_{ij}}{h}\right) + \frac{\Delta_y^-}{h}\left(\frac{\Delta_y^+ u_{ij}}{h}\right) \\ &= \frac{1}{h^2}(\Delta_x^-\Delta_x^+ u_{ij} + \Delta_y^-\Delta_y^+ u_{ij}) = \frac{u_{i,j+1} - 2u_{i,j} + u_{i,j-1}}{h^2} + \frac{u_{i,j+1} - 2u_{i,j} + u_{i,j-1}}{h^2}. \end{aligned}$$

There are two basic types of finite difference schemes, the explicit and implicit schemes. An explicit scheme is one which calculates the state of the system at a future time from the state at the current time, i.e., if $u^n = u(x, n\Delta t)$, $u^{n+1} = G(u^n)$ for some operator G. In an implicit scheme, we find an approximation for the future state by solving a system of equation involving both the future and current time step, i.e., $G(u^{n+1}) = u^n$. Generally, we can attain higher order of approximation than the explicit scheme. However, for nonlinear operator G, an implicit scheme is hard to implement.

Since we are using finite difference scheme to approximate (5.8), we have to assume the domain Ω is rectangular and the initial values of on grid points $\{u_{ij}^0\}$ are given. For non rectangular domain, we can expand it to a rectangular domain by multiplying a characteristic function.

We design our numerical scheme based on the predictor-corrector method. In numerical analysis, a predictor-corrector is a two-step process which first calculates an rough approximation of the desired quality, and then refines this initial approximation by another mean.

Denote r_i the discretion of the nonlinear function $\frac{1}{\sqrt{1+|\nabla\phi|^2}}$ in the diffusion term $\mathrm{div}\left(\frac{\nabla\phi}{\sqrt{1+|\nabla\phi|^2}}\right)$. In order to follow the "fair" rule, we use two sets of approximations of r_i. Since it is a nonlinear function, we use the explicit scheme here.

$$r_{ij}^x = \frac{1}{\sqrt{1+((\triangle_-^x\phi_{i,j}^n)/h)^2+((\triangle_c^y\phi_{i,j}^n)/2h)^2}}$$

$$r_{ij}^y = \frac{1}{\sqrt{1+((\triangle_-^y\phi_{i,j}^n)/h)^2+((\triangle_c^x\phi_{i,j}^n)/2h)^2}}$$

Then we have

$$\begin{aligned}
&\mathrm{div}\left(\frac{\nabla\phi}{\sqrt{1+|\nabla\phi|^2}}\right)\\
\simeq\ & \frac{1}{h^2}\left(\Delta_x^+(\Delta_x^-\phi_{ij}r_{ij}^x)+\Delta_y^+(\Delta_y^-\phi_{ij}r_{ij}^y)\right)\\
=\ & \frac{1}{h^2}\left(\phi_{i+1j}r_{i+1j}^x+\phi_{i-1j}r_{ij}^x+\phi_{ij+1}r_{ij+1}^y+\phi_{ij-1}r_{ij}^y-\phi_{ij}(r_{i+1j}^x+r_{ij}^x+r_{ij+1}^y+r_{ij}^y)\right).
\end{aligned}$$

Let

$$C_{ij} = \nu+\lambda_1(u_{i,j}-u_{i,j}^1)^2-\lambda_2(u_{i,j}-u_{i,j}^2)^2.$$

In the prediction step, the implicit discrete form of (5.8) is given as follows:

$$\begin{aligned}
\frac{\phi_{i,j}^{n+1}-\phi_{i,j}^n}{\triangle t} =\ & \frac{\mu\delta(\phi_{i,j}^{n+1})}{h^2}(r_{ij}^x\phi_{i-1,j}^{n+1}+r_{i+1j}^x\phi_{i+1,j}^{n+1}+r_{ij}^y\phi_{i,j-1}^{n+1}+r_{ij+1}^y\phi_{i,j+1}^{n+1})\\
&-\frac{\mu\delta(\phi_{i,j}^{n+1})}{h^2}(r_{i+1j}^x+r_{ij}^x+r_{ij+1}^y+r_{ij}^y)\phi_{i,j}^{n+1}-\delta(\phi_{i,j}^{n+1})C_{ij}\\
&+\frac{\tau}{h^2}(r_{ij}^x\phi_{i-1,j}^{n+1}+r_{i+1j}^x\phi_{i+1,j}^{n+1}+r_{ij}^y\phi_{i,j-1}^{n+1}+r_{ij+1}^y\phi_{i,j+1}^{n+1})\\
&-\frac{\tau}{h^2}(r_{i+1j}^x+r_{ij}^x+r_{ij+1}^y+r_{ij}^y)\phi_{i,j}^{n+1}.
\end{aligned} \tag{5.9}$$

Then move all the linear terms of $\phi_{i,j}^{n+1}$ to the left hand side:

$$\begin{aligned}
&\left(1+\left(\frac{\mu\triangle t}{h^2}\delta(\phi_{i,j}^{n+1})+\frac{\tau\triangle t}{h^2}\right)(r_{ij}^x+r_{i+1j}^x+r_{ij}^y+r_{ij+1}^y)\right)\phi_{i,j}^{n+1}-\phi_{i,j}^n \qquad (5.10)\\
=\ & \triangle t\delta(\phi_{i,j}^{n+1})\left(\frac{\mu}{h^2}(r_{ij}^x\phi_{i-1,j}^{n+1}+r_{i+1j}^x\phi_{i+1,j}^{n+1}+r_{ij}^y\phi_{i,j-1}^{n+1}+r_{ij+1}^y\phi_{i,j+1}^{n+1})\right)-\triangle t\delta(\phi_{i,j}^{n+1})C_{ij}\\
&+\frac{\tau\triangle t}{h^2}(r_{ij}^x\phi_{i-1,j}^{n+1}+r_{i+1j}^x\phi_{i+1,j}^{n+1}+r_{ij}^y\phi_{i,j-1}^{n+1}+r_{ij+1}^y\phi_{i,j+1}^{n+1}).
\end{aligned}$$

Next we replace ϕ^{n+1} in all nonlinear terms by ϕ^n:

$$\begin{aligned}
&\left(1+\left(\frac{\mu\triangle t}{h^2}\delta(\phi^n_{i,j})+\frac{\tau\triangle t}{h^2}\right)(r^x_{ij}+r^x_{i+1j}+r^y_{ij}+r^y_{ij+1})\right)\phi^{n+1}_{i,j}-\phi^n_{i,j} \qquad (5.11)\\
=\;& \triangle t\delta(\phi^n_{i,j})\left(\frac{\mu}{h^2}(r^x_{ij}\phi^{n+1}_{i-1,j}+r^x_{i+1j}\phi^{n+1}_{i+1,j}+r^y_{ij}\phi^{n+1}_{i,j-1}+r^y_{ij+1}\phi^{n+1}_{i,j+1})\right)-\triangle t\delta(\phi^n_{i,j})C_{ij}\\
&+\frac{\tau\triangle t}{h^2}(r^x_{ij}\phi^{n+1}_{i-1,j}+r^x_{i+1j}\phi^{n+1}_{i+1,j}+r^y_{ij}\phi^{n+1}_{i,j-1}+r^y_{ij+1}\phi^{n+1}_{i,j+1}).
\end{aligned}$$

To predict ϕ^{n+1}, we replace all linear terms of ϕ^{n+1} by ϕ^n on the right hand side of (5.11) to get the predictor $\bar{\phi}^{n+1}$,

$$\begin{aligned}
&\left(1+\left(\frac{\mu\triangle t}{h^2}\delta(\phi^n_{i,j})+\frac{\tau\triangle t}{h^2}\right)(r^x_{ij}+r^x_{i+1j}+r^y_{ij}+r^y_{ij+1})\right)\bar{\phi}^{n+1}_{i,j}-\phi^n_{i,j} \qquad (5.12)\\
=\;& \triangle t\delta(\phi^n_{i,j})\left(\frac{\mu}{h^2}(r^x_{ij}\phi^{n}_{i-1,j}+r^x_{i+1j}\phi^{n}_{i+1,j}+r^y_{ij}\phi^{n}_{i,j-1}+r^y_{ij+1}\phi^{n}_{i,j+1})\right)-\triangle t\delta(\phi^n_{i,j})C_{ij}\\
&+\frac{\tau\triangle t}{h^2}(r^x_{ij}\phi^{n}_{i-1,j}+r^x_{i+1j}\phi^{n}_{i+1,j}+r^y_{ij}\phi^{n}_{i,j-1}+r^y_{ij+1}\phi^{n}_{i,j+1}).
\end{aligned}$$

Finally, in the correction step we replace ϕ^{n+1} in all nonlinear terms, and the right hand side of (5.11) with $\bar{\phi}^{n+1}$,

$$\begin{aligned}
&\left(1+\left(\frac{\mu\triangle t}{h^2}\delta(\bar{\phi}^{n+1}_{i,j})+\frac{\tau\triangle t}{h^2}\right)(r^x_{ij}+r^x_{i+1j}+r^y_{ij}+r^y_{ij+1})\right)\phi^{n+1}_{i,j}-\phi^n_{i,j} \qquad (5.13)\\
=\;& \delta(\bar{\phi}^{n+1}_{i,j})\left(\frac{\mu}{h^2}(r^x_{ij}\bar{\phi}^{n+1}_{i-1,j}+r^x_{i+1j}\bar{\phi}^{n+1}_{i+1,j}+r^y_{ij}\bar{\phi}^{n+1}_{i,j-1}+r^y_{ij+1}\bar{\phi}^{n+1}_{i,j+1})\right)-\delta(\bar{\phi}^{n+1}_{i,j})C_{ij}\\
&+\frac{\tau}{h^2}(r^x_{ij}\bar{\phi}^{n+1}_{i-1,j}+r^x_{i+1j}\bar{\phi}^{n+1}_{i+1,j}+r^y_{ij}\bar{\phi}^{n+1}_{i,j-1}+r^y_{ij+1}\bar{\phi}^{n+1}_{i,j+1}).
\end{aligned}$$

Solving the above equation, we get ϕ^{n+1}.

5.4.2 Numerical Examples

We first apply the Chan-Vese active contour method in variate image processing problems: such as texture detecting, object identification and image segmentation. Then we give two examples of edge-adaptive triangulation based on the segmentation by active contour method. In the following, we use the term "ACM" for short "Active Contour Method".

Example 5.4.1 *In Fig. 5.5 and Fig. 5.6, we demonstrate how to use the active contour model to identify objects. In the pictures of zebra and leopard, since the gray-level of the*

animals' body is similar to the background, we can not apply the ACM to separate the animals from the background directly. Therefore we first calculate the structure tensors (cf.[10]) of the images. Applying ACM on the graph of the structure tensor, we are able to separate the animals from the background. Using a similar idea, we can use ACM to identify different texture. A such example is given in Fig. 5.7.

Example 5.4.2 *In Fig. 5.8, we study the difference of ACM on grey-level image and gradient level image. (b) is the segmentation after applying ACM on the grey-level image directly. In this case the two coarse patches are unable to be distinguished from the background. On the other hand, applying ACM to the gradient image in (c), the two coarse patches are able to be singled out.*

Example 5.4.3 *We can also use ACM to identify the locations of clustered data. Suppose some data are spreading over an area with different densities. Our purpose is to locate those regions of highest data density and classify them. We can consider this as segmentation problem and use ACM to solve it. A such example is shown in Fig. 5.9.*

Example 5.4.4 *Fig. 5.10 and Fig. 5.11 show two examples of the edge-adaptive triangulation based on edge graphs from the ACM-segmentation.*

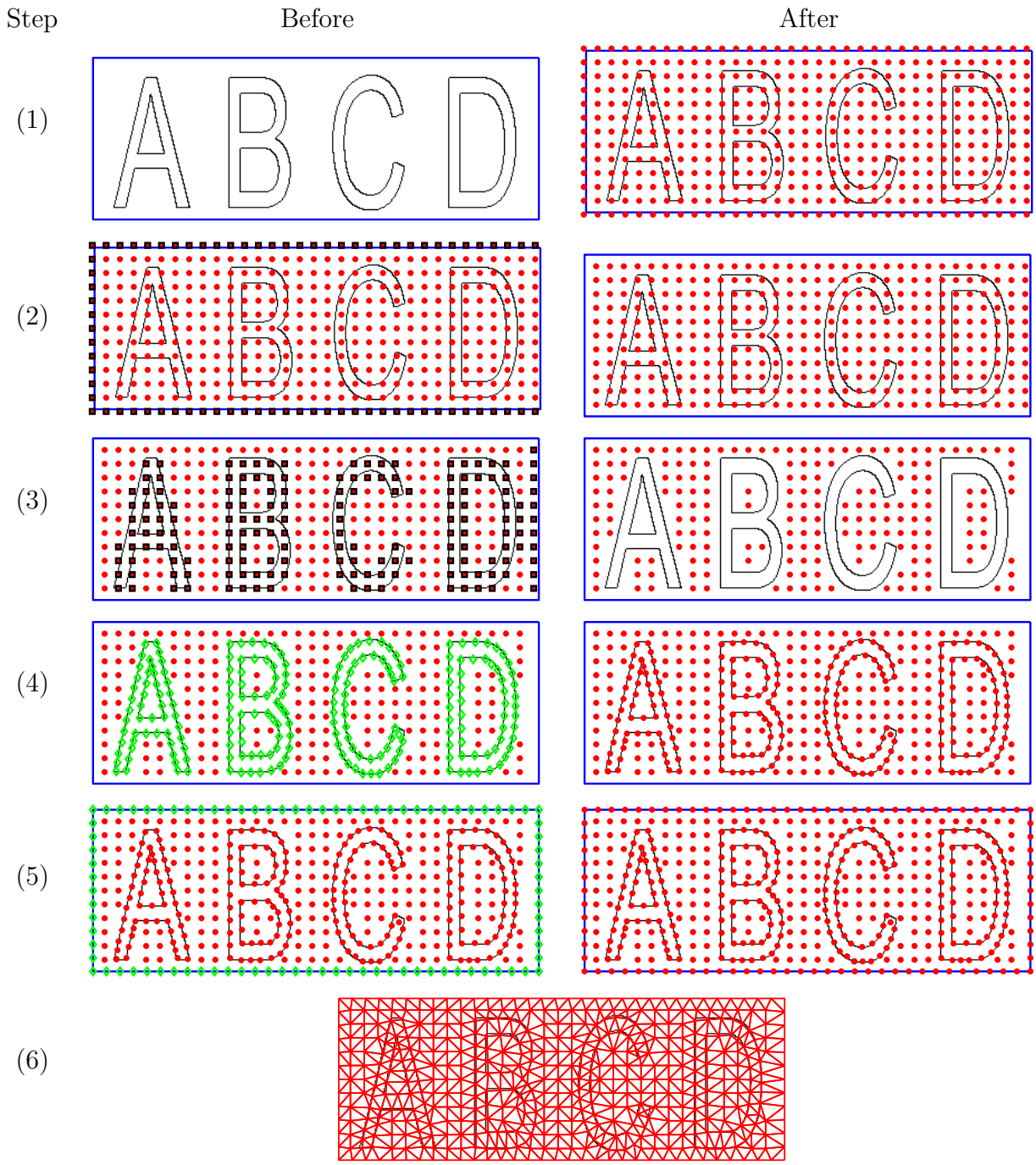

Figure 5.4: Demonstration of the six steps in the edge-adaptive triangulation algorithm. Blue lines are boundaries. Black curves are edges. In each step, points will be deleted are marked in black, and points will be added are marked in blue.

(a): Original Image

(b): Structure Tensor

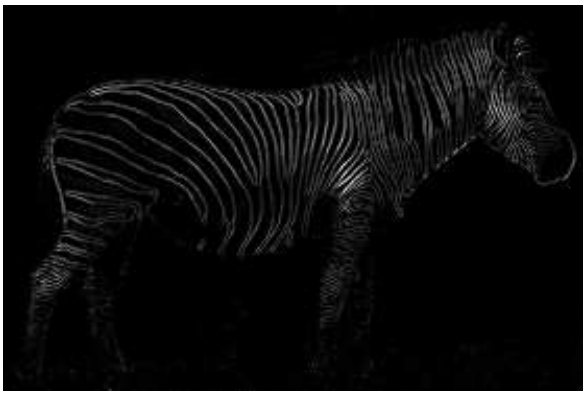

(c) The ACM-Segmentation

(d):Edge

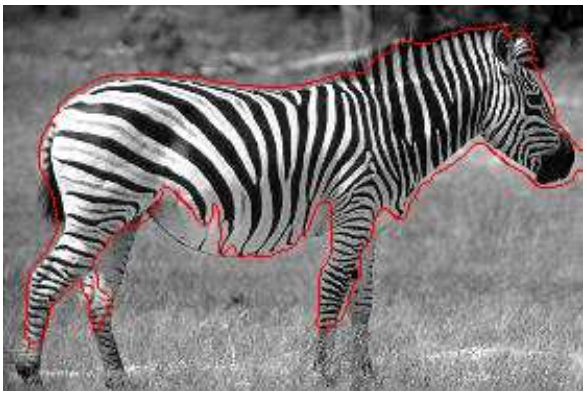

Figure 5.5: (a) An image of a zebra. (b) The structure tensor of the zebra. (c)ACM-segmentation of the structure tensor in (b). (d)The edge of the ACM-segmentation.

(a): Original Image

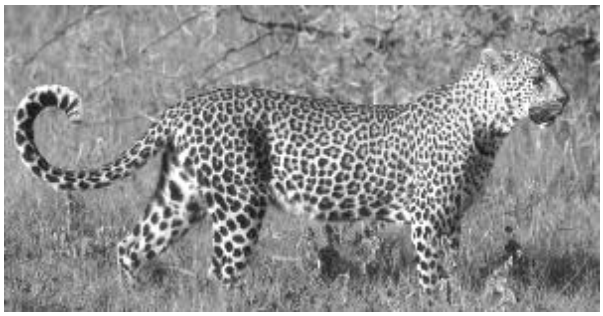

(b):Structure Tensor

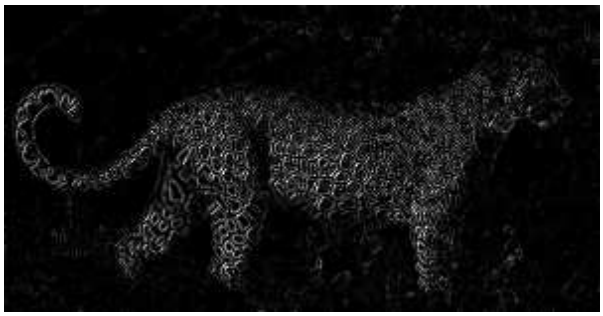

(c): ACM-Segmentation

(d): Edge

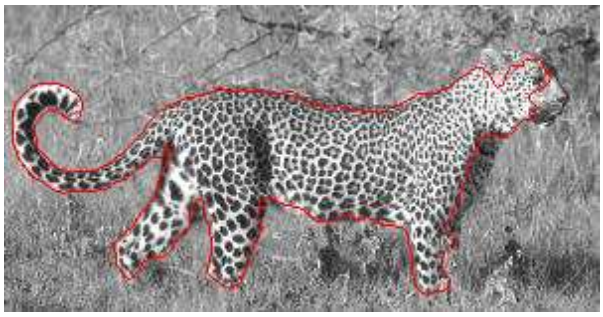

Figure 5.6: (a) An image of a leopard. (b) The structure tensor of the leopard. (c) The ACM-segmentation of the structure tensor in (b). (d) The edge of the ACM-segmentation.

(a):Original Image

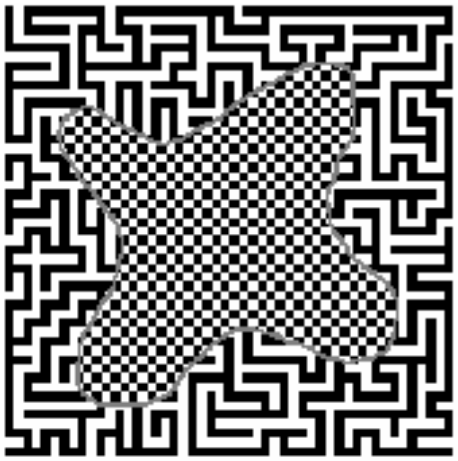

(b):Structure Tensor

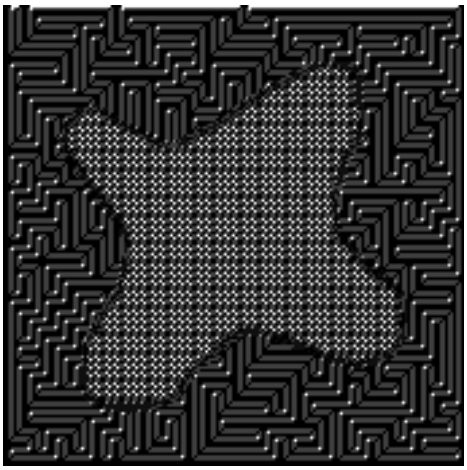

(c):Segmentation

(d):Edge

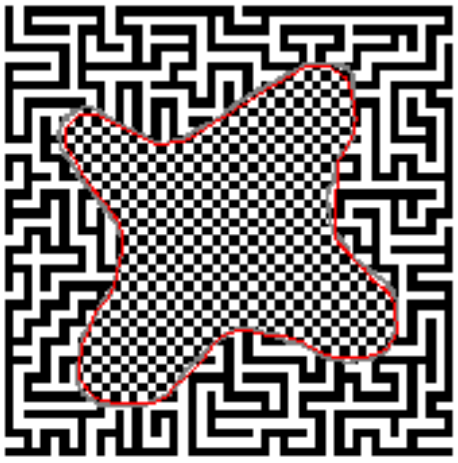

Figure 5.7: Original image of some special textures. (b) The structure tensor of the texture image. (c) ACM-segmentation of the structure tensor in (b). (d) Boundary of the ACM-segmentation.

(a): Original Image

(b): ACM-Segmentation of grey-level

(c): Gradient Image

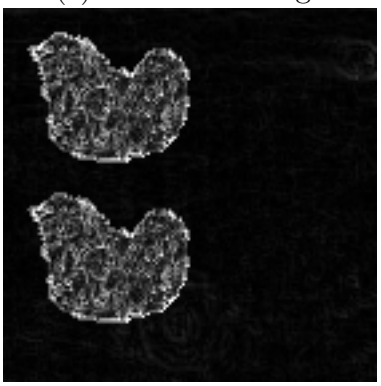

(d): ACM-Segmentation of gradient level

Figure 5.8: ACM-Segmentations based on grey level and gradient level respectively

(a):Clustered Data

(b):ACM-Segmentation

(c):Edges

(d): True Locations and Edges

Figure 5.9: In (a), some data are clustered together. In (b) the locations of clustered data are identified by ACM-segmentation. In (c) the identified locations are compared to the clustered data. In (d) the true locations of the clustered data are compared to the ACM-identified locations.

(a):Original Image

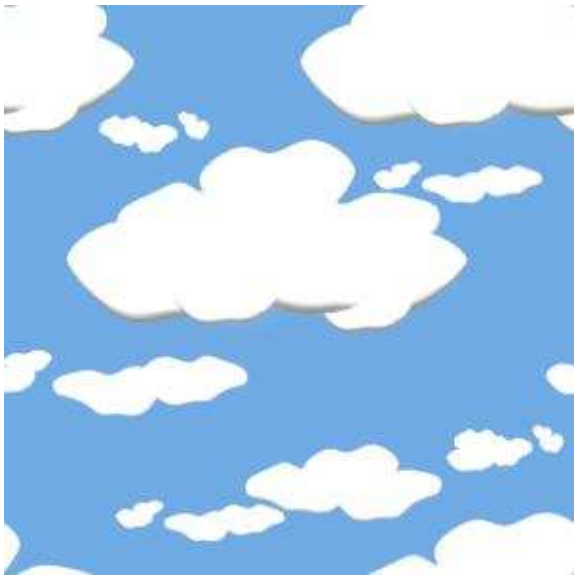

(b):ACM-Segmentation

(c):Original Image and Triangulation

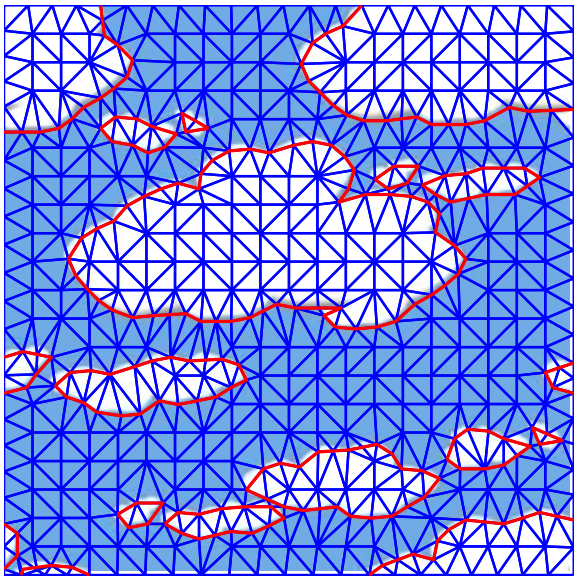

(d):Edges and Triangulation

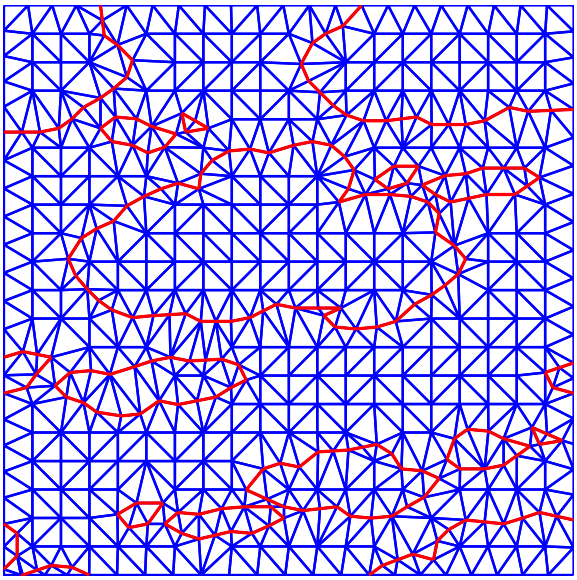

Figure 5.10: (a) The original image of clouds. (b) ACM-segment. (c) is the triangulation based on ACM-segmentation with original image as the background. (d) is the triangulation and edges from the ACM-segmentation.

(a):Original Image

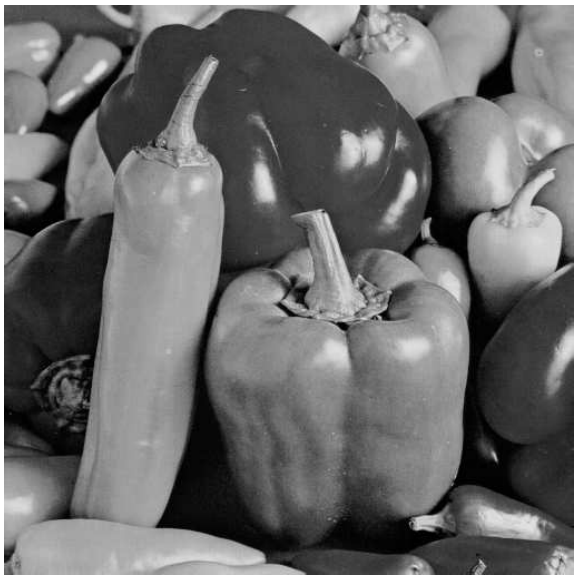

(b):ACM-Segmentation

(c):Original Image and Triangulation

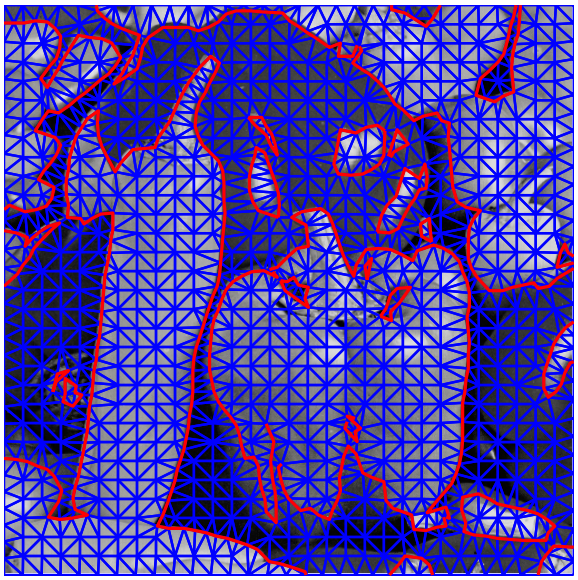

(d):Edges and Triangulation

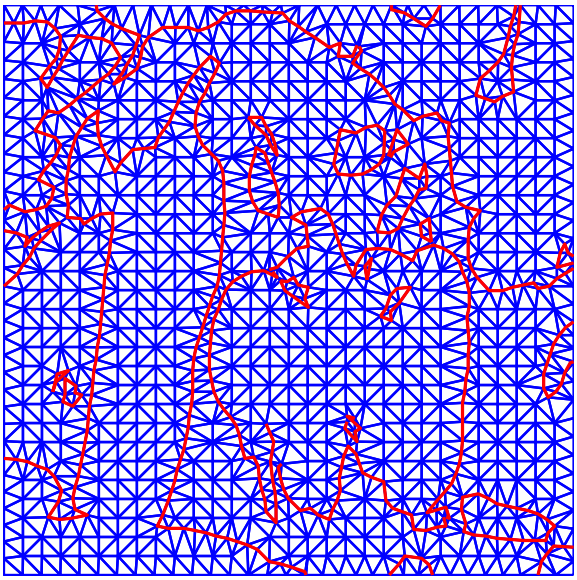

Figure 5.11: (a) is the original image of peppers. (b) is the ACM-segmentation. (c) is the triangulation based on the ACM-segmentation with original image as the background. (d) is the triangulation and the edges.

Bibliography

[1] Acar R., C.R. Vogel (1994): Analysis of bounded variation penalty methods for ill-posed problems, Inverse Problems, 10, 1217–229.

[2] Alliney, S. Digital filters as absolute norm regularizers. IEEE Transactions on Signal Processing. 40:6 (1992), pp. 1548–1562.

[3] Alliney, S. Recursive median filters of increasing order: a variational approach. IEEE Transactions on Signal Processing. 44:6 (1996), pp. 1346 – 1354.

[4] Alliney, S. A property of the minimum vectors of a regularizing functional defined by means of the absolute norm. IEEE Transactions on Signal Processing. 45:4 (1997), pp. 913–917.

[5] G. Aubert and P. Kornprobst, *Mathematical Problems in Image Processing*, Springer, 2006.

[6] G. Aubert and L. Vese. A variational method in image recovery. SIAM Journal of Numerical Analysis, 34E):1948-1979, 1997.

[7] L. Vese. Problemes variationnels et EDP pour Vanalyse d'images et revolution de courbes. PhD thesis, Universite de Nice Sophia-Antipolis, November 1996.

[8] G. Awanou, M. J. Lai, and P. Wenston, *The multivariate spline method for numerical solution of partial differential equations and scattered data interpolation*, in Wavelets and Splines: Athens 2005, edited by G. Chen and M. J. Lai, Nashboro Press, Nashville, TN, 2006, 24–74.

[9] G. Awanou and M. J. Lai, On the convergence rate of the augumented Lagrangian algorithm for the nonsymmetric saddle point problem, J. Applied Numerical Mathematics, (54) 2005, 122–134.

[10] T. Brox, J. Weickert, B. Burgeth, and P. Mráazek. Nonlinear structure tensors. Image and Vision Computing, 24(1):41–55, 2006.

[11] A. Chambolle, An algorithm for total variation minimization and applications, Journal of Mathematical Imaging and Vision, **20** (2004), Issue 1-2, 89-97.

[12] Chambolle, A., and Lions, P.-L.: Image recovery via total variation minimization and related problems, *Numer. Math.* **76**(2) (1997), 167-188.

[13] A. Chambolle and P.-L. Lions, Image recovery via total variation minimization and related problems, Numer. Math. **76**(1997), 167-188.

[14] A. Chambolle, R. A. DeVore, N. Lee, and B. J. Lucier, Nonlinear wavelet image processing: variational problems, compression, and noise removal through wavelet shrinkage, IEEE Trans. Image Process., **7**(1998), 319–335.

[15] T.F. Chan and S. Esedoglu, Aspects of total variation regularized L_1 function approximation, SIAM Journal on Applied Mathematics, 65 (2005), pp. 1817-1837.

[16] T. Chan, L. A. Vese, Active Contour Without Edge, IEEE Transactions on Image Processing, VOL. 10, No.2, 2001, 266-277.

[17] Chan, T. F.; Vese, L. A. Active contour and segmentation models using geometric PDE's for medical imaging, Geometric methods in bio-medical image processing, 6375, Math. Vis., Springer, Berlin, 2002,

[18] F. Ciarlet, The Finite Element Method for Elliptic Problems, North- Holland, Amsterdam, New York, 1978.

[19] A. Cohen, R. DeVore, P. Petrushev, and H. Xu, Nonlinear approximation and the space BV, American Journal of Mathematics 121 (1999), 587-628.

[20] D. C. Dobson and C. R. Vogel. Convergence of an iterative method for total variation denoising. SIAM J. Numer. Anal., 34(1997), 1779–1791.

[21] L. Demaret, N. Dyn, and A. Iske, Image compression by linear splines over adaptive triangulations, IEEE Signal Process Letters, 86 (2006) 1604–1616.

[22] L. Demaret and A. Iske, Adaptive Image Approximation by Linear Splines over Locally Optimal Delaunay Triangulations, IEEE Signal Process Letters,

[23] V. Duval, J. Aujol, and Y. Gousseau, The TV-L_1 model: a geometric point of view,

[24] Duval, V. J.-F. Aujol and L. Vesse, A projected gradient algorithm for color image decomposition, CMLA Preprint 2008–21.

[25] I. Ekeland and R. Temam, Convex Analysis and Variational Problem, Cambridge University Press, 1999.

[26] L. C. Evans, Partial Differential Equations, American Mathematical Society, 2002, pp 629-631.

[27] Faádi Bruno, F. , "Sullo sviluppo delle Funzioni" (in Italian), Annali di Scienze Matematiche e Fisiche 6, 1855, pp 479-80.

[28] X. Feng and A. Prohl. Analysis of total variation flow and its finite element approximations, Math. Mod. Num. Anal., 37(2003) 533–556, 2003.

[29] X. Feng, M. von Oehsen, and A. Prohl. Rate of convergence of regularization procedures and finite element approximations for the total variation flow, Numer. Math., 100(2005), 441–456.

[30] Enrico Giusti, Minimal Surfaces and Functions of Bounded Variation, Birkh$^{'}$auser Boston, Inc., 1984.

[31] M. von Golitschek, M. J. Lai, L. L. Schumaker, *Error bounds for minimal energy bivariate polynomial splines*, Numer. Math. 93(2002), 315–331.

[32] M. von Golitschek and L. L. Schumaker, *Penalized least squares fitting*, Serdica 18 (2002), 1001–1020.

[33] M. von Golitschek and L. L. Schumaker, *Bounds on projections onto bivariate polynomial spline spaces with stable local bases*, Const. Approx. 18(2002), 241–254.

[34] M. von Golitschek and L. L. Schumaker, *Penalized least squares fitting*, Serdica 18 (2002), 1001–1020.

[35] Q. Hong and M. -J. Lai, Bivariate splines for Image Enhancement, submitted, 2010.

[36] M.-J. Lai, Multivariate splines for data fitting and approximation, Approximation Theory XII, San Antonio, 2007, edited by M. Neamtu and L. L. Schumaker, Nashboro Press, 2008, Brentwood, TN, pp. 210–228.

[37] M. -J. Lai and L. L. Schumaker, Approximation power of bivariate splines, Advances in Comput. Math., 9(1998), pp. 251–279.

[38] M. -J. Lai and L. L. Schumaker, *Spline Functions on Triangulations* , Cambridge University Press, 2007.

[39] M. -J. Lai and L. L. Schumaker, *Domain decomposition technique for scattered data interpolation and fitting*, SIAM J. Numerical Analysis, 47(2009), 911-928.

[40] D. Mumford and J. Shah, Optimal approximation by piecewise smooth functions and associated variational problems, Commun. Pure Appl. Math, vol. 42, pp. 577–85, 1989.

[41] Nikolova, M. Minimizers of cost-functions involving nonsmooth data-fidelity terms. SIAM Journal on Numerical Analysis. 40:3 (2002), pp. 965–994.

[42] Nikolova, M., A variational approach to remove outliers and impulse noise, Journal Math. Imaging and Vision, 20 (2004), pp. 99–120.

[43] J. von Neumann, Various techniques used in connection with random digits. Monte Carlo methods, Nat. Bureau Standards, 12 (1951), pp. 36–8.

[44] Osher, and Sethian, Fronts propagating with curvature-dependent speed: Algorithms based on Hamilton-Jacobi formulations, J. Comput. Phys. 79: 12C49, 1988.

[45] P. Parona and J. Malik, Scale-Space and Edge Detection Using Anisotropic Diffusion, 12 (1990), pp. 629–639.

[46] Robert, C.P. and G. Casella, **Monte Carlo Statistical Methods**, (second edition), New York: Springer-Verlag, 2004.

[47] L. Rudin and S. Osher. Total variation based image restoration with free local constraints. In Proceedings of the International Conference on Image Processing, volume I, pages 31-35, 1994.

[48] L. Rudin, Osher, S., Fatemi, E., Nonlinear total variation based noise removal algorithms. Physica D 60 (1992), 259-268.

[49] E. M. Stein, Singular Integrals and Differentiability Properties of Functions, Princeton University Press, 1970.

[50] F.Santosa and W.Symes, Reconstraction of blocky impedance profiles from normal-incidence refection seismographs which are band-limited and miscalibrated, Wave Motion, vol.10(1988), pp. 209-230.

[51] X.-C.-Tai et al., eds., *Scale Space and Variational Methods in Computer Vision*, Lecture Notes in Computer Science, Vol. 5567, Springer Berlin, Heidelberg, 2009.

[52] L. Vese, A study in the BV space of a denoising-deblurring variational problem, Applied Maht. Optim, 44(2001), 131–161.

[53] C.R.Vogel, Total Variation regularization for ill-posted problems, Department of Mathematical Sciences Technical Report, April 1993, Montana State University.

[54] C. R. Vogel and M. E. Oman, Iterative methods for total variation denoising. SIAM J. Sci. Comput. 17 (1996), no. 1, 227-238,

[55] D.D. Wackerly, W. Mendenhall III, and R.L. Scheaffer, Mathematical Statistics with Applications, Sixth Edition, Duxbury Thomson Learning, pp. 429-433, 2002.

[56] J.Wang, Error Bound for Numerical Methods for the ROF Image Smoothing Model, Ph.D Dissertation, University of Purdue, 2008.

[57] J. Wang and Lucier, B., Error bounds for finite-difference methods for Rudin-Osher-Fatemi image smoothing, submitted, 2009.

[58] W. Yin, D. Goldfarb, and S. Osher, A comparison of three total variation based texture extraction models, Journal of Visual Communication and Image Representation, 18 (2007), pp. 240-252.

[59] W. Yin, W. Goldfarb, and S. Osher, The total variation regularized L_1 model for multiscale decomposition, SIAM Journal on Multiscale Modeling and Simulation, 6 (2007), pp. 190-211.

[60] J. Yuan, J. Shi and X. C. Tai, A Convex and Exact Approach to Discrete Constrained TV-L1 Image Approximation, UCLA Dept. of Math. CAM Report, August 2010.